57 Orbital Fractures

Ananthanarayanan Parameswaran,
Madhulaxmi Marimuthu, Shreya Panwar,
and Beat Hammer

57.1 Introduction

Orbital fractures are unique among cranio-maxillofacial (CMF) fractures. They have functional, cosmetic, and psychological implications. Most importantly they are among the few true emergencies in the realm of CMF trauma. Management of orbital fractures poses a challenge to every surgeon because of its complex anatomy, relationship to vital structures such as the globe and the brain, and its direct influence on the most precious of senses, *Vision.*

The orbit is a small bony cone filled with numerous vital and delicate structures, which require absolute precaution while handling and immense precision in its reconstruction. The principles of managing orbital trauma differ significantly from rest of the CMF fractures, which mandate a thorough understanding of its morphology and biodynamics. Choosing the appropriate indication for intervention and management protocol is critical in achieving the desired surgical outcome. This chapter aims to answer the questions of the *When*, *Why*, and *How* of managing orbital trauma.

57.2 Surgical Anatomy of the Orbit

The orbits are bilateral bony cavities which house the globes. Each orbit is made up of seven bones: the maxilla, frontal bone, zygomatic, sphenoid, ethmoid, lacrimal, and the palatine bones (Fig. 57.1). The orbital cavity is a pyramidal structure with a quadrilateral base anteriorly, forming the orbital aperture, and the apex posteriorly which ends at the optic foramen. The apex is superomedially placed, while the base is directed anterior and lateral. The orbit encases two fissures: (1) the inferior orbital fissure also called the sphenozygomatic fissure and (2) the superior orbital fissure otherwise called as the inter-sphenoidal fissure (Fig. 57.2). The major structures within the orbit are provided in Box 57.1.

Electronic Supplementary Material The online version of this chapter (https://doi.org/10.1007/978-981-15-1346-6_57) contains supplementary material, which is available to authorized users.

A. Parameswaran (✉)
Department of Oral and Maxillofacial Surgery, Meenakshiammal Dental College and Hospital, Chennai, India

Department of Orbit, Oculoplasty, Reconstructive and Aesthetic Surgery, Shankara Nethralaya, Chennai, India

Department of Orbit and Oculoplasty, Aravind Eye Hospitals, Chennai, India

M. Marimuthu
Department of Oral and Maxillofacial Surgery, Saveetha Dental College and Hospital, Chennai, India

S. Panwar
Department of Oral and Maxillofacial Surgery, Meenakshiammal Dental College and Hospital, Chennai, India

B. Hammer
CFC Hirslanden Kopf Zentrum, Aarau, Switzerland
e-mail: Beat.Hammer@hirslanden.ch

K. Bonanthaya et al. (eds.), *Oral and Maxillofacial Surgery for the Clinician*, https://doi.org/10.1007/978-981-15-1346-6_57

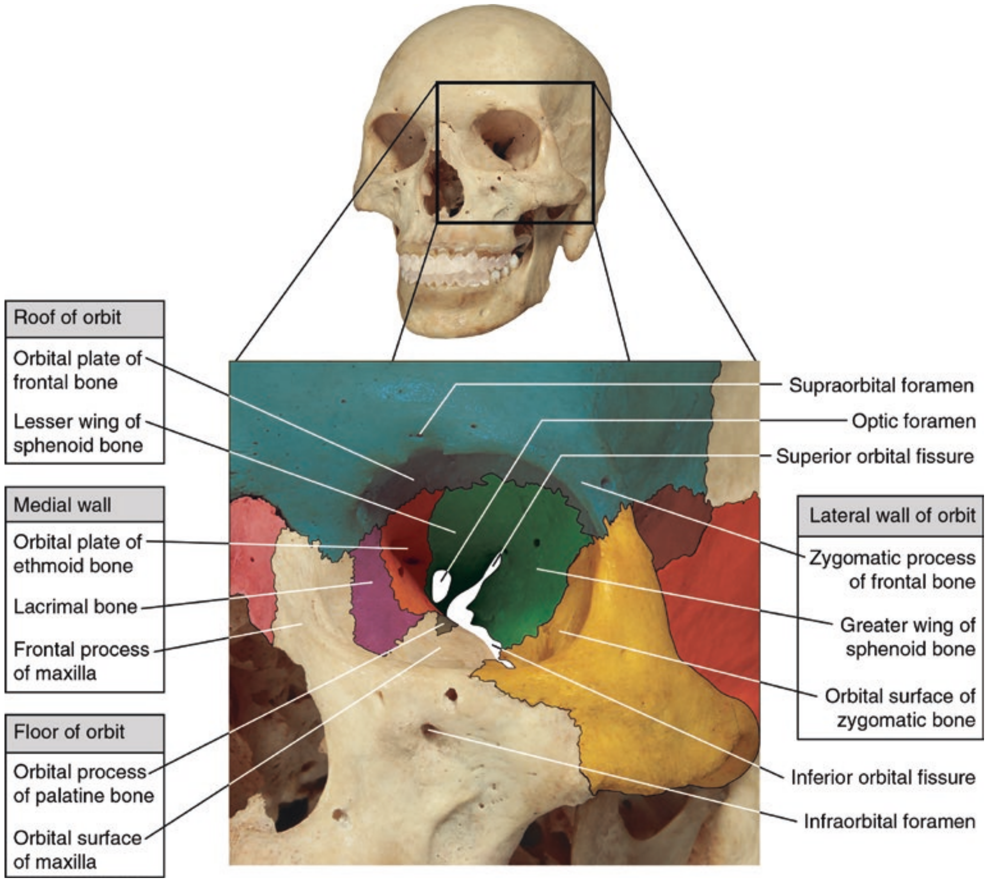

Fig. 57.1 Bones forming the orbit

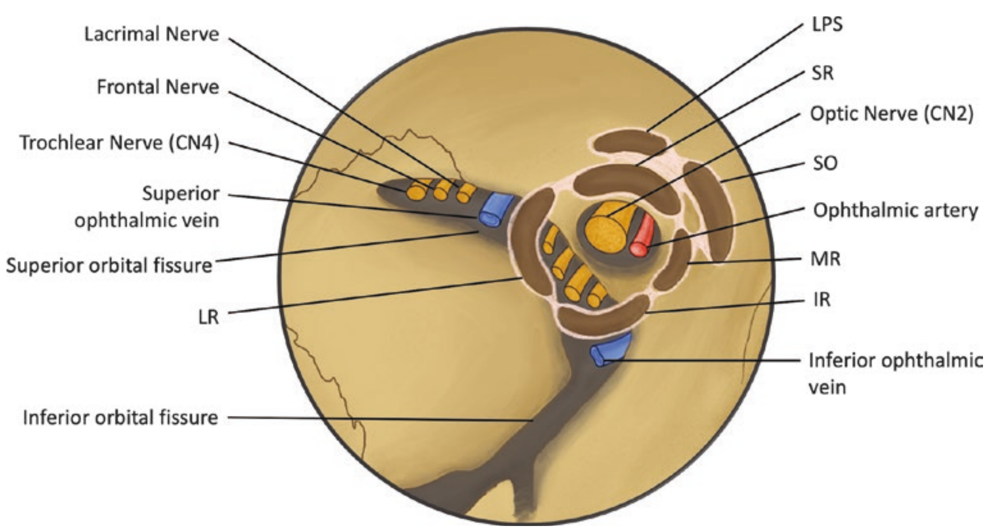

Fig. 57.2 Structures passing through the superior and inferior orbital fissures

Box 57.1 The Major Structures that Occupy the Orbit

- Eye/globe
- Orbital fat
- Extraocular muscles
- Ciliary parasympathetic ganglion
- Nasolacrimal apparatus
- Optic nerve
- Oculomotor
- Trochlear
- Abducent nerves
- V1 and V2 of trigeminal nerve
- Ophthalmic vessels

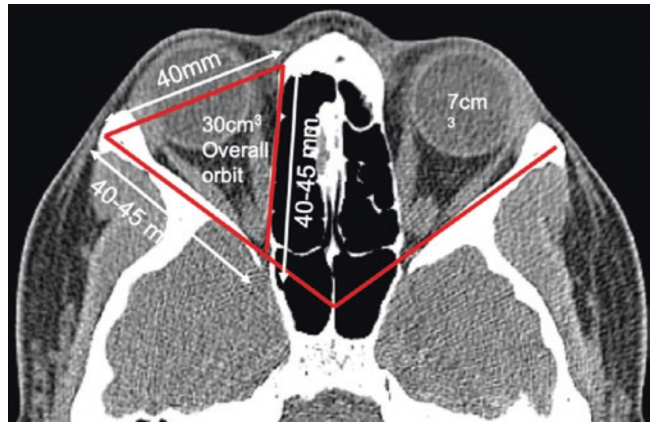

Fig. 57.3 Diagrammatic representation of the various measurements of the orbit and the globe

The orbits have an average height of 35 mm and a mediolateral width of 40 mm [1–3]. The intra-orbital volume of an adult is approximately 30 cc, while the volume of the globe is 7 cc [4]. Generally, the orbital and globe volumes are bilaterally symmetrical at any stage of growth. The medial walls are parallel to each other and around 45–50 mm in length, while the lateral walls are around 90° to each other and 40–45 mm long (Fig. 57.3).

The orbital skeleton may essentially be divided into walls and rims. These include the orbital roof, floor, and medial and lateral walls. The rims include the inferior, superior, medial, and lateral orbital rims. A brief description of the structure of the orbital cavity is provided below.

57.2.1 Orbital Walls

The roof (Fig. 57.4a) is formed by a concave broad plate of the frontal bone which delineates the orbital contents from the cranial cavity. The posterior portion of the roof has a small contribution from the lesser wing of the sphenoid. The anterolateral portion has a shallow depression called the lacrimal fossa, while 5 mm behind the medial aspect of the supraorbital rim is the trochlear fossa which has the cartilaginous pulley of the superior oblique muscle. The roof is triangular in shape and ends in optic foramen, which is the entry of the optic nerve into the orbit.

In older patients there may be spots of resorption in the orbital roof which may cause the dura to adhere to the periorbita of the roof. The junction of the medial wall and the roof has a suture line which lies in close proximity to the cribriform of the ethmoid and is prone for fragmentation. This may be a major concern for CSF leak into the orbits or the nose or at times both.

The roof is separated from the lateral orbital wall by the superior orbital fissure which serves as a passage of entry for the cranial nerves III, IV, V1, and VI into the orbit. The other structure coursing through the fissure is the ophthalmic vein. On the anterior aspect of the roof, at the junction between the medial 1/3rd and the lateral 2/3rd of the supraorbital rim is the supraorbital foramen which transmits the supraorbital neurovascular bundle [1–3, 5].

The medial wall (Fig. 57.4c) is quadrangular in shape and is constituted by the ethmoid bone in the center. The anterosuperior aspect is formed by the frontal bone, while the anteroinferior part is formed by the lacrimal bone. The sphenoid bone forms the posterior part of the medial wall. The infraorbital rim continues along the anterior aspect of the medial wall forming the anterior lacrimal crest which is a part of the frontal process of the maxilla, while the superomedial aspect of the supraorbital rim continues inferiorly as the posterior lacrimal crest which is formed by the lacrimal bone. Between these crests lie the fossa which houses the lacrimal sac. This is of importance during access planning for surgery of the medial wall and the anteromedial aspect of the infra-orbital rim.

The anterior and posterior ethmoidal foramen are located along the fronto-ethmoidal suture which signifies the height of the cribriform plate. The anterior ethmoidal foramen which transmits the anterior ethmoidal artery and nerve lies approximately 22–25 mm behind the medial orbital rim while the posterior ethmoidal foramen which transmits the posterior ethmoidal artery and the spheno-ethmoidal nerve is present about 12 mm posterior [6]. The optic foramen is in continuation of the medial wall and is approximately placed 45–50 mm behind the medial rim. The safe distances the sur-

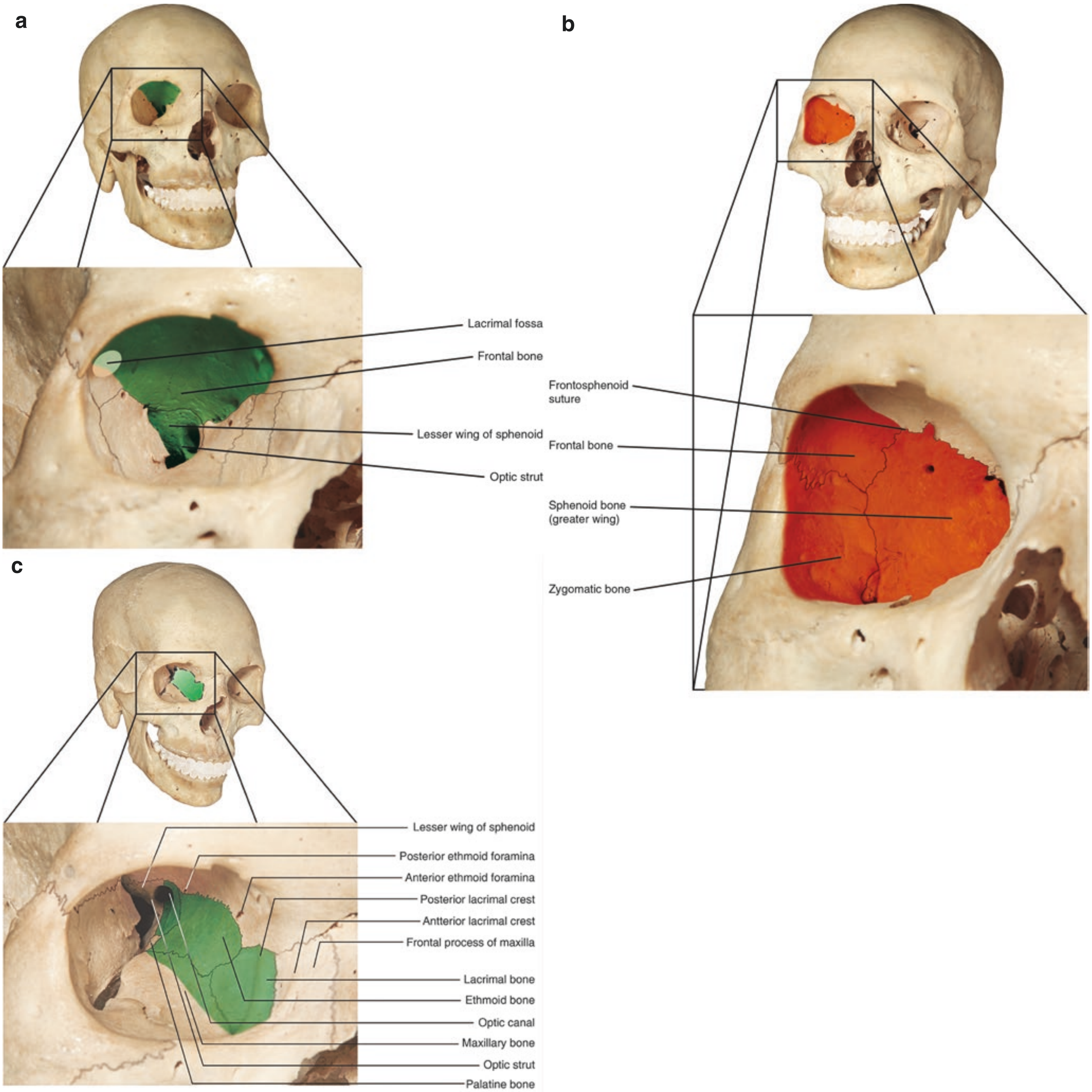

Fig. 57.4 (**a**) Roof, (**b**) lateral wall, and (**c**) medial wall of the orbit

geon needs to remember are 24 mm for the anterior ethmoidal artery, with an additional 12 mm for the posterior ethmoidal vessel and a further 6 mm as the limit to stay away from the optic foramen making it *24-12-6*, an easy formula to remember. One important structure which may be involved in medial wall trauma is the medial rectus muscle which can get entrapped causing ocular motility disturbances.

The lateral wall (Fig. 57.4b) is the thickest wall and is made primarily by the orbital surface of the zygomatic bone and the greater wing of the sphenoid. A small bony projection seen on the lateral wall is the Whitnall's tubercle which lies 11 mm below the fronto-zygomatic suture and 4 mm behind the rim (Fig. 57.7).

This tubercle forms the attachment of the 4L's:

1. The suspensory ligament of Lockwood
2. The lateral horn of the levator aponeurosis
3. The ligaments of the lateral rectus muscle
4. The lateral palpebral ligament

A small groove may be seen at the anterior end of the inferior orbital fissure which transmits the zygomatico-facial and zygomatico-temporal vessels. These course through the zygoma and exit through independent foramina to supply the face and the temporal regions.

The floor (Fig. 57.5a, b) follows a gentle slope from its medial to lateral side. The highest point lies in the postero-medial aspect of the floor forming a bulge called the "Hammer's key area" [7] (Fig. 57.5a), which influences the position of the globe in the anteroposterior axis. In the sagittal view, the floor follows a "lazy S" shape with the anterior part concave and the posterior convex. The reconstruction of this convexity is important to maintain the anterior position of the globe (Fig. 57.5b). The floor is separated from the lateral wall by the inferior orbital fissure. The fissure communicates with the pterygopalatine fossa extra-orbitally. The maxillary division of the V nerve and its branches, the infra-orbital artery, and branches of the sphenopalatine ganglion are transmitted through the posteromedial aspect of the fissure, while the inferior ophthalmic veins pass through the lateral aspect to communicate with the pterygoid plexus. The floor is formed by the zygomatic bone and the maxilla with a small contribution from the orbital process of the palatine bone in the posteromedial aspect. A rough area at the antero-medial angle of the floor behind the infra orbital rim forms the attachment of the inferior oblique muscle. The infra-orbital groove originates from the inferior orbital fissure and transmits the infra-orbital neurovascular bundle.

Orbital Rims:
The rims are superior, inferior, medial, and lateral. Three major bones—the maxilla, zygomatic bone, and frontal bone—make up the rims of the orbit. The width of the rims is greater than its height making it into a rectangular form. The presence of the maxillary sinus and the insertion of the inferior oblique muscle make the infra-orbital rim more prone for fracture and comminution.

57.2.2 Muscles of the Orbit (Fig. 57.6a)

Muscles in relation to the orbit can be divided into

- the muscles associated with the lids
- and the muscles associated with the globe.

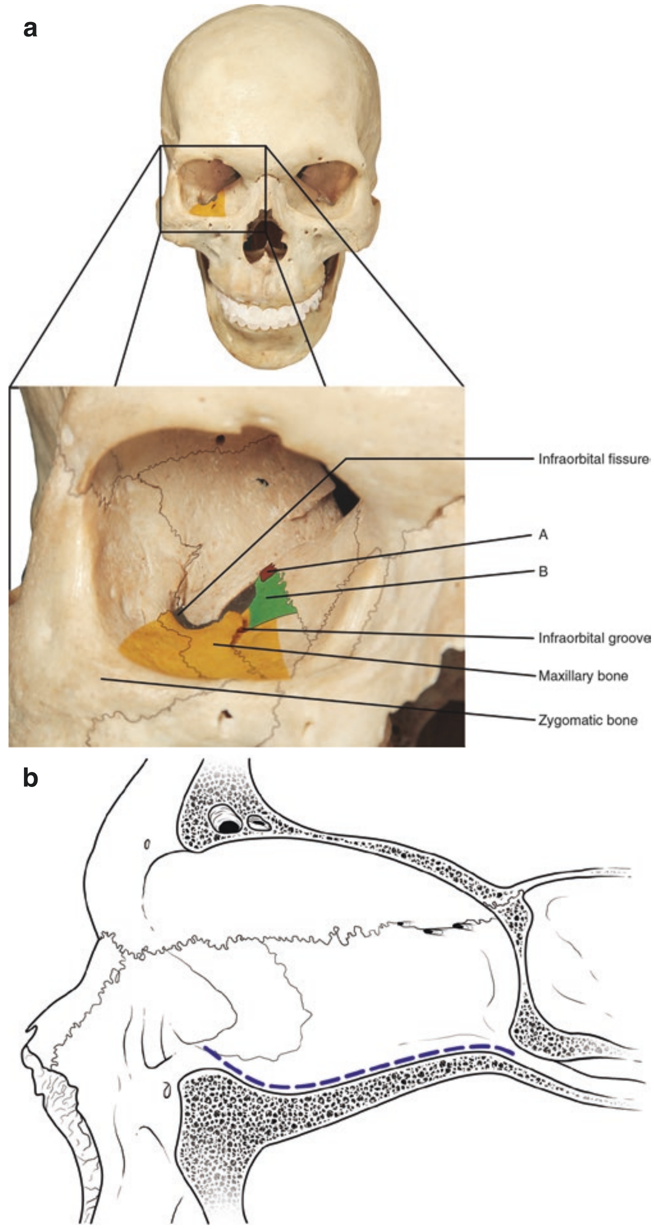

Fig. 57.5 The orbital floor in (**a**) frontal view demonstrating the (A) orbital process of palatine bone and (B) "Hammer's key area." (**b**) Sagittal view of the floor with the "lazy S" form

The muscles of the lid are:

1. The orbicularis oculi which has a palpebral portion (upper and lower eyelids), the intervening orbital septum, and the inner layer connecting the tarsus
2. The levator palpebrae superioris which is the elevator of the upper eyelid
   The levator palpebrae superioris along with the four recti, and the two obliques form the seven extraocular muscles of the human eye.

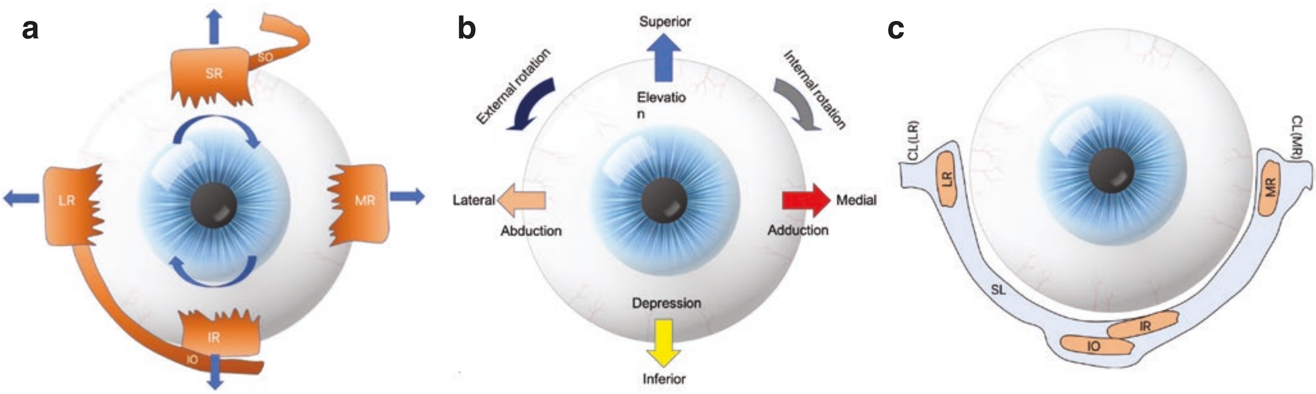

Fig. 57.6 Diagram of right eye demonstrating (**a**) the extraocular muscles and (**b**) the movements they cause. (**c**) The fascial sheath. (*SR* - Superior Rectus, *IR* - Inferior Rectus, *MR* - Medial Rectus, *LR* - Lateral Rectus, *SO* - Superior Oblique, *IO* - Inferior Oblique, *CL(MR)* - Check Ligament of Medial Rectus, *CL(LR)* - Check Ligament of Lateral Rectus, *SL* - Suspensory Ligament

The origin of the superior rectus is from the common tendinous ring superolateral to the optic canal, and its insertion is into the upper part of the sclera. Its function is to produce elevation of the eye and to move the cornea upward and medially helping in adduction and medial rotation.

The origin of the medial rectus is from the medial aspect of the tendinous ring and inserts into the medial surface of the sclera. The medial rectus helps in moving the eye medially (adduction), and bilateral action of the medial rectus helps in medial convergence of both the corneas. A suspensory attachment to the lacrimal crest is also seen on the medial orbital wall where it blends with the medial canthus and the check ligament (Fig. 57.6c) [2, 3, 6, 8]. The origin of the lateral rectus is from the lateral part of the common tendinous ring, and it inserts into the lateral surface of the sclera. Its primary function is to move the eye laterally (abduction).The inferior rectus arises from the common tendinous ring, below the optic canal, and inserts into sclera below the cornea. It is responsible for depression and lateral rotation of the eye.

The inferior rectus followed by the medial rectus are the most common muscles to be entrapped secondary to orbital trauma and may need to be explored and released surgically as indicated. Delayed release of the recti may cause significant necrosis and fibrosis of the muscles hampering return to normal function.

The superior oblique arises superomedial to the optic canal. It has a pulley action at the trochlea on the anteromedial aspect of the orbital roof and inserts into the sclera behind the equator of the globe. The contraction of the muscle produces depression of the cornea and movement of the eye laterally with medial rotation (intorsion).

The inferior oblique muscle arises from the orbital surface of the maxilla lateral to the nasolacrimal groove and inserts into the lateral part of the sclera behind the equator between the inferior and lateral recti muscle. It produces elevation of the cornea and helps in moving the eye laterally with lateral rotation (extorsion).

57.2.3 Movements of the Eye and Their Innervation

Box 57.2 The Movements of the Eye

- Elevation
- Depression
- Adduction
- Abduction
- Intorsion
- Extorsion (Fig. 57.6b)

The different movements of the eye are enumerated in Box 57.2. These are facilitated by the extraocular muscles described above and are contained by the check ligaments. The inferior oblique and inferior rectus muscles which course the floor of the orbit serve as the inferior check ligaments. The fascia of the levator palpebrae superioris, which is anchored to the Whitnall's tubercle laterally and the trochlea medially, acts as the superior check ligament [8].

The contraction of the orbicularis oculi innervated by the facial nerve dictates the closure of the upper eyelid. The movements of the globe within the orbit are however dictated by the synchronous movements of the extraocular muscles of the orbit. The oculomotor nerve innervates all the extraocular muscles other than the lateral rectus which is supplied by the abducent nerve and the superior oblique supplied by the trochlear nerve. Reflex closure of the eyelids occurs via the sympathetic pathways traveling to the smooth muscles of the upper and lower eyelids.

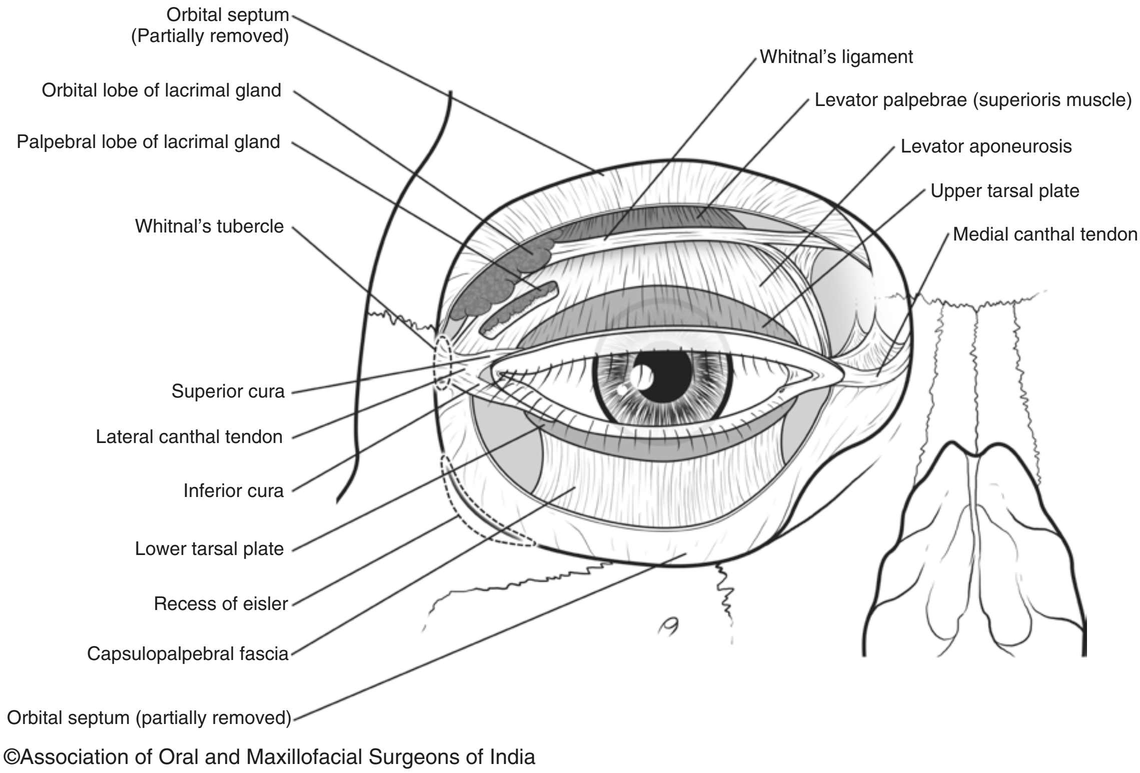

Fig. 57.7 The tarsal apparatus and the orbital septum

57.2.4 Orbital Septum and Tarsal Plates (Fig. 57.7)

The supporting framework for the eyelid is formed by a dense fibrous tissue called the orbital septum which condenses at the lids as the tarsal plates. The orbital septum which separates the orbital and lid contents attaches to the bone and becomes the periorbita inside the orbit and periosteum outside the orbit. The septum of the lower eyelid attaches to the orbital rims, while the septum of the upper eyelid is attached intra-orbitally behind the equator of the globe. The tarsal plates add rigidity to the lids and also serve attachments of multiple muscles and membranes [1, 3].

57.2.5 Conjunctiva

The conjunctiva is the transparent mucous membrane that covers the front surface of the globe and the inner surface of the eyelids.

This has two segments:

1. The bulbar conjunctiva that covers the anterior part of the sclera (the "white" of the eye)
2. The palpebral conjunctiva otherwise known as tarsal conjunctiva which covers the inner aspect of the eyelids

57.2.6 Fascial Sheath of the Eyeball (Fig. 57.6c)

The fascial sheath of the eyeball is called the Tenon's capsule [8]. It extends from the optic foramen to the sclerocorneal junction enveloping the eyeball on the inferior aspect. It attaches to the sclera on the anterior and posterior surfaces of the eyeball and becomes continuous with the fascia of the muscles posteriorly and around the inferior oblique muscle. The fascial sheath of all muscles blend together and form a continuous fascial band called the suspensory ligament of the eye that provides support for the eyeball [8, 9].

57.2.7 Orbital Fat

The orbital fat is present both intra- and extra-conally. They cushion the globe and muscles of the orbit. The extra-conal fat determines and influences the position of the globe. This may be altered either due to herniation or atrophy secondary to fractures of the orbit resulting in enophthalmos.

57.3 Classification System

Manson [10] and colleagues classified the fractures based on the energy of impact, the degree, and extent of comminution and displacement observed on CT:

(a) Trap door fractures—low-velocity injuries
(b) Medial blowout fractures—intermediate-velocity injuries
(c) Lateral blowout fractures—high-velocity fractures

Converse and Smith [11] termed them "pure" or "impure" based on the involvement of orbital rims (Fig. 57.8):

(a) Pure (blow-in or blowout fractures)—fracture of the internal walls with intact rims
(b) Impure (complex with involvement of one or more rims)—associated fractures of the rims

Hammer [7] described four classes of orbital fractures based on their occurrence with other fractures of the face (Fig. 57.9):

(a) *Type I*: Orbito-zygomatic fractures—These involve the fractures of the walls of the orbit along with the zygomatic complex.
(b) *Type II*: Internal orbital fractures—These involve isolated fractures of any of the walls, roof, and floor.
(c) *Type III*: Naso-orbito-ethmoid-type fractures—These involve fractures of the naso-orbito-ethmoid complex which involve the orbit.
(d) *Type IV*: Complex fractures of the face—This type involve fractures of the orbit with concomitant fractures of the face other than the ones mentioned above [7].

57.4 Blowout and Blow-In Fractures

Smith and Converse in 1960 recognized the phenomenon of blowout fractures (Fig. 57.10a). These fractures may involve entrapment or herniation of periorbital tissues resulting in restricted eye movements and/or enophthalmos due to reduction in the volume of intra-orbital contents [3, 11].

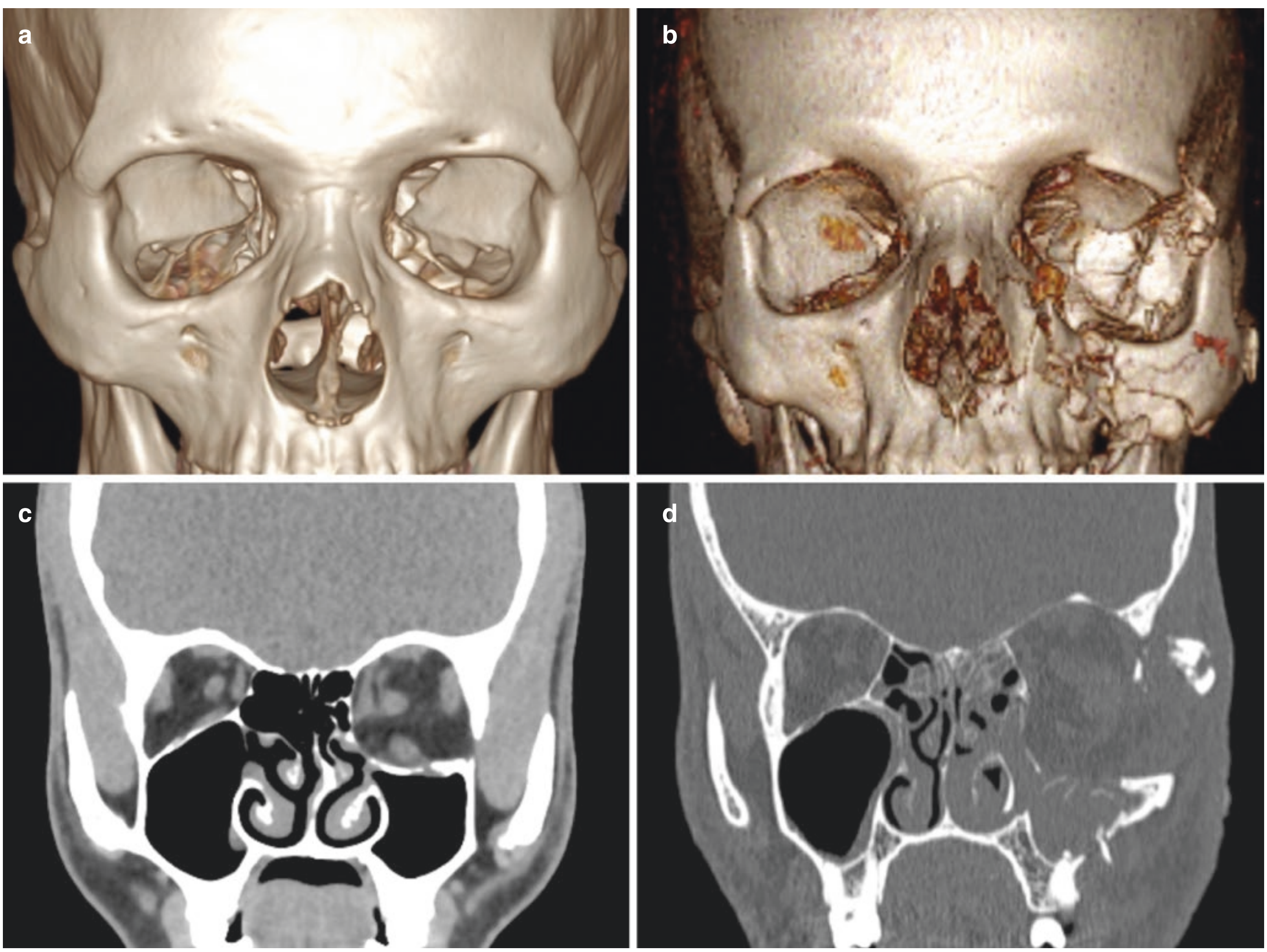

Fig. 57.8 CT scans showing Pure (**a** and **c**) and impure (**b** and **d**) blowout fractures of the orbit

"Blow-in" type of orbital fractures was described by Dingman and Natvig [3, 12] in 1964 wherein the intra-orbital space is reduced by an internally displaced bony fragment (Fig. 57.10b). Such types of fractures are usually accompanied with proptosis on the affected side [13].

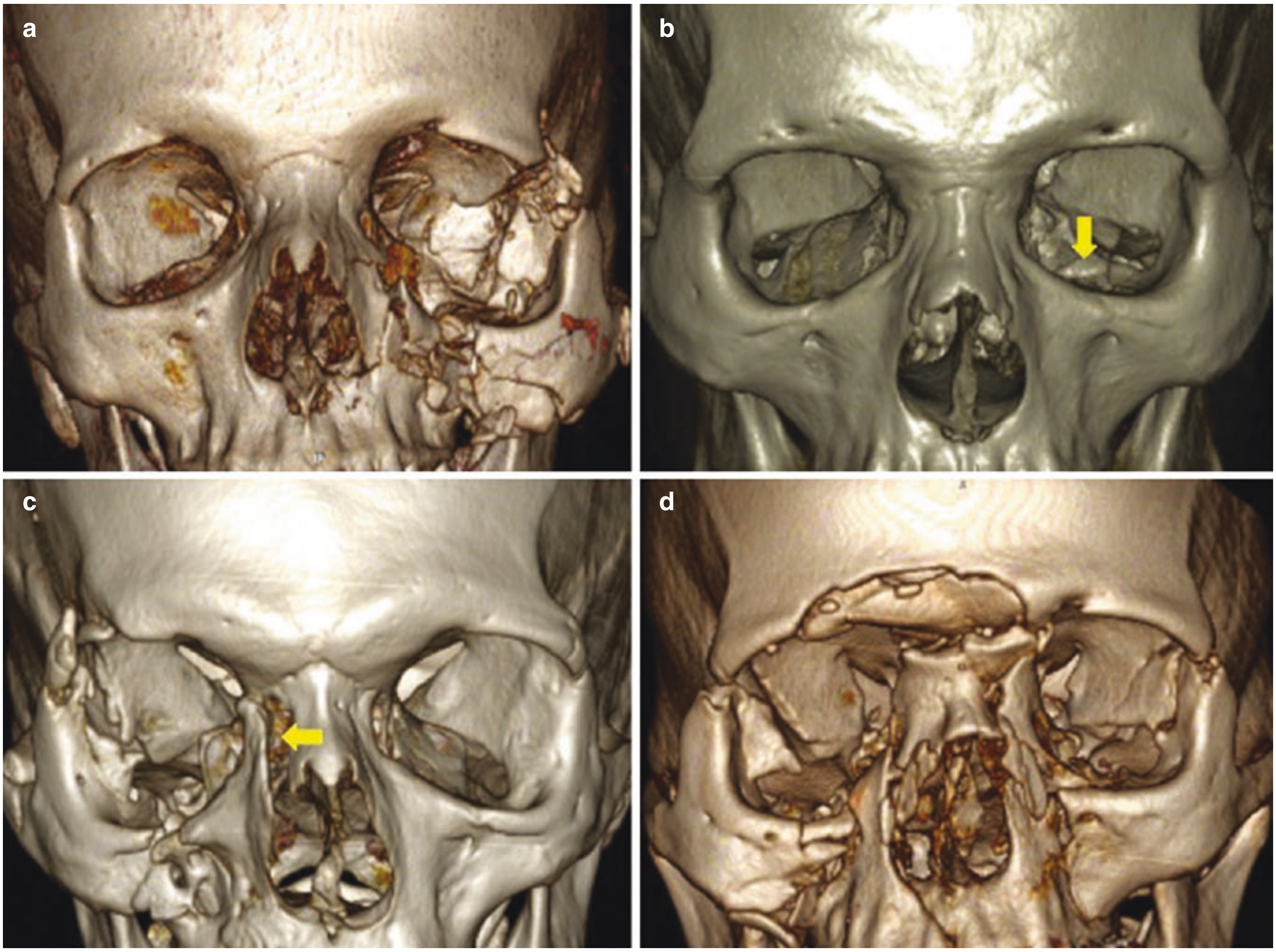

Fig. 57.9 CT scan images showing types of orbital fractures: (**a**) orbito-zygomatic, (**b**) internal orbital, (**c**) naso-orbito-ethmoid type, and (**d**) orbit with complex facial fractures

Fig. 57.10 CT scans demonstrating a blowout of the medial orbital wall and floor (**a**) and a blow-in fracture of the orbital roof (**b**)

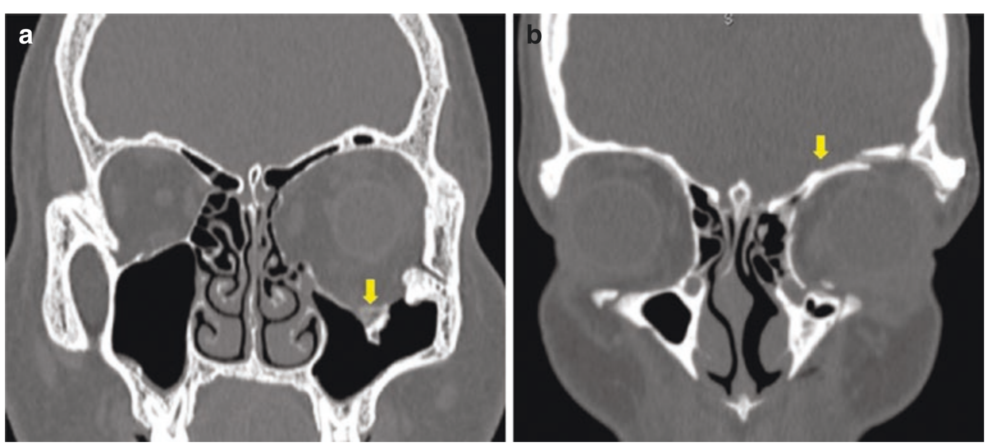

57.5 Biomechanics of Injury

One of the first mechanisms of orbital wall fractures was suggested by Pfeiffer [14] in 1943, called *globe-to-wall theory or hydraulic theory* (Fig. 57.11a), wherein posterior displacement of the globe after sustaining a direct hit was propounded to transmit force along the walls resulting in fracture of the thinner walls. There are two more widely accepted mechanisms of orbital wall fractures, namely, the:

(i) *Retropulsion theory* (Fig. 57.11b)
(ii) *Buckling mechanism* [15] (Fig. 57.11c)

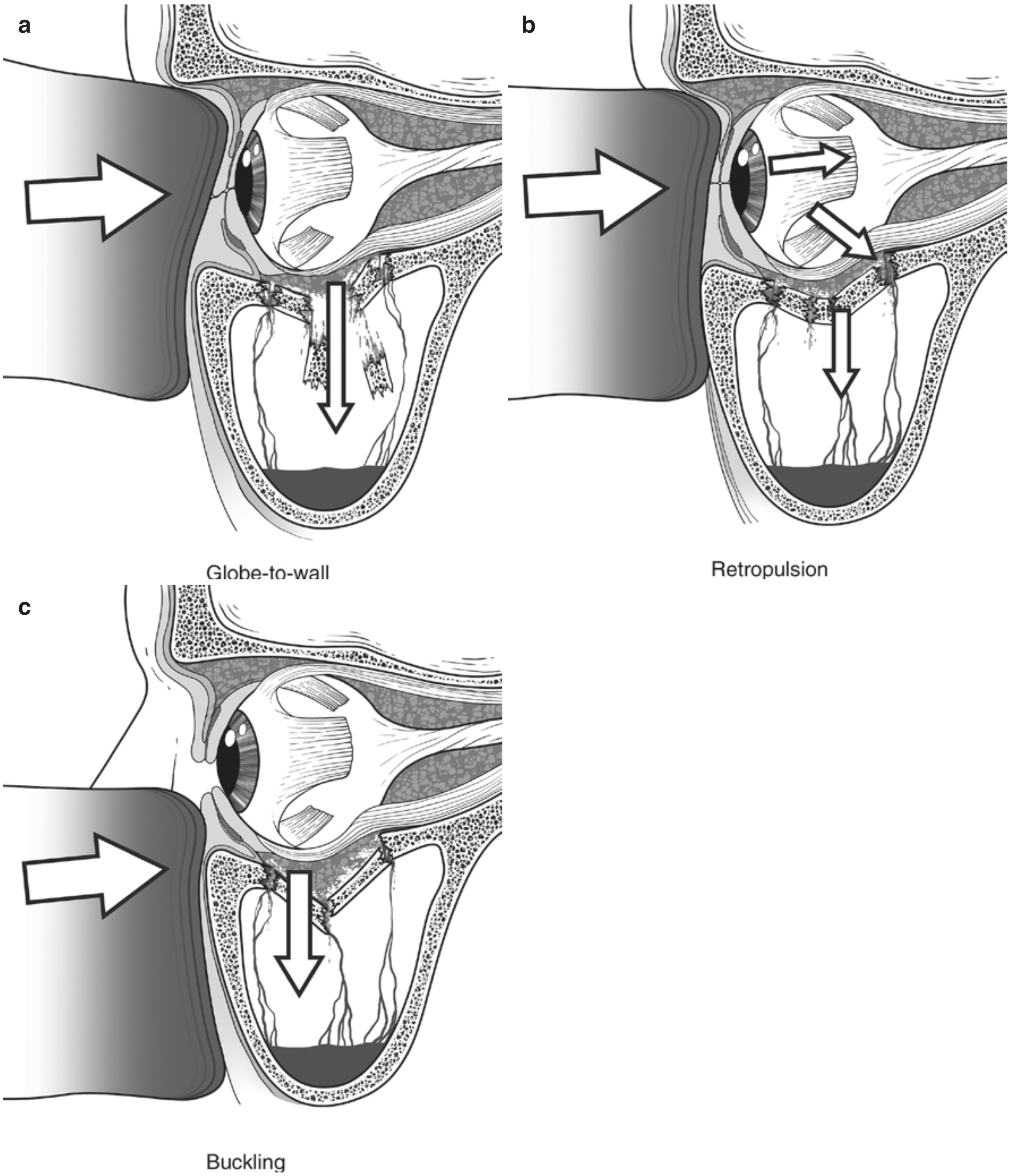

Fig. 57.11 Diagrammatic representation of (**a**) hydraulic theory, (**b**) retropulsion theory, and (**c**) buckling mechanism

First proposed by King [16] in 1944, retropulsion theory suggests that sudden increase in intra-orbital pressure caused by direct hit from a large object creates stresses along the orbital walls resulting in fractures at the areas of least thickness. The buckling theory or transmission theory explains the injury through a ripple effect created in the floor. The ripple thus created causes compression in an anteroposterior direction and resultant fracture at the posteromedial part of the orbital floor commonly [17, 18].

57.6 Initial Assessment

After initial stabilization of the patient, a thorough facial examination is performed in a way similar to any facial fracture. Special consideration is given to a detailed ophthalmic evaluation followed by eliciting signs and symptoms significant for periorbital trauma which are discussed below. The frontal area and supraorbital rim are examined first, with a logical progression downward, including the lateral and infra-orbital rims, although extensive edema in this area may obscure any steps making the palpatory examination difficult [3, 7, 19–22].

57.6.1 Ophthalmologic Examination

The American Association of Ophthalmology [23] advocates an 8-point ophthalmological examination which includes the following (Box 57.3):

1. *Visual acuity*: Visual acuity test for each eye is recorded using a Snellen chart (Fig. 57.12a) and includes ability to read letters, count fingers, perceive hand movements, and light perception. If visual acuity is extremely poor and recording of a chart test fails, the patient is subjected to a finger counting test or at times even assessed for primary light perception alone.
2. *Pupillary examination*: Pupillary examination is done to note the
   (a) size,
   (b) shape,
   (c) symmetry,
   (d) and direct/indirect reflex to light.
   Glaucoma, previous history of surgery, and/or injury to ocular system may also account for anisocoria or irregular pupils. Peaked or irregular pupils may also be indicative of perforation of the globe. The swinging flashlight test is performed for relative afferent pupillary defect (RAPD) (Fig. 57.12b).
3. *Extraocular motility and alignment*: The patient is first screened for all the six cardinal gazes (Fig. 57.12c). First checked binocularly for versions of both sides and then checked monocular for ductions. A thorough heterotropia check is also performed. Diplopia and restrictions in gazes are noted. Clinically, a forced duction test under topical anesthesia is done to elicit mechanical impediment to movement of the globe. This may also be performed under general anesthesia intraoperatively (Figs. 56.21, 57.13). A Hess chart examination is a part of the orthoptic assessment protocol for evaluation of ocular motility.
4. *Intraocular pressure*: Tonometry should be performed to evaluate intraocular pressure either in a clinic setting using a Goldmann applanation method or outside using a mobile/portable device. This examination is skipped if there is a suspicion of ruptured globe. The normal IOC

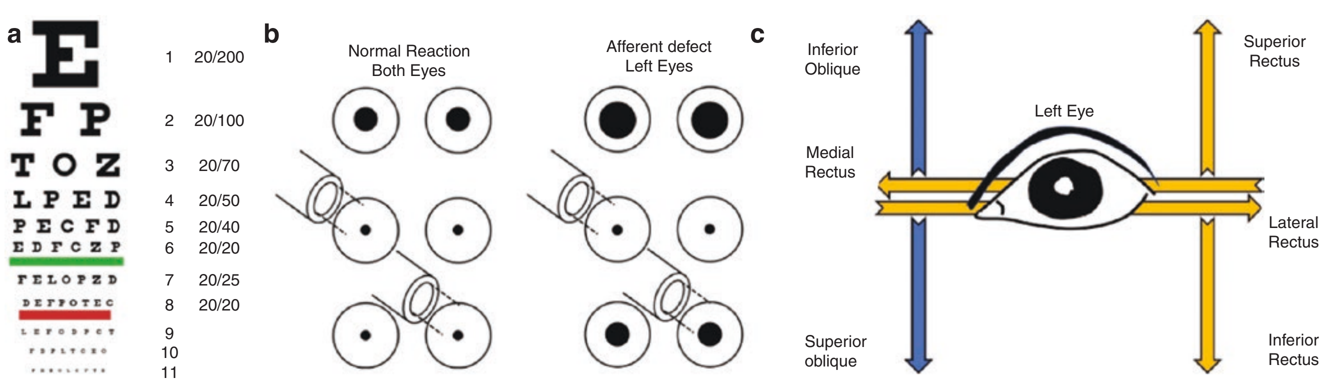

Fig. 57.12 Picture showing (**a**) the Snellen chart, (**b**) swinging flash light test, and (**c**) the six cardinal signs of gazes

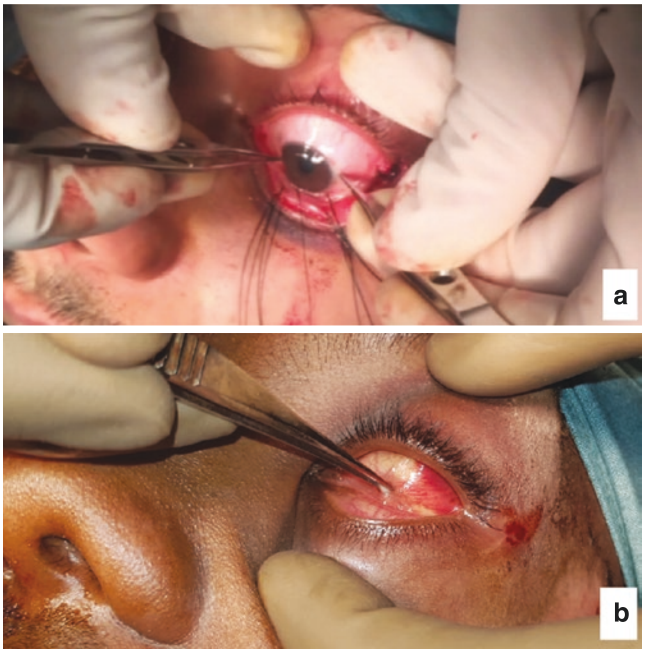

Fig. 57.13 Demonstration of the method of performing intraoperative forced duction test (**a**) by grasping the limbus (sclero-corneal junction) and (**b**) by grasping the inferior rectus muslce

is a range between 10 and 21 mmHg with the mean being around 15 mmHg. Low IOP may be suggestive of a ruptured globe or detached retina, while increased IOP may indicate hyphema, glaucoma, or an orbital compartment syndrome like "retrobulbar hemorrhage." A pressure of more than 30 mmHg is an ophthalmological emergency.

5. *Visual fields*: Visual fields for each eye are checked by asking the patient to determine movements at the periphery of the examiner's own visual field, while at a distance of about 2 ft from each other. Loss of field may be suggestive of compressive or ischemic injuries to the optic nerve with or without damage to the visual pathway. Goldmann visual field test can also be employed to objectively chart binocular visual field loss wherein patient is asked to look at a center of the chart and is required to track a point source of light.
6. *External examination/periorbital screening*: A thorough clinical evaluation is performed to note down all clinical features detailed below. Orbital trauma is generally associated with possible adnexal injuries which also need to be assessed for intervention and management.
7. *Slit-lamp examination*: A formal slit lamp test is performed if it may be allowed. This provides information about the lids, lashes, lacrimal system, conjunctiva, sclera, anterior chamber, iris, the lens, and the anterior vitreous.
8. *Fundoscopic examination*: A fundoscopic examination is performed to assess the retina, optic nerve head, and the vessels. This is done by the use of an ophthalmoscope. It also provides information about presence of intraocular hemorrhages and foreign bodies.
9. *Globe position*: An important feature in examination of orbital trauma from a cranio-maxillofacial perspective includes the examination of globe positions. This is performed both clinically and by using an exophthalmometer. The Hertel's exophthalmometer is used in common settings for the evaluation of proptosis or enophthalmos. In case of injuries involving the lateral face, like a fracture of the ZMC, the Naugle's exophthalmometer is used.

Box 57.3 "8-Point" Ophthalmic Examination Advocated by the American Association of Ophthalmology [23]

1.	Visual acuity and visual fields
2.	Pupillary examination
3.	Extraocular motility and alignment
4.	Intraocular pressure
5.	External examination/periorbital screening
6.	Slit-lamp examination
7.	Fundoscopic examination
8.	Globe position

57.6.2 Clinical Features

A good evaluation of the skeletal and soft tissue components of the orbit as well its associated adnexa (eyelids, lacrimal apparatus, etc.) is mandated. The common clinical features that are presented with in orbital trauma are provided in Box 57.4.

Box 57.4 Common Clinical Features in Orbital Trauma Are Enumerated Below

- Periorbital edema (Fig. 57.14a)
- Periorbital ecchymosis and subconjunctival hemorrhage (Fig. 57.14b)
- Contusions and hematomas
- Subcutaneous emphysema with crepitus
- Lacerations involving the eyelids (Fig. 57.14c)
- Injuries to the canthal apparatus (medial and lateral)
- Neurological deficits of the infra-orbital and facial nerves

Fig. 57.14 Clinical pictures demonstrating (**a**) edema of the left periorbital region, (**b**) left-sided periorbital ecchymosis and subconjunctival hemorrhage, and (**c**) soft tissue injury of the left eyelid and supraorbital region

Clinical signs and symptoms that are more exclusive to orbital trauma are discussed further in more detail.

57.6.2.1 Enophthalmos/Hypophthalmos (Fig. 57.15a, b)

Any change in the orbital volume directly impacts the position of the globe and its anteroposterior projection and supero-inferior position [24]. Clinically enophthalmos can be detected by an exaggerated suprapalpebral fold and reduced projection on viewing from an inferior view or worm's view. Hertel's or Naugle's exophthalmometer can also be used to quantify and measure the discrepancy. Other causes of enophthalmos implicated are traumatic atrophy of intra-orbital fat, infections causing cicatricial contraction of retrobulbar tissues, and dislocation of trochlear attachment of superior oblique muscle due to trauma [25, 26]. Hypophthalmos is noted as a change in the horizontal pupillary levels.

57.6.2.2 Retrobulbar Hemorrhage (Fig. 57.16)

Retrobulbar hemorrhage is a vision threatening emergency which occurs due to accumulation of blood in the retrobulbar space. This causes increased intra-orbital pressure resulting in compression or stretching of the optic nerve and reduced perfusion to the eye. Orbital trauma especially blunt injury may be associated with retrobulbar hemorrhage which warrants immediate attention. However this may also occur as a complication following surgery to the orbit or pathologies like an aneurysm. Acute post-septal hemorrhage limited anteriorly by the orbital septum and posteriorly by bone may cause permanent loss of vision by creating a compartment syndrome [27]. It presents as reduced ocular motility, elevated intraocular pressure, proptosis, and diminishing vision. In unconscious patients, pupillary assessment, increased pressure, and presence of relative afferent pupillary defect or RAPD are usually diagnostic.

57.6.2.3 Lacrimal System Injuries

Due to its close topographical location to the orbital complex, nasolacrimal system especially the duct may be involved in traumatic injuries to the orbit. Injury to the canaliculi or the nasolacrimal ducts in naso-orbito-ethmoidal injuries may present as epiphora [28]. Patency of

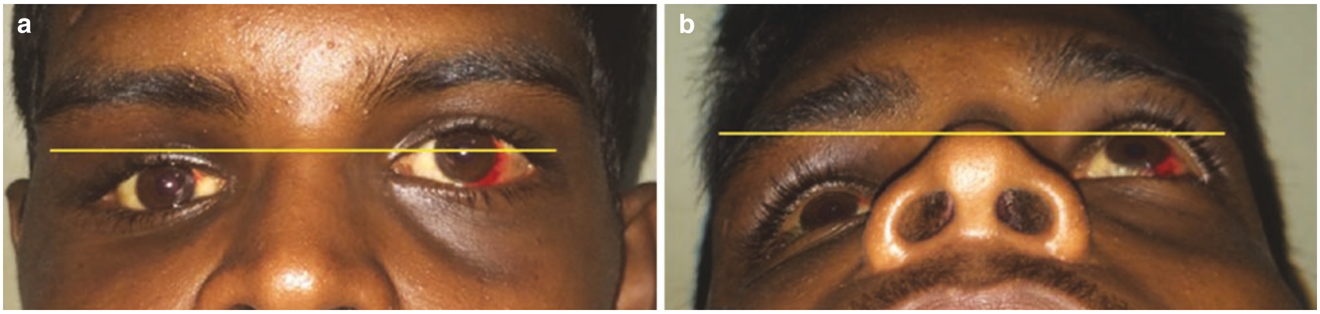

Fig. 57.15 Clinical photograph of a patient with both (**a**) hypophthalmos and (**b**) enophthalmos of the right globe

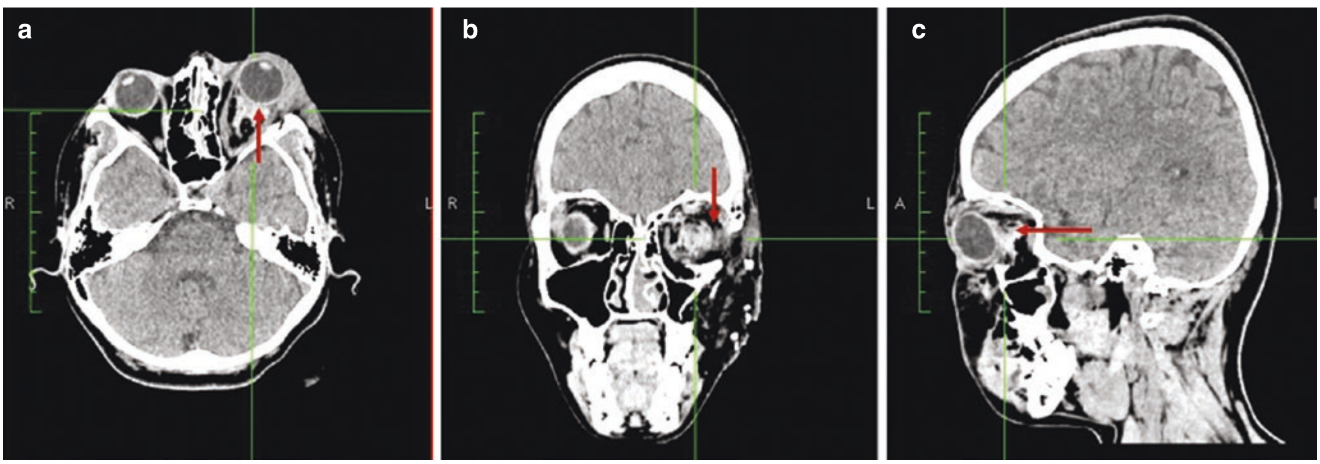

Fig. 57.16 (**a**) Axial, (**b**) coronal, and (**c**) sagittal section CT scan images demonstrating left-sided retrobulbar hemorrhage

the naso-lacrimal duct and sac can be verified by the Jones tests 1 and 2 or by a simple lacrimal probing test with insertion of a Crawford silicone intubation tubes though the canaliculi and visualization of the same at the distal end of the disruption. ROPLAS test or regurgitation on pressure over lacrimal sac may be performed clinically to elicit post-traumatic blockage of the nasolacrimal duct (Fig. 57.17c). Confirmation however is obtained with a CT dacryocystogram or CT-DCG (Fig. 57.17a, b). Reconstruction of the lacrimal drainage system is achieved by simple intubations or a formal dacryocystorhinostomy as indicated by the clinical scenario.

57.6.2.4 Oculocardiac Reflex (Trigeminocardiac Reflex)

First described by Dagnini and Aschner in 1908, oculocardiac reflex is bradycardia on manual compression of the eyes. The most common traumatic etiology is the incarceration of inferior rectus muscle in trap-door fractures of the orbital floor [29, 30]. Other causes that may present with oculocardiac reflex are retrobulbar hemorrhage, white-eyed blowout fractures and orbital surgery.

57.6.2.5 Superior Orbital Fissure Syndrome (Box 57.5)

Post-traumatic superior orbital fissure syndrome may be attributed to pressure exerted on the contents of the superior orbital fissure due to hemorrhage or impingement by fractured fragments.

Superior orbital fissure syndrome was first described by Hirschfield in 1858 [31, 32] and symptoms include:

(i) Ophthalmoplegia due to involvement of III, IV, and VI cranial nerves.
(ii) Paresthesia over the forehead due to involvement frontal nerve of first division of trigeminal nerve.
(iii) Ptosis due to impeded action of levator palpebrae superioris and Muller's muscle.
(iv) Pupillary dilatation due to paresis of circular sphincter muscle and unrestricted action of dilator pupillae.
(v) Impairment of direct pupillary reflex due to blocked ipsilateral efferent arc, whereas consensual reflex is preserved due to intact ipsilateral efferent and contralateral efferent arcs.

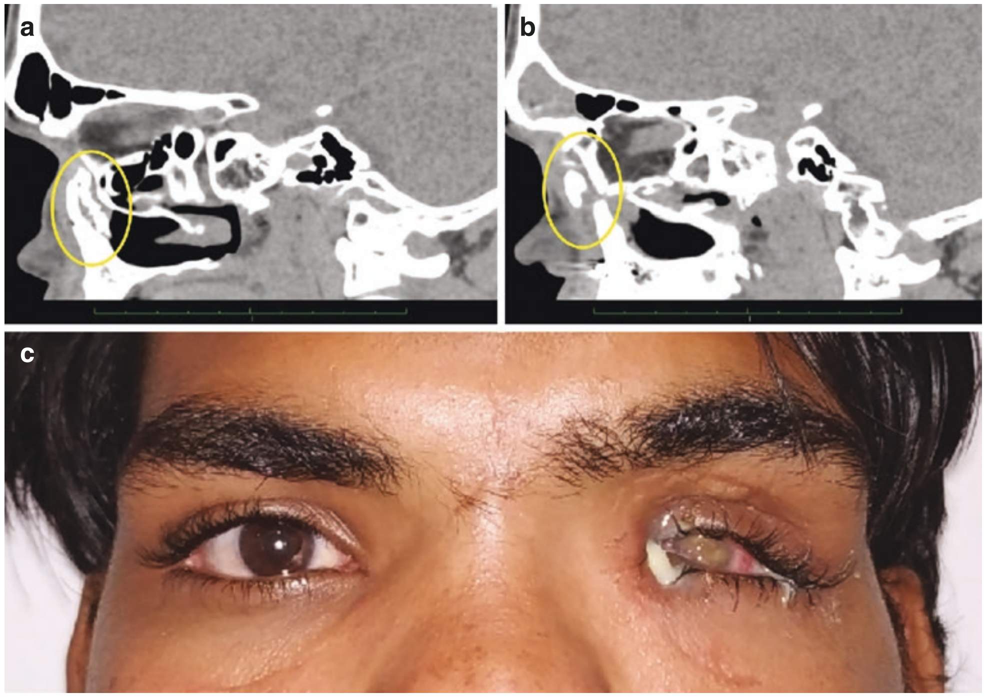

Fig. 57.17 (**a**) Sagittal section CT DCG demonstrating patent NLD with draining dye and (**b**) blocked NLD with no drainage of the dye. (**c**) Clinical photograph of patient with left-sided NOE fracture demonstrating regurgitation of contents due to blocked left naso-lacrimal duct ROPLAS positive

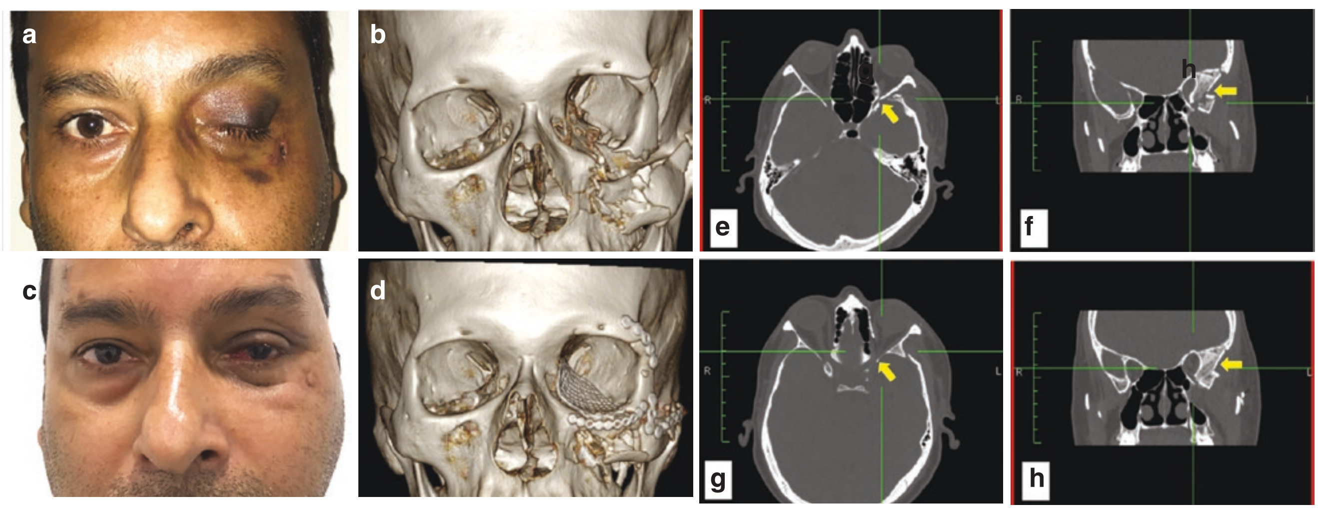

Fig. 57.18 Clinical pictures and CT scans of patient with orbital apex syndrome. (**a**) Clinical picture demonstrating left-sided orbito-zygomatic trauma with clinically evident ptosis, (**b**) 3D CT demonstrating comminuted zygomatico-orbital fracture with medial displacement of the greater wing of sphenoid, (**c**) clinical picture of patient 2 weeks post-surgery with resolution of ptosis, (**d**) post-operative 3D CT showing ORIF, (**e**) pre-operative axial CT demonstrating total compression of the left optic canal (yellow arrow), (**f**) pre-operative coronal CT demonstrating compression of the left superior orbital fissure (yellow arrow), (**g**) post-operative CT showing decompressed left optic canal (yellow arrow) and (**h**) post-operative coronal CT showing decompresison of the left superior orbital fissure (yellow arrow)

(vi) Impaired accommodation is because of impaired parasympathetic pathway to the ciliary ganglion.
(vii) Loss of corneal reflex due to lack of transmission via the nasociliary branch of ophthalmic nerve.
(viii) Proptosis either due to presence of hemorrhage or paresis and laxity of extraocular muscles which normally aid in globe retraction.

Management may be conservative or exploratory surgery of the orbit including surgical decompression [33].

57.6.2.6 Orbital Apex Syndrome (Fig. 57.18) (Box 57.5)

In severe orbital trauma, optic nerve may also be implicated due its close proximity to the superior orbital fissure [31, 34]. The term orbital apex syndrome was first coined by Kjaer in 1945 [35], and the symptoms include all features

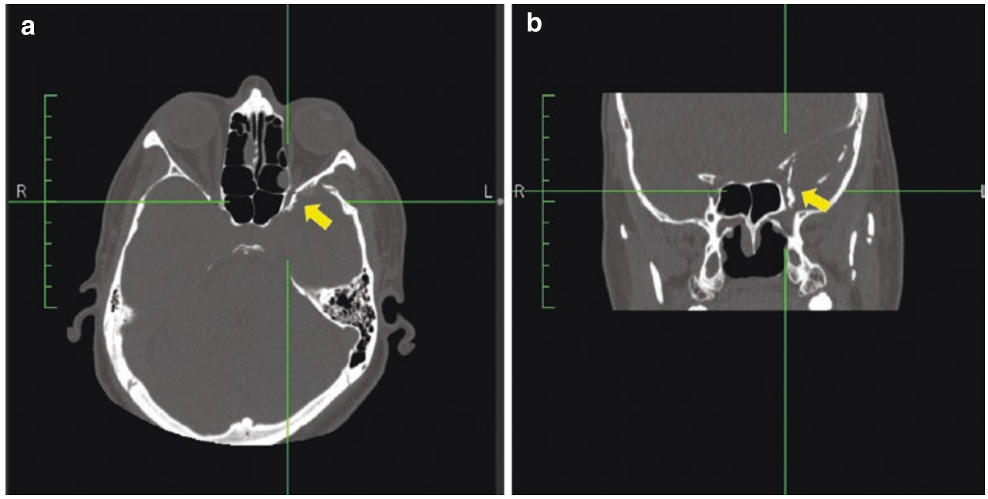

Fig. 57.19 (**a**, **b**) Axial CT scan of patient with direct traumatic optic neuropathy demonstrating a skull base fracture and bony spicule at the entry of the optic nerve into the canal

of superior orbital fissure syndrome along with partial or loss of vision.

57.6.2.7 Traumatic Optic Neuropathy (TON) (Box 57.5)

TON may be defined as an acute injury to the optic nerve with impairment of visual function. It may occur as a result of:

(i) Direct trauma to the optic nerve (Fig. 57.19) (physical damage or nerve sheath compression due to compartment syndromes)
(ii) An indirect insult due to diffuse axonal damage secondary to conduction of forces from blunt head trauma
The occurrence may be unilateral or bilateral.

Clinical features of TON include:

(i) Afferent pupillary defect
(ii) Diminished visual acuity
(iii) Diminished color perception
(iv) Varying reduction in visual fields

Management of TON is handled under the section of orbital emergencies.

Box 57.5 Comparison of Clinical Features of Traumatic Optic Neuropathy, Superior Orbital Fissure, and Orbital Apex Syndromes

Traumatic optic neuropathy (TON)	Superior orbital fissure syndrome	Orbital apex syndrome
Unilateral or bilateral	Ophthalmoplegia with involvement of cranial nerves III, IV, & VI	All features of superior orbital fissure syndrome
Relative afferent pupillary defect (RAPD) except in symmetrical bilateral cases	Forehead paresthesia	Partial or total loss of vison
Variable loss of visual acuity (from normal to no vision)	Ptosis	
Impaired color vision	Dilated pupil	
Variable visual field defects	Impaired direct but preserved consensual pupillary reflex. Impaired accommodation	
	Loss of corneal reflex	
	Proptosis	

57.6.3 Investigations

Conventional radiographs have a minimal role in the diagnosis and planning of orbital fractures. CT scans (Fig. 57.20a–c) have long been considered the “gold standard” in orbital trauma. The scans are usually ordered in fine cuts of 0.5 mm and taken in all the three planes. The coronal and the sagittal scans are important in the diagnosis

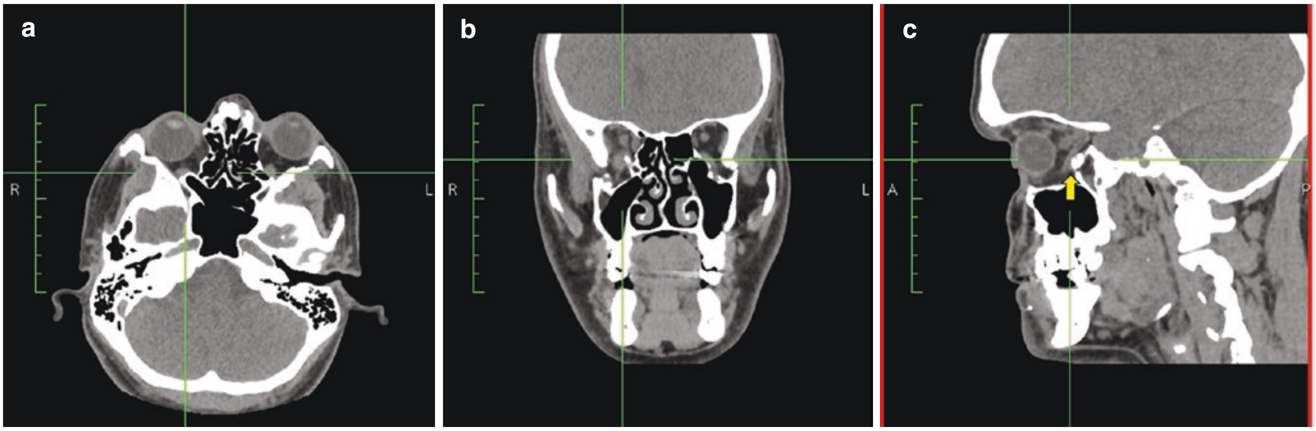

Fig. 57.20 CT scans showing (**a**) axial section with fracture of the medial wall of the right orbit, (**b**) coronal section showing fractures of the medial wall and floor, and (**c**) sagittal section showing fracture of the floor with fibrosis of the inferior rectus to the posterior ledge (yellow arrow)

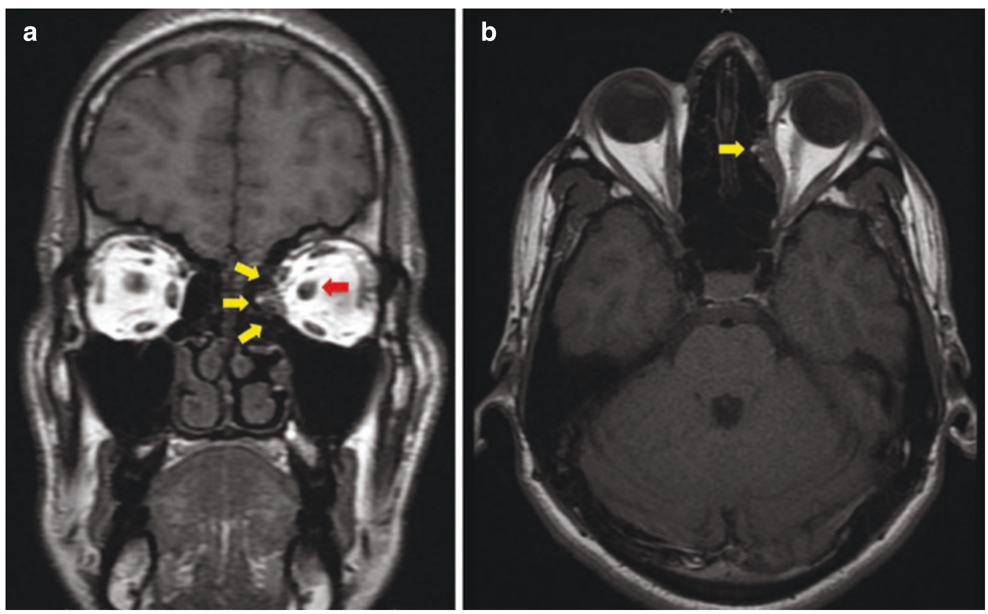

Fig. 57.21 MRI (**a**) coronal and (**b**) sagittal sections, demonstrating entrapment of the medial rectus (yellow arrows) and medial displacement of the optic nerve (left orbit)

of fractures of the floor and the roof, while the axial scans provide better information regarding the fractures of the medial and lateral walls. Axial sections are also important to study the optic canal integrity.

Indications for an MRI (Fig. 57.21a, b) scan are limited to determining soft tissue injuries and entrapment of muscles and to assessing damage to the optic nerve. It is also used to identify intra-orbital herniation of brain in the case of blow-in fractures.

57.7 Approaches to the Orbit

Box 57.6 Surgical Approaches to the Orbit

- Transcutaneous-medial and lateral
- Trans-caruncular
- Transconjunctival

57.7.1 Transcutaneous Approaches

1. Lynch
2. Extended glabellar approach
   (a). Lateral transcutaneous approaches
      (i) Lateral brow incision
      (ii) The upper lid blepharoplasty and the sub brow approaches
   (b). Lower eyelid approaches (Also refer Figs. 56.44, 56.45)
      (i) Sub-ciliary
      (ii) Sub-tarsal
      (iii) Infra-orbital (Video 57.1)

57.7.1.1 Lynch

This incision described by Lynch [36] in 1921 is a semilunar-shaped incision (Fig. 57.22a) placed between the nasal dorsum and the medial canthal ligament that provides direct access to the canthal apparatus and the medial orbital rim and wall. The major drawbacks of this particular incision are chances of developing a web and hence an unsightly scar. There may also be risk of damage to the medial canthal tendon and the lacrimal apparatus that is present infero-laterally. Recent modifications of the Lynch incision have accommodated options to reduce the scarring by the use of "Z" plasties (Fig. 57.22b, c) and other esthetic incision designs.

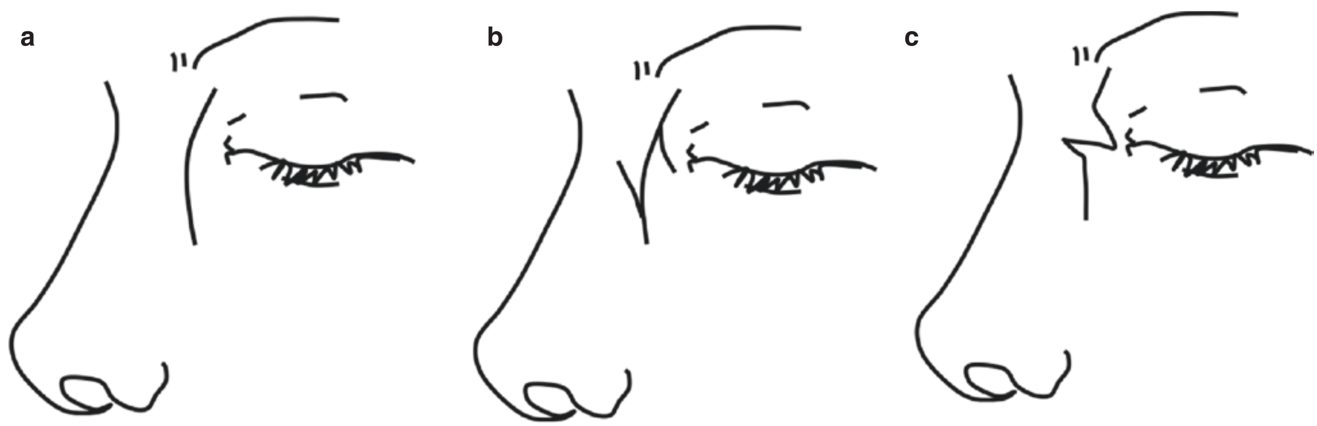

Fig. 57.22 Diagrammatic representation of the (**a**) classical Lynch incision and (**b, c**) modification with "Z" plasty

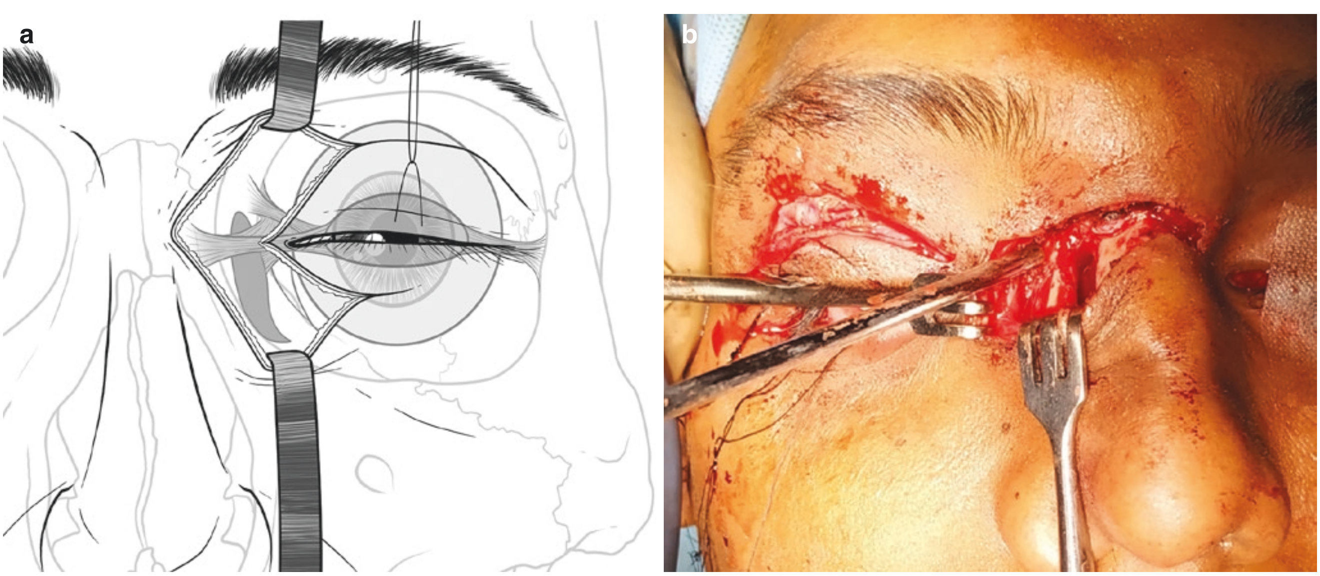

Fig. 57.23 Diagram and intraoperative picture showing extended glabellar approach to the medial orbit

57.7.1.2 Extended Glabellar Approach (Fig. 57.23)

The extended glabellar incision or a horizontal "Y" approach involves a small Y-shaped incision with the fork extending over the upper and lower lid crease with the long arm across the nasal dorsum over the glabellar region. This approach provides excellent access to the medial canthal tendon apparatus and also provides enough room for medial orbital wall exploration cephalad to the tendon.

57.7.2 Trans-caruncular Approach

The trans-caruncular route provides excellent exposure to the medial orbit without causing any esthetic concern. The caruncle is a papular structure seen medial to the plica semilunaris which is a fold of conjunctiva in medial canthal region. An avascular plane is located deep to the caruncle between the medial orbital septum and the Horner's muscle which on dissection exposes the medial wall of the orbit (Fig. 57.24a) [37].

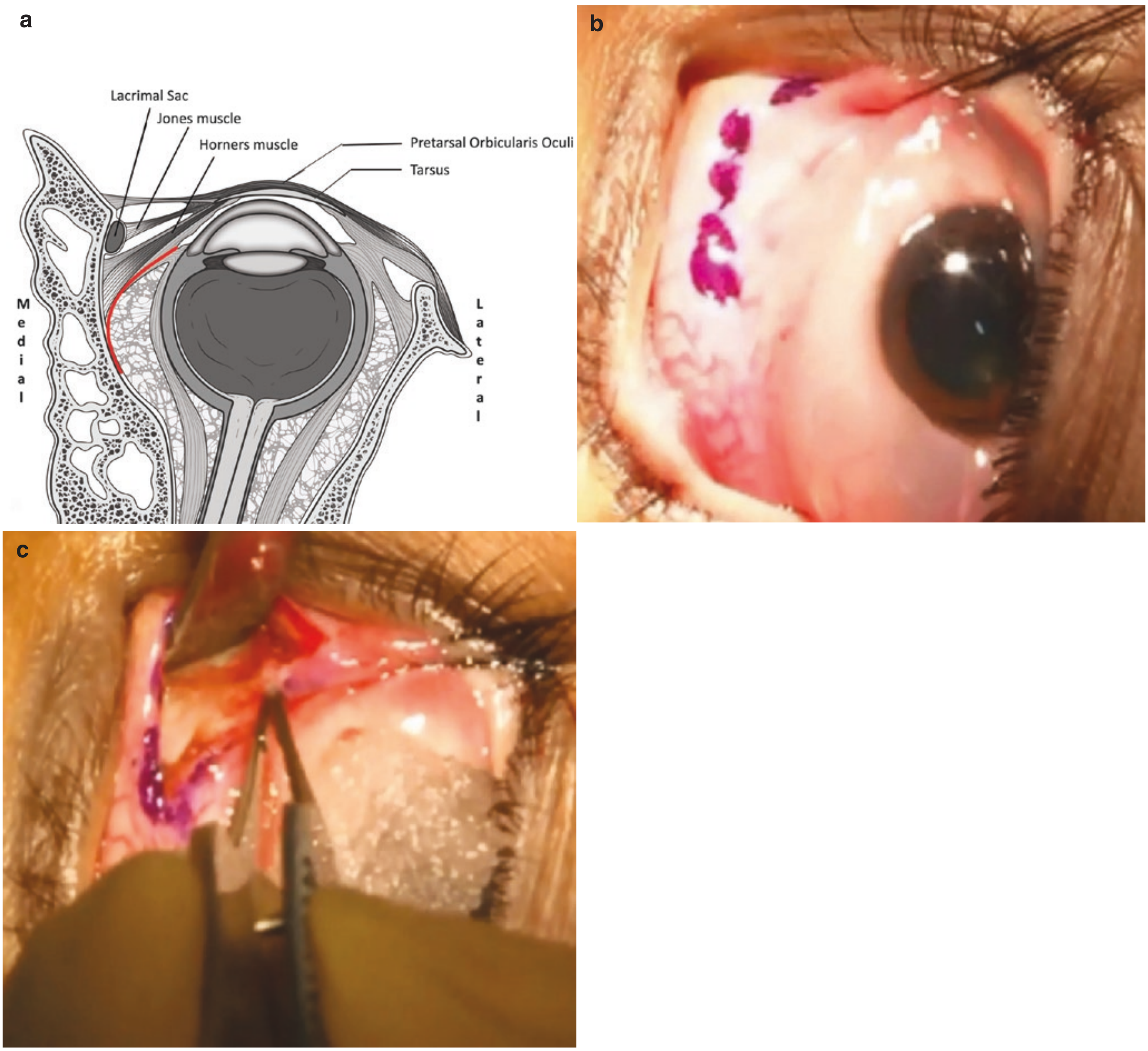

Fig. 57.24 (**a**) Diagram and (**b**) intraoperative pictures showing marking for trans-caruncular approach to the medial orbit and (**c**) exposure of the medial orbital wall. (Courtesy: Dept of Orbit & Oculoplasty, Shankara Nethralaya, Chennai)

After placing retraction sutures on upper and lower eyelids, gentle medial traction is applied over the skin of the nasal dorsum, and incision is placed lateral to the caruncle, while avoiding injury to the lacrimal puncta or canaliculi (Fig. 57.24b). The length of the incision is between 1.5 and 2.5 cm. Dissection through the fibers of the Muller's muscle exposes the medial wall just posterior to the posterior lacrimal crest (Fig. 57.24c). For additional exposure of associated orbital floor fractures, a C-shaped approach can be used including a transconjunctival incision with or without lateral canthotomy and inferior cantholysis in conjunction with the trans-caruncular approach.

As the lateral transcutaneous and lower lid approaches also find use in the management of fractures of the zygomatic complex fractures, they are discussed in detail in chapter on zygomatic complex fractures.

57.7.3 Transconjunctival Approach (Fig. 57.25)

The infra-orbital rim and orbital floor defects can be accessed through a transconjunctival incision (Video 57.2).

Its advantages include:

(i) Excellent cosmesis
(ii) Minimal incidence of ectropion
(iii) Extensive access up to 270° including the floor and medial and lateral walls, with the modifications to the conventional approach

A historical perspective of the description of the transconjunctival approach and its evolution into the most favored approach for access to the floor and medial wall of the orbit along with the infra-orbital rim is provided in Box 57.7.

Box 57.7 Evolution and Modifications of the Transconjunctival Approach

Author	Year	Description
Bourget J	1924	Conjunctival approach for blepharoplasty
Tenzel & Miller	1971	Post-septal approach
Tessier P	1973	Pre-septal approach
McCord & Moses	1979	"Swinging eyelid" with lateral canthotomy
Garcia GH	1998	Trans-caruncular approach

Pre-septal Approach (Fig. 57.26)

The incision is marked 2–3 mm posterior to the tarsal plate along the mediolateral length of the lower palpebral conjunctiva. Dissection is performed along the subconjunctival plane and is carried down toward the inferior orbital rim. This maintains the plane anterior to the orbital septum. Retraction sutures may be placed on the vestibular portion of the conjunctival flap with traction in superior direction, to provide additional protection to the globe. On reaching the facial surface of the infra-orbital rim, the periosteum is incised about

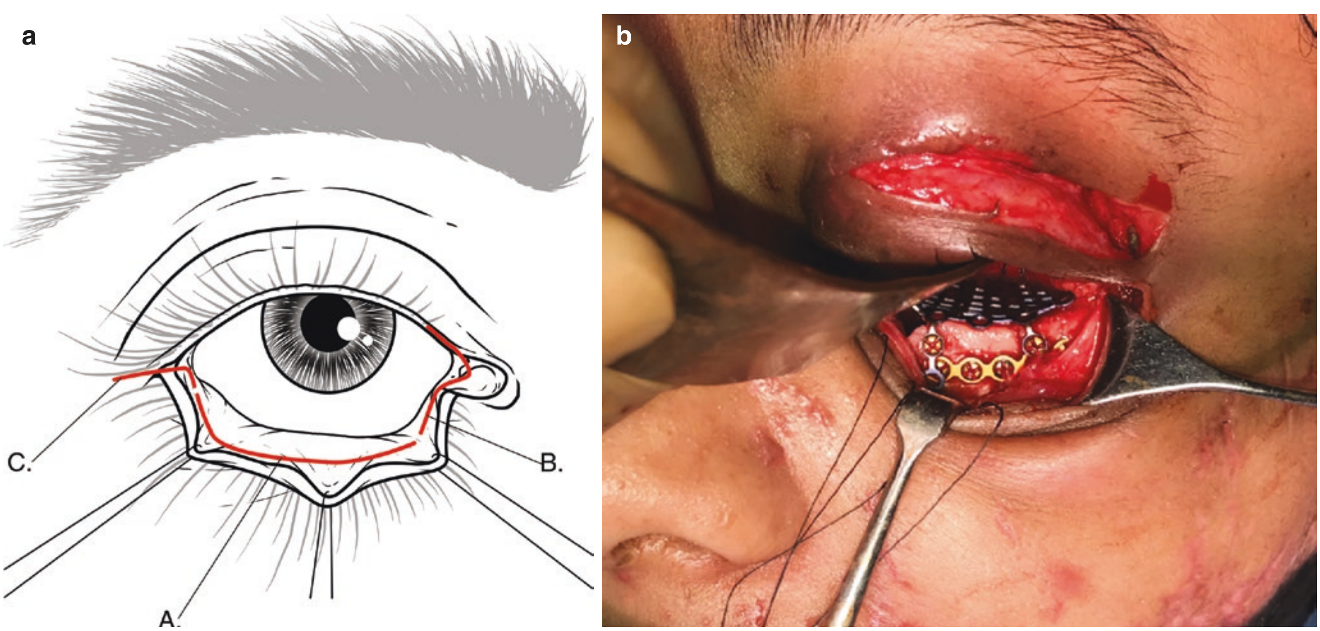

Fig. 57.25 (**a**) Diagram showing trans-conjunctival approach and its modifications - A. Transconjunctival, B. Trans-caruncular & C. Lateral canthotomy. (**b**) Intra-operative picture of trans-conjunctival with the lateral canthotomy modification. The picture also shows an upper lid blepharoplasty incision used to access the fronto-zygomatic suture

2 mm inferior to the rim. This is followed by subperiosteal dissection and exploration of the orbital floor by retracting the globe and orbital contents superiorly. Approximately 2–3 mm distance must be maintained from the lower end of the tarsal plates while making the initial conjunctival incision failing which there is vertical shortening of the lower eyelid and entropion post-operatively.

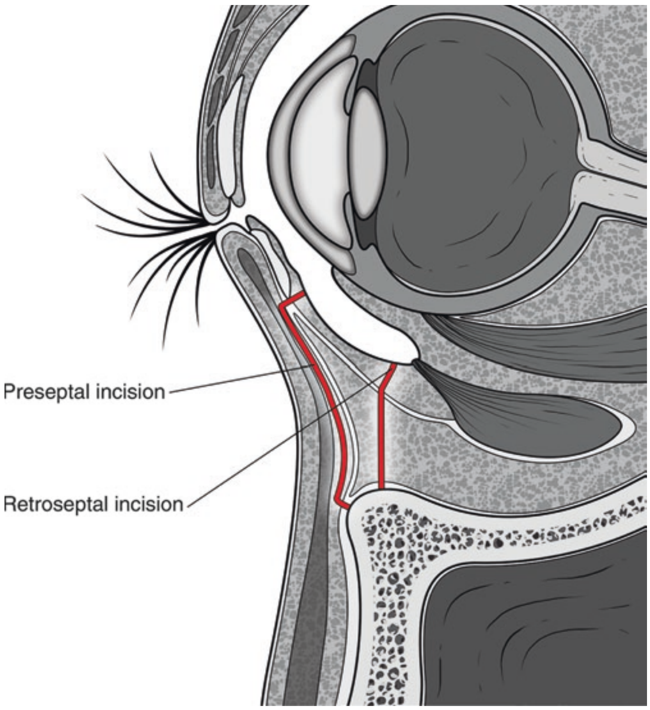

©Association of Oral and Maxillofacial Surgeons of India

Fig. 57.26 Diagrammatic representation of the pre-septal and retro-septal modifications of the transconjunctival approach

Retroseptal Approach (Fig. 57.26)

In the retroseptal type, the conjunctival incision is made near the fornix spanning mediolaterally just short of the caruncle. Dissection is posterior to the orbital septum providing a fast and direct access to the floor when compared to the pre-septal type [38]. However, orbital fat is encountered before approaching the orbital floor, which may prove bothersome for dissection and manipulation. The periorbita is incised immediately posterior to the rim after superior retraction of the fat and globe with a malleable retractor. This is followed by subperiosteal dissection and exploration of the floor defect. Excessive manipulation of the orbital fat during orbital reconstruction increases the risk of enophthalmos due to fat disintegration [39, 40]. Placement of the incision too low into the fornix may damage the inferior oblique muscle and retractors of the lower eyelid, compromising esthetics post-operatively due to lower lid entropion.

57.7.4 Trans-antral Endoscopic-Assisted Approach (Fig. 57.27a, b)

The trans-antral approach was attempted by Converse and Smith [41] as early as the 1960s. Entry to the antrum is gained through a transoral Caldwell Luc procedure and a 0° or 30° endoscope may be used to visualize the orbital floor.

57.7.5 Coronal Approach

The coronal approach offers the most extensive exposure of the entire upper and middle third of the face including the orbit. A detailed description of the same is provided in Chap. 85 on access osteotomies.

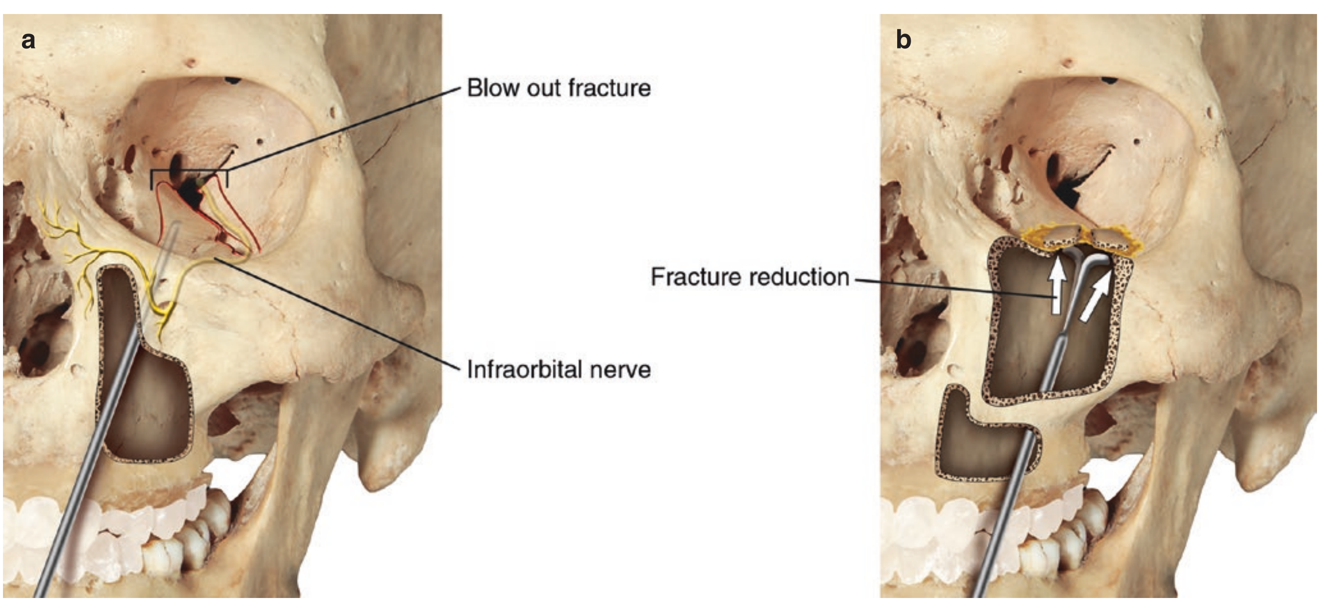

©Association of Oral and Maxillofacial Surgeons of India

Fig. 57.27 (**a**, **b**) Diagram of the trans-antral endoscopy assisted approach to the orbital floor

57.8 A Clinical Sequence for Treatment Planning and Management of Orbital Fractures

A clear understanding of the various patterns of orbital fractures and their clinical implications is absolutely necessary to design and formulate a plan for their reconstruction. The basic management guidelines for the common variations in orbital fractures are detailed below (see Hammer [7] classification, Fig. 57.9).

57.8.1 Type I (Orbito-Zygomatic)

Concomitant fractures of the zygomatic complex and the orbit mandate ORIF of the zygomatic complex first, followed by internal orbital reconstruction. This sequence is favored because the orbital rims provide the most accurate guidance for restoration of the internal orbital architecture.

Box 57.8 The Surgical Objectives for Type I Fractures

- Restoration of transverse dimension of the face, malar prominence, and the arch anatomy
- Restoration of rim architecture
- Correction of orbital dystopia
- Correction of the axis of the palpebral fissure and
- Reconstruction of the internal orbit

Figures 57.28a–d and 57.29a–d demonstrate a type I fracture managed using the above principles.

Fig. 57.28 3D CT scans of patient with orbito-zygomatic fracture. (**a** and **b**) Pre-operative frontal and basal views demonstrating the fracture, (**c** and **d**) post-operative frontal and basal views demonstrating fixation of fractures

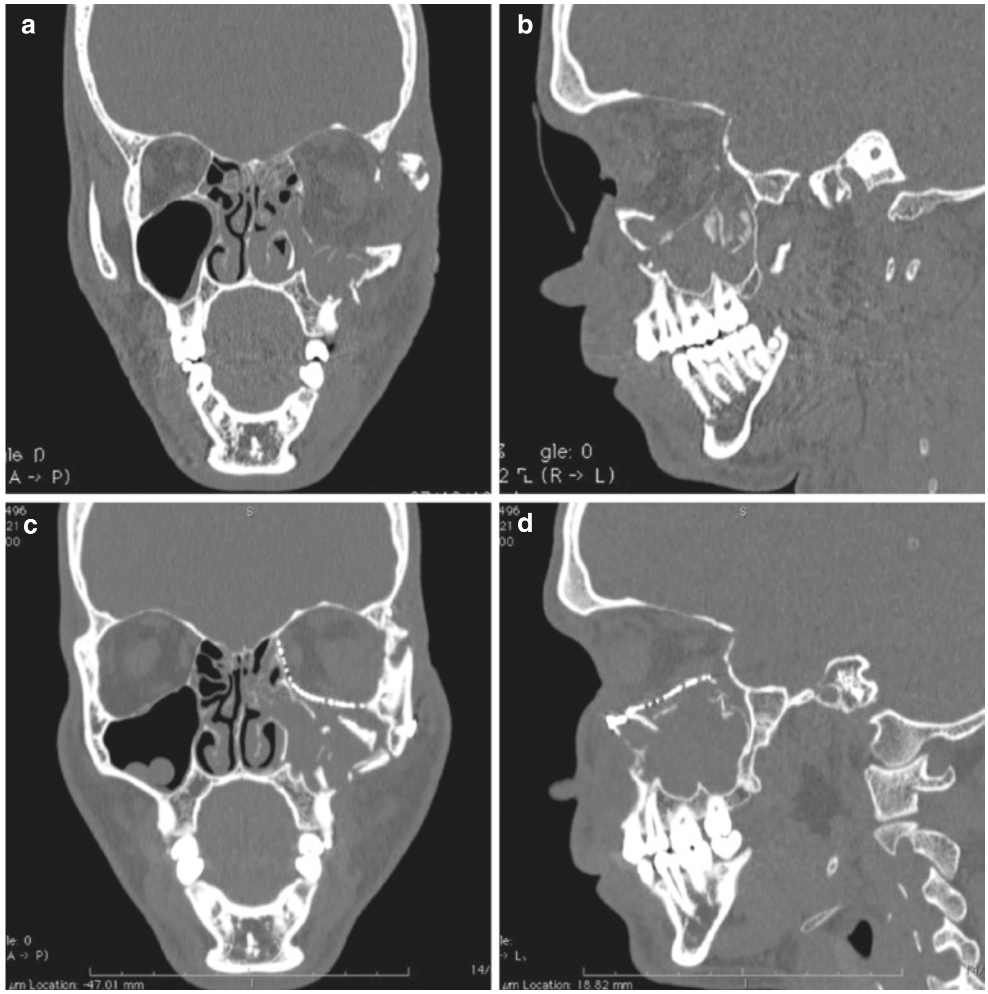

Fig. 57.29 Axial and sagittal scans of the patient in Fig 57.28, with orbito-zygomatic fracture. (**a** and **b**) Sections demonstrating fracture of the left zygomatic complex with a large defect of the orbital floor. (**c** and **d**) Post-operative sections revealing optimal reduction of the fracture and floor reconstruction with anatomical orbital floor implant

57.8.2 Type II (Internal Orbital)

Management of type II orbital fractures, which are essentially the internal fractures (both blow-in and blowout) of the orbit including (1) the roof, (2) the floor, and (3) the medial and (4) lateral walls are detailed below.

> **Box 57.9 The Management of All Internal Orbital Fractures Can Be Handled Essentially by Answering the Following Basic Questions** *(Clinical Tip)*
>
> (i) Is there a need for intervention?
> (ii) When is the best time to intervene?
> (iii) Is there a need for reconstruction?
> (iv) What to use for reconstruction?

57.8.2.1 Fractures of the Orbital Roof

Isolated fractures of the orbital roof are extremely rare. They usually occur as a part of fronto-basilar fractures, fractures of the frontal sinus, or may occur concomitant with fractures of the supraorbital rim. Orbital roof fractures are present in approximately 5% of all orbital and cranial fractures, while incidence of isolated orbital roof fractures may be as low as 0.7% of all orbital and cranial fractures. The most common etiological factors include motor vehicle accidents, assaults, or falls.

Orbital roof fractures may be associated with more severe neurological symptoms including dural tears, CSF leak, tension pneumocephalus, diffuse cerebral edema, and contusions of the frontal lobe [42]. It is imperative for a neurological and ophthalmological consult prior to management.

In general, orbital roof fractures may be categorized into four types (Fig. 57.30).

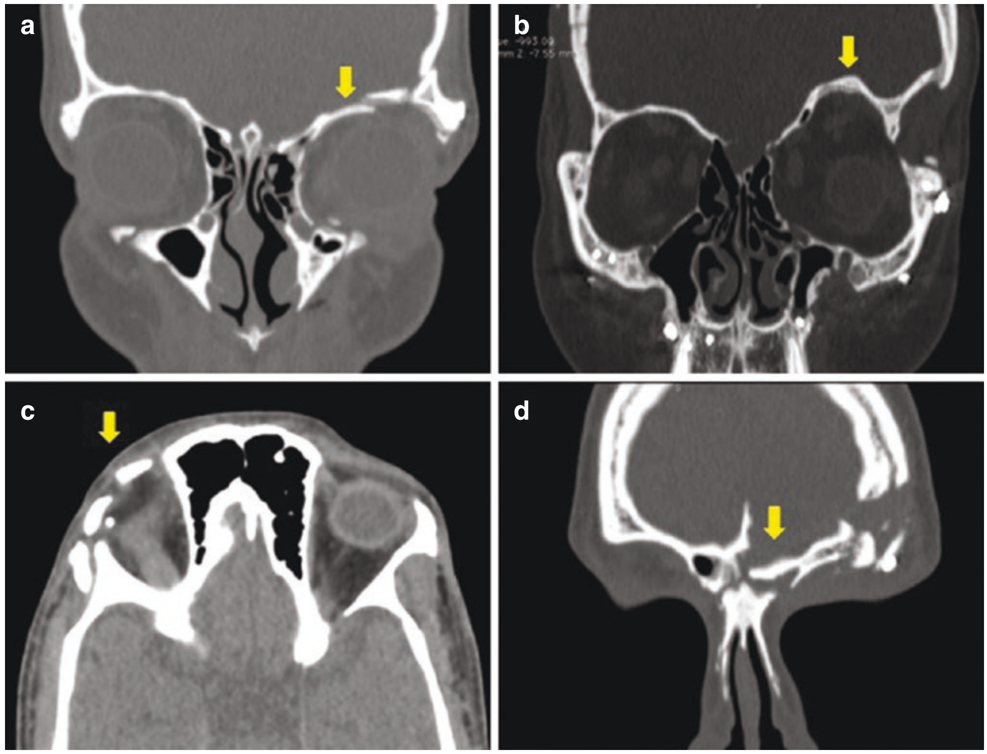

Fig. 57.30 CT scan images showing types of roof fractures (**a**) blow-in fracture, (**b**) blowout fracture, (**c**) fracture of the supraorbital rim, and (**d**) fronto-basilar fracture

- I—Blow-in fractures of the orbital roof where there is caudal displacement of the orbital roof with or without herniation of the brain. These may be undisplaced or displaced fractures. Comminuted fractures may leave fragments within the orbital cavity and may produce functional deficits with ophthalmic signs including restriction of extraocular muscle movement, diplopia, ptosis, and even blindness. These are generally caused due to increase in the intra-cranial pressure secondary to injuries.
- II—Blowout fractures of the orbital roof where there is cephalad displacement of the orbital roof into the cranial cavity due to increased intra-orbital pressure pushing the roof above. These injuries may be associated with neurological symptoms.
- III—Fractures involving the supraorbital rim. These may be seen as impure fractures of the orbital roof with an associated fracture of either a blow-in or a blowout nature.
- IV—Fractures involving the frontal sinus and the fronto-basilar complex. These fractures are more severe in nature and may often be associated with severe neurological implications.

Less than 10% of orbital roof fractures may need any form of surgical intervention [42]. Most are amenable to conservative management with observation and follow-up of neurological and ophthalmic status.

The need for management of fractures of the orbital roof may depend on:

(i) The presence of CSF leak which may need to be addressed
(ii) The necessity to retrieve displaced intra cranial fragments
(iii) Ophthalmic signs with compromise on vision
(iv) Large displacement of fragments which may act as mechanical impediments or significantly alter intra-orbital volume producing enophthalmos or exophthalmos.

Interventions may be indicated immediately or late primary depending on the indications mentioned above. Reconstruction of the roof of the orbit is not a procedure routinely indicated. However in cases where there is an absolute necessity for reconstruction like prevention of brain herniation or restoration of intra orbital volume which has been significantly altered, the choice may vary between the use of titanium meshes (Fig. 57.31) or porous polyethylene implants fixed with micro-screws to split calvarial grafts.

Figure 57.32a–f demonstrates the management of a malunited fronto-basilar fracture along with a blow-in fracture of the orbital roof compressing the eyeball producing restriction of movement.

57.8.2.2 Fractures of the Lateral Orbital Wall

Lateral orbital walls are the strongest of all the orbital walls [43]. The lateral wall generally shows diastasis and displacement in the case of fractures involving the zygomatico-orbital complex and is restored to its normal anatomy when the reduction of the zygomatic complex is achieved [44]. However this wall gets comminuted in high-velocity injuries [45] necessitating reconstruction in the primary intervention.

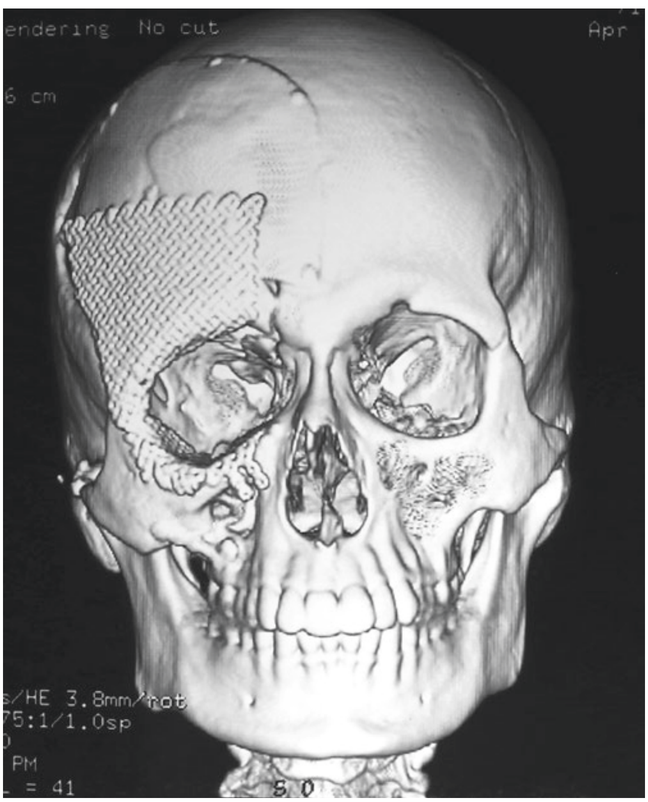

Fig. 57.31 Reconstruction of complex defect of the frontal bone, orbital roof, and supraorbital rim with a titanium mesh

The anatomy of the lateral wall plays an important role in the internal orbital volume as demonstrated by development of enophthalmos in unrestored lateral wall fractures [46]. Restoration of the architecture or augmentation of the same ensures correction of enophthalmos.

> Reconstruction of the lateral orbital walls is usually accomplished with the use of:
> (i) Alloplasts including titanium meshes, porous polyethylene sheets, and custom-made polyether ether ketone (PEEK) implants
> (ii) Bone grafts which may be harvested from either the calvarium or ilium

Figure 57.33a, b demonstrates the management of fracture of the lateral walls of the orbit in a patient with concomitant fracture of the zygomatic complex.

57.8.2.3 Medial Wall Fractures

The medial wall and the floor are the thinnest walls of the orbit and have the propensity to fracture the most [47, 48]. Though the incidence of concomitant fractures of the medial wall with that of the orbital floor have been reported over a wide range of 5–71%, its occurrence in isolation is very rare. Most fractures of the medial wall are incidental findings when CT scans are obtained to study other cranial, facial, or orbital fractures.

The most common type of clinical presentation would either involve a combination of the medial wall and floor (36%) or medial wall, floor, and zygomatic complex (28%) [49–51].

Fractures of the medial wall were managed conservatively in the past, but current literature proposes clear indications [49–51] for the exploration and reconstruction of the medial wall fractures and defects, which include:

1. Restriction of ocular motility
2. Diplopia
3. Clinically significant enophthalmos

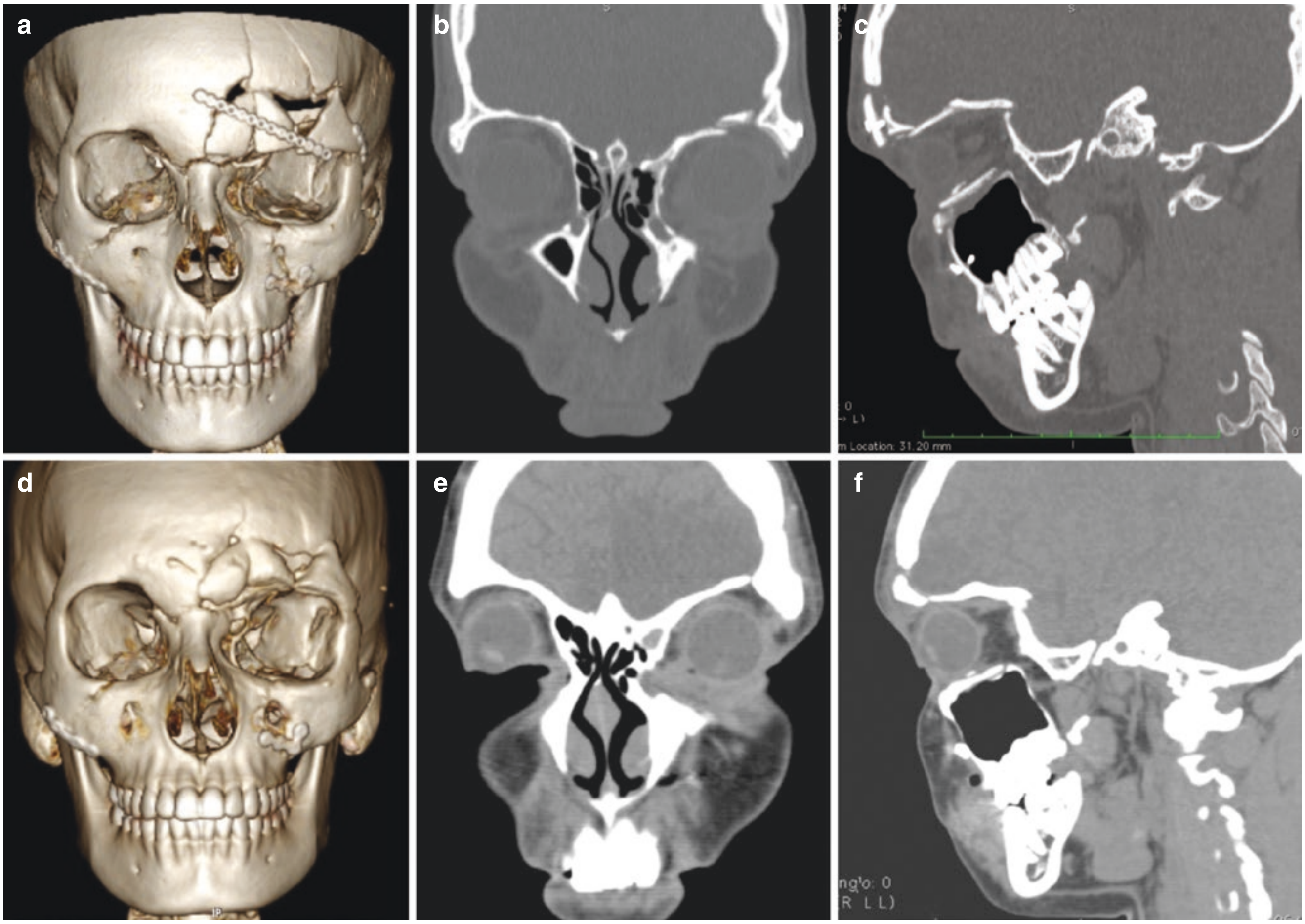

Fig. 57.32 CT images of patient with malunited fractures of the orbital roof. (**a**–**c**) Pre-operative images demonstrating malunited fracture of the frontal bone and orbital roof of the left side with decrease in intra-orbital volume and compression on the globe. (**d**–**f**) Post-operative images showing recontouring of the supraorbital rim and roof using ultrasonic aspirator system, with resultant expansion of the intra-orbital volume

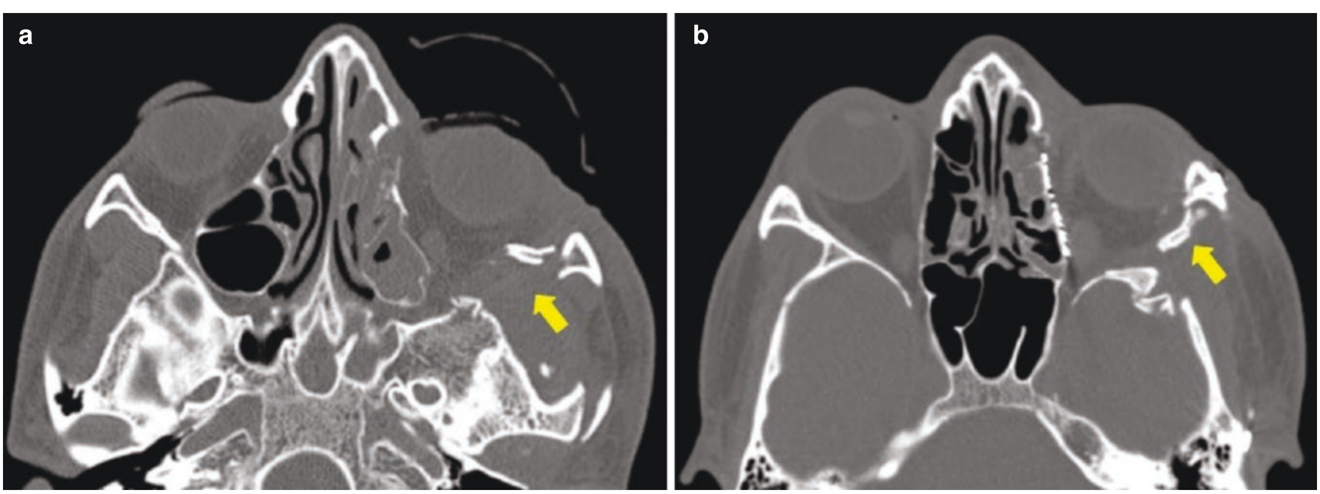

Fig. 57.33 CT scan images of lateral orbital wall with concomitant fracture of the zygomatic complex. (**a**) Pre-operative image showing fracture and displacement of the lateral wall and (**b**) post-operative image showing reduction of the lateral wall and re-establishment of the sphenozygomatic suture continuity

Box 57.10 A Clinically Useful Classification of Medial Wall Fractures Has Been Described by Nolasco et al. [47] in 1995 Based on CT Scan Findings

They describe four patterns of presentations (Fig. 57.34)

- Type I: Isolated medial wall fractures
- Type II: Fracture involving the medial wall and the orbital floor
- Type III: Fractures involving the medial wall, floor, and the zygomatic complex
- Type IV: Medial wall plus complex fractures of the face (maxillary, NOE, etc.)

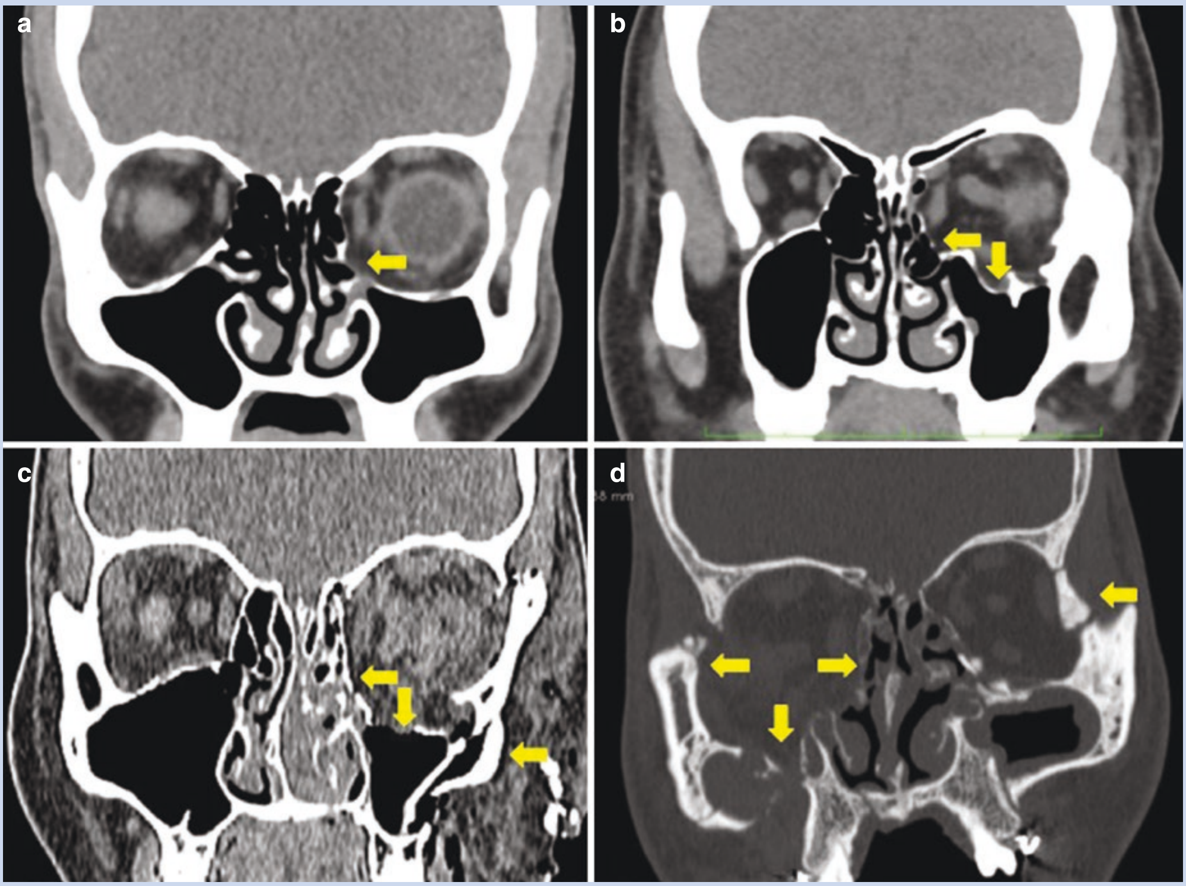

Fig. 57.34 CT scans showing types of medial wall fractures. (**a**) Isolated medial wall fracture; (**b**) fracture of medial wall with floor; (**c**) fracture involving medial wall, floor and zygomatic complex; and (**d**) concomitant fractures of the medial wall, floor, and midface at LeFort 3 level

Contrary to earlier belief the loss of medial wall integrity also significantly contributes to development of enophthalmos [49]—with any defect involving an area of more than 1.9 cm^2 or volume expansion of excess of 0.9 ml [50, 51] producing clinically significant enophthalmos (2 mm or more).

Approaches to the medial wall have already been described in detail earlier. The most favored being the transcaruncular/retro-caruncular approaches which give excellent exposure and access to the medial wall for both exploration and reconstruction [37, 52].

Options for reconstruction include a multitude of materials which may be autogenous or alloplastic as shown in Table 57.1. Bioactive resorbable sheets are also found to produce good outcomes [53].

Figure 57.35a, b demonstrates reconstruction of a medial wall fracture with a Titanium mesh.

57.8.2.4 Orbital Floor Fractures

The fractures involving the orbital floor are the most common fractures of the internal orbit either in isolation or concomitant with other facial fractures. A comprehensive classification of floor fractures with clinical guidelines for management is described by Jaquiery [54] et al. which lays emphasis on the morphology of the defect and the role of the infero-medial strut of the inferior orbital fissure.

The internal orbit is divided into three zones which helps in evaluating the difficulty of approach and exposure:

(i) Anterior third
(ii) Middle third
(iii) Dorsal third

Table 57.1 Commonly used biomaterials for orbital reconstructions

Material	Stability / fixation (S/F)	Contouring	Biological behavior	Permeability for inflammatory exudate	Donor site morbidity	Radio-opacity	Availability
Titanium	S+++ F++	++	++ (allows tissue in-growth)	+	+	+	+
Bone graft	S++ F+	-	+++	-	-	+	+/–
Porous polyethylene	S+/– F+/– (when thin)	+	++ (allows tissue in-growth)	–	+	-	+
Composite porous polyethylene/Ti	S++ F++	+	++ (allows tissue in-growth)	–	+	+	+
Resorbable (PLLA)	S+/– F+/–	+	+ (inflammatory response)	(non-perforated)	+	–	+
Pre-formed anatomical implant	S+++ F++	+++ (minimal contouring needed)	++ (allows tissue in-growth)	+	+	–	+

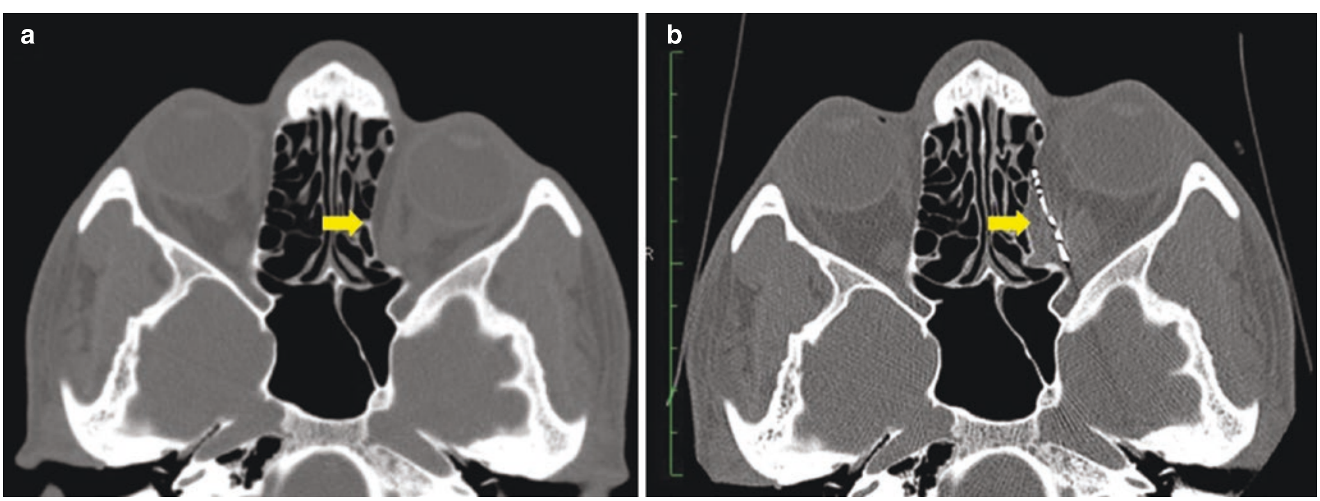

Fig. 57.35 CT images of patient with medial wall fracture. (**a**) Fracture of the medial orbital wall of the left orbit showing displaced medial rectus. (**b**) Post-operative image demonstrating medial orbital reconstruction with titanium mesh

Table 57.2 The classification of orbital wall defects (Jaquiery et al. modified by Dubois et al.) [53–55]

Category of fracture	Complexity of reconstruction	Defect description	Clinical finding
I	Low	Isolated defect of floor or medial wall, 10–20 mm^2 within zone 1 or 2	
II	Moderate	Defect of floor and/or medial wall >20 mm^2 within zone 1 and 2	Bony infero-medial strut of the inferior orbital fissure present
III	High	Defect of floor and/or medial wall >20 mm^2 within zone 1 and 2	Infero-medial strut of inferior orbital fissure absent
IV	High	Defect of the entire orbital floor with medial wall involving zone 3	Infero-medial strut of inferior orbital fissure absent. The posterior ledge of the floor also may be absent

The fractures themselves are then classified into four categories of defects (Table 57.2; Fig. 57.36a–d).

Which Fractures of the Orbital Floor Need Intervention?

Indications and contraindications for floor exploration and repair are well defined.

Absolute Indications

1. Acute injury to the orbit showing evidence of immediate clinical enophthalmos and/or hypophthalmos [55] (Fig. 57.15), necessitating a primary surgical intervention. Post-surgical outcome may get compromised with delay due to progressive atrophy of intra-orbital fat.
2. Severe restriction of ocular motility with CT or MRI evidenced muscle entrapment or incarceration of periorbital soft tissue.

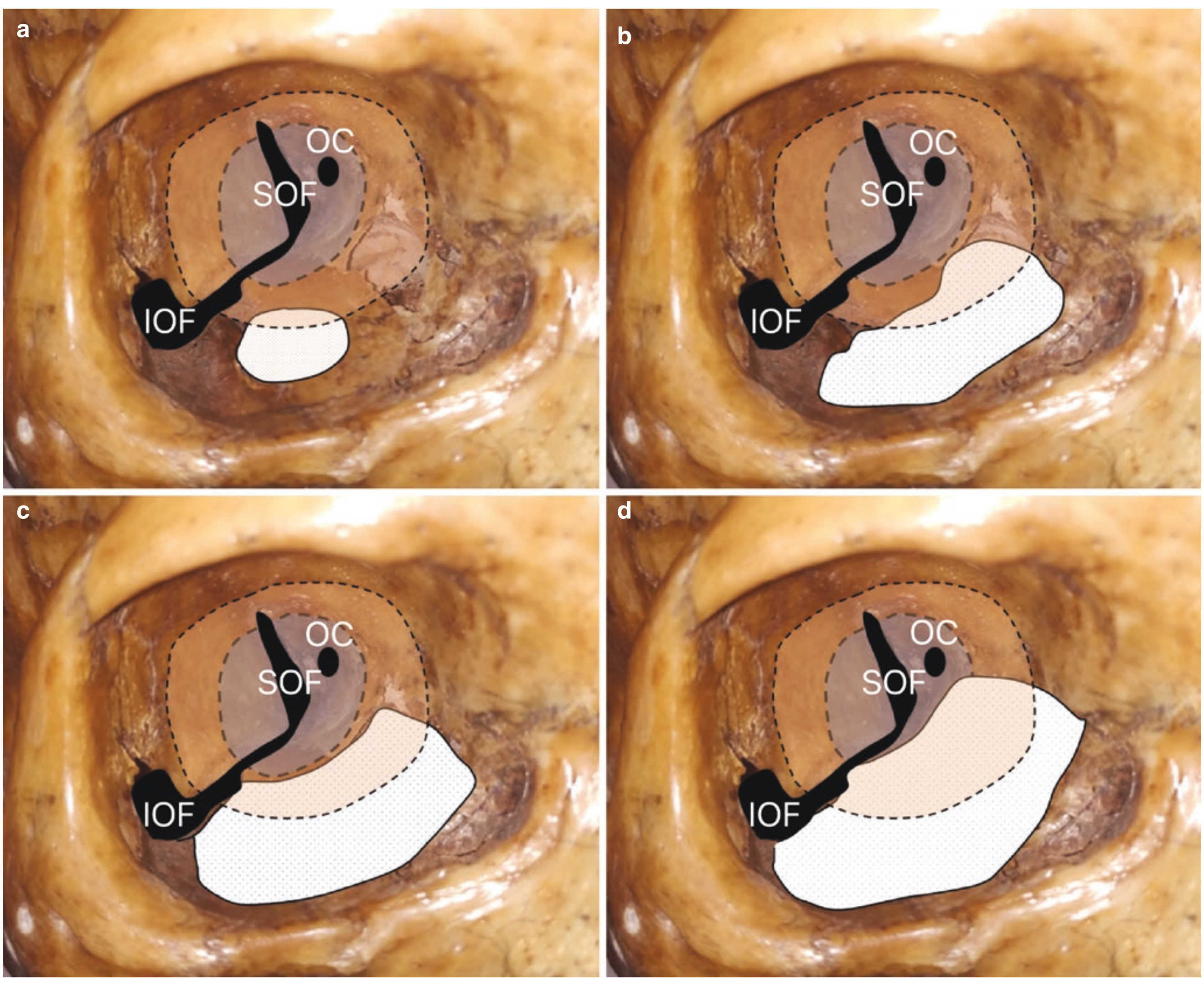

Fig. 57.36 Diagrammatic representation of the different types of defects of the orbital floor which indicate the grades of difficulty to reconstruct. (**a**) Type I, (**b**) Type II, (**c**) Type III and (**d**) Type IV

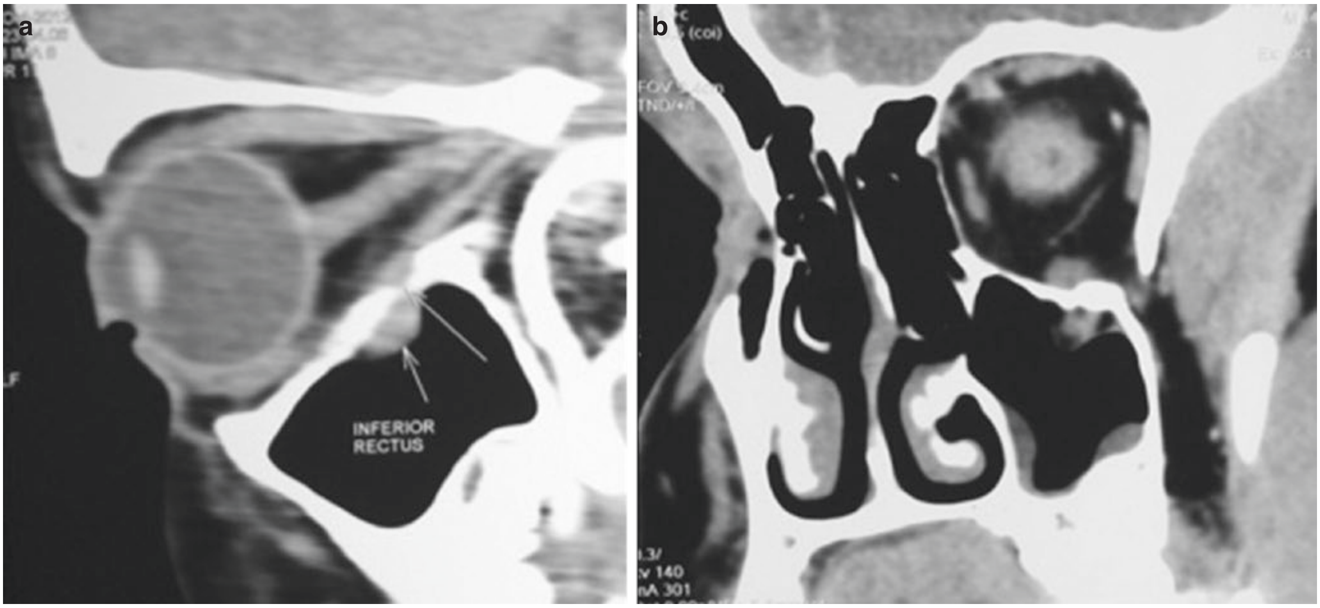

Fig. 57.37 CT scan images of a young boy with history of orbital trauma. (**a**) Sagittal and (**b**) coronal sections demonstrating a "springing trapdoor" fracture of the orbital floor on the left side with entrapped inferior rectus muscle. (Courtesy: Dept of Orbit & Oculoplasty, Shankara Nethralaya, Chennai)

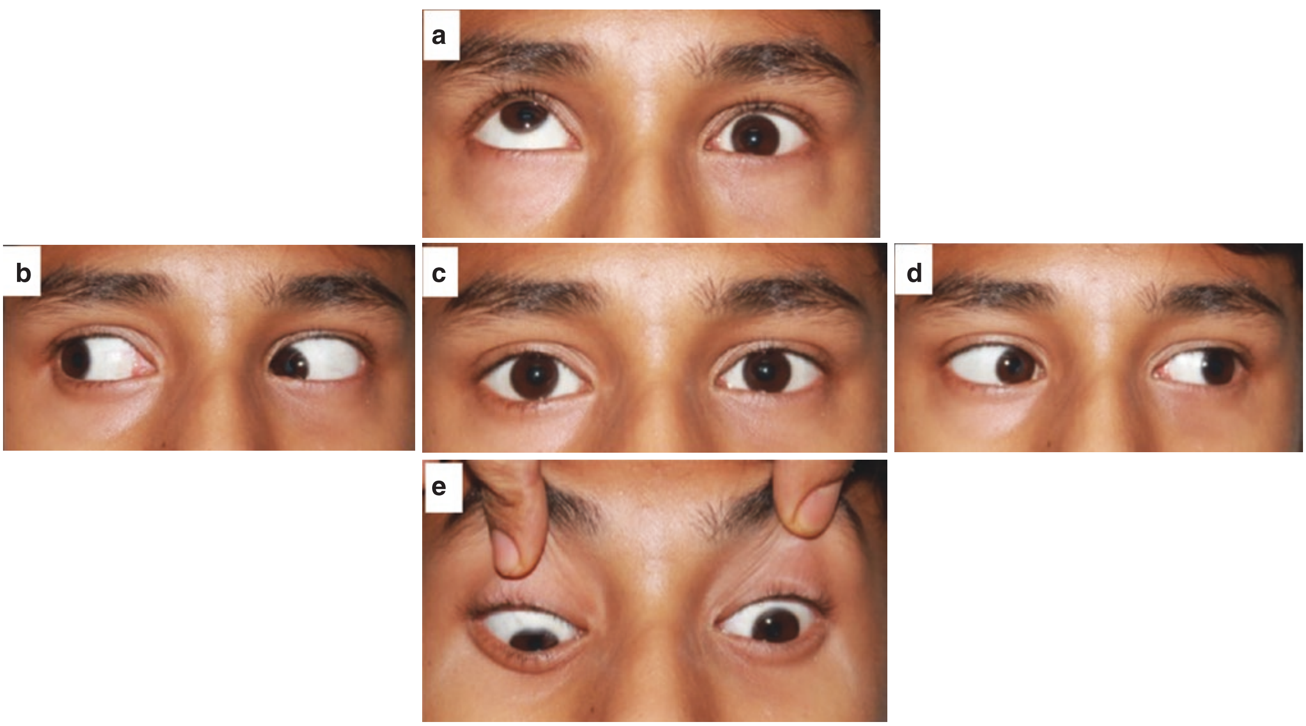

Fig. 57.38 Clinical photographs of a boy with "White eye blowout" fracture, showing restriction of ocular motility in the left eye in the superior (**a**) and inferior (**e**) gazes. The other gazes (**b**, **c** and **d**) show no abnormalities. (Courtesy: Dept of Orbit & Oculoplasty, Shankara Nethralaya, Chennai)

3. "White eye blowout" fracture in a child or young adult with severe restriction of ocular motility (Figs. 57.37a, b and 57.38) and vagal symptoms.

Relative Indications

1. Defects of the orbital floor often larger than 50% of the orbital floor area or greater than 20 × 20 mm of defect size especially in the zone between the floor and the medial wall (Fig. 57.39a).
2. Diplopia which is non-resolving and persistent for more than 2 weeks due to entrapment or fibrosis of orbital soft tissue (Fig. 57.39b) [56, 57].

Relative Contraindications

1. Associated ophthalmic injuries like retinal tears, hyphema, displacement of lens, ruptured globe, avulsion injuries of the globe, etc.
2. Loss of vision in one eye with the only seeing eye involved in a fracture

Figure 57.40a–f demonstrates the delayed management of a patient with an isolated fracture of the floor and medial walls. The CT scan shows fibrosis and adhesion of the inferior rectus muscle to the residual posterior ledge producing diplopia and restriction in superior gaze.

Surgery for Special Indications in Orbital Floor Fractures

Enophthalmos

Enophthalmos is the displacement of the eyeball in a posterior direction and is attributed to increase in the intra-orbital volume. Numerous studies have shown that there is a correlation between increase in intra-orbital volume and the presenting enophthalmos. It is proved that an increase in intra-orbital volume by 0.5–1 cc would produce posterior displacement of the globe by 1 mm. Enophthalmos of 2 mm or more may be clinically perceivable and warrant surgical intervention [58, 59]. An important aspect of orbital reconstruction lies in the fact that it is the only fracture in CMF region where the onus is not in recreating the anatomical form but rather in the restitution of the intra-orbital volume. Care should be taken to reconstruct the posteromedial aspect of the orbit (Hammer's key area) to achieve anterior projection of the globe. It is imperative to understand that reconstruction of the floor posterior to the equator of the globe influences anterior projection of the globe, while reconstruction of the equatorial region of the floor influences only the supero-inferior position of the globe (Fig. 57.41).

Figure 57.42a–d shows a case of delayed correction of enophthalmos in a patient with an orbital floor fracture.

Hypophthalmos

This is otherwise called hypoglobus and signifies the downward displacement of the globe due to the interruption in the anatomical integrity of the orbital floor. The clinical presence of hypoglobus needs to be differentiated from orbital dystopia which essentially means that the entire bony orbit with its contents is displaced caudally, unlike hypophthalmos, where only the globe is displaced caudally.

However decision-making for surgical intervention based on both enophthalmos and hypophthalmos is challenging as they may or may not present immediately following trauma. (Refer to clinical scenario 1. Figs. 57.57, 57.58 and 57.59).

Diplopia

Clinically demonstrable double vision is termed diplopia. Generally post-traumatic diplopia due to edema and hemorrhage is self-limiting and shows spontaneous resolution.

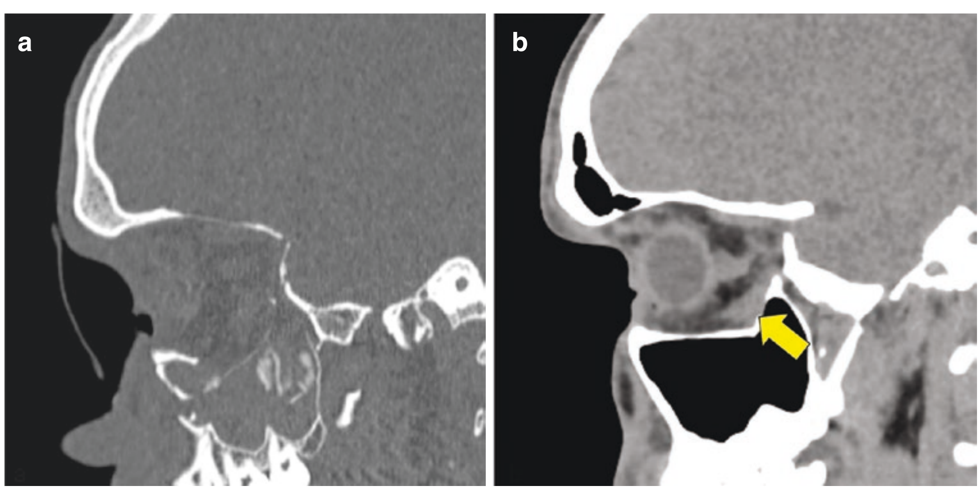

Fig. 57.39 (**a**) Sagittal section CT demonstrating large defect of the orbital floor. (**b**) Sagittal section CT demonstrating fibrosis and adhesion of the inferior rectus (yellow arrow) to the posterior ledge of the orbital defect

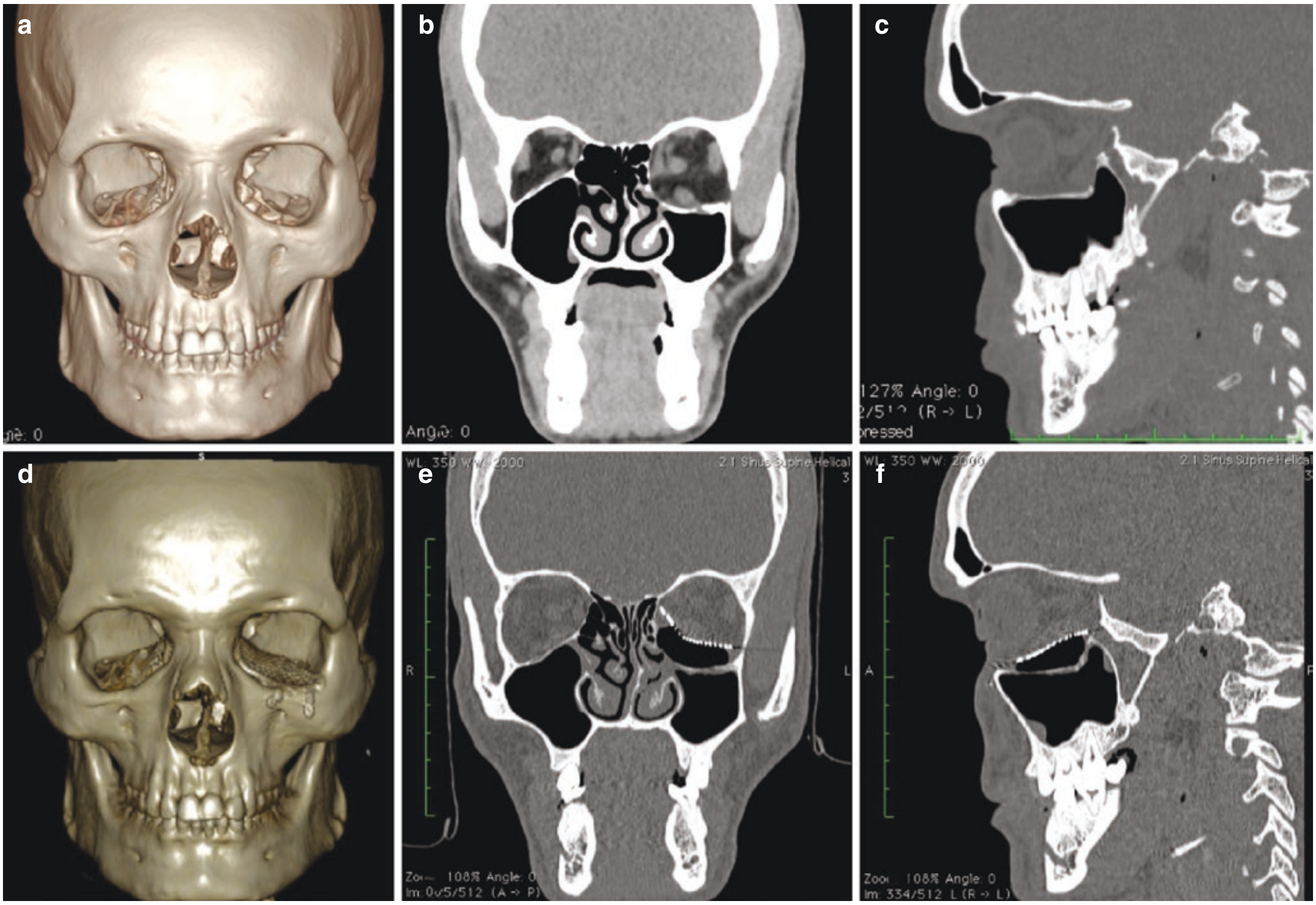

Fig. 57.40 CT scan images of patient with internal orbital fracture. (**a**–**c**) 3D, coronal, and sagittal images demonstrating isolated fracture of the left orbital floor and medial wall. (**d**–**f**) post-operative images demonstrating reconstruction of the defect with anatomical orbital implant

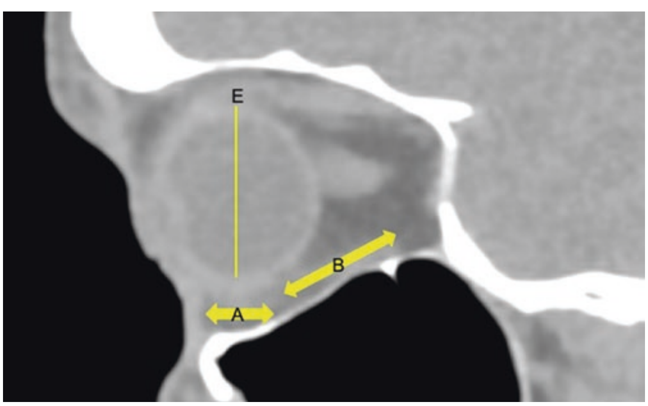

Fig. 57.41 Graphical representation of the equator of the globe (E) and the associated equatorial (A) and post-equatorial (B) zones of the floor

Diplopia can manifest in two forms:

(i) Monocular (diplopia present when seeing through one eye with the other eye closed) which is of more concern where the pathology is generally due to an ophthalmic problem (corneal, retinal, etc.) or neurological where the problem may be due to the optic nerve or the optic disk being injured.

(ii) Binocular diplopia (diplopia present only when seeing with both eyes, while absent on seeing with one eye) with CT proven muscle entrapment is seen as an indication for immediate intervention. However, it may also be attributed to other reasons including (a) intra-orbital edema or hemorrhage, physical bony spicules or fragments acting as impediments following trauma, (b) entrapment of the periorbita, and in rare cases (c) large changes in intra-orbital volume including massive

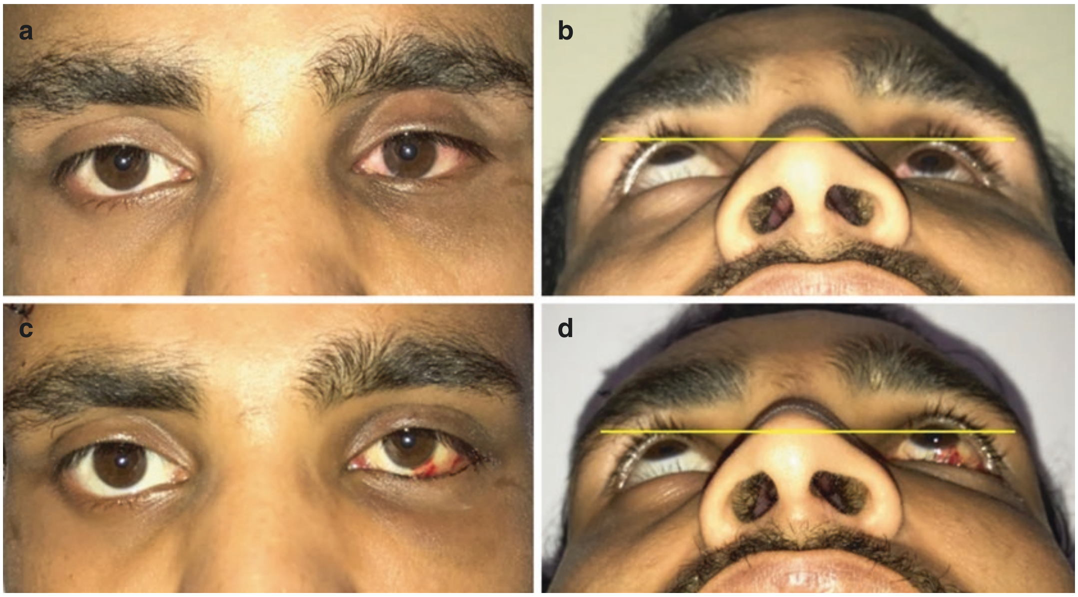

Fig. 57.42 Clinical photographs of patient with enophthalmos. (**a** and **b**) Pre-operative pictures demonstrating significant enophthalmos of the left globe. (**c** and **d**) Post-operative pictures demonstrating good surgical outcome

herniations or atrophy of periorbital fat, which do not mandate immediate intervention. Refer to clinical scenario 2.

When Is the Right Time to Intervene?

The timing for intervention for fractures of the orbital floor can be divided into three categories—immediate, early, and late. The indication for all three categories are well discussed in literature [57] and are listed in Fig. 57.43.

Indications for immediate repair are of an urgent nature and may require priority as surgical emergencies, generally less than 6 h following trauma.

What to Use for Reconstruction of the Orbital Defect?

A plethora of material both autogenous and alloplastic have been used and documented. A table is provided with the list of the most commonly used materials and their relative merits (Table 57.1). However, contemporary literature favors the use of stock titanium meshes and custom patient specific implants which provide optimal corrections (Fig. 57.44a, b).

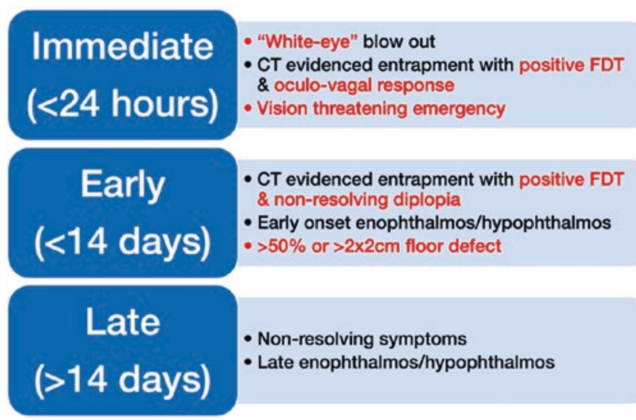

Fig. 57.43 Chart showing timing for intervention for orbital reconstruction

Guidelines for Deep Orbital Dissection

The dissection of the deep orbit is always a challenge for the surgeon due to the high concentration of vital structures within a limited space [60]. A few anatomical landmarks that have been suggested for guidance while dissecting in the deep orbit include:

(a) *Infra-orbital nerve*: the course of the infra-orbital nerve within the orbit is a very important landmark in floor dissection. The point of its entry from the pterygopalatine fossa at the genu/bend where inferior orbital fissure takes a turn and ascends laterally to continue as the superior orbital fissure signifies the safe limit for the posterior extent of floor dissection. Even in the case of badly comminuted fractures or delayed corrections, the nerve may be identifiable and provides a reliable clue to the end of the pre confluence area.

(b) *Inferior orbital fissure*: the inferior orbital fissure forms a pathway for an extended exposure of the lateral orbit as the contents of the fissure can be safely divided using bipolar cautery dissection. This facilitates easy navigation into the deep orbit behind the fissure and trace the greater wing of sphenoid. It may be of clinical relevance to note that the structures of the lateral orbit are much stronger and less prone to comminution when compared to the medial orbital structures. This makes the lateral approach to the deep orbit more predictable. Furthermore, the medial strut of the inferior orbital fissure is an important entity to identify and utilize for reconstruction of the internal orbit.

(c) *The greater wing of the sphenoid*: this is a thick and strong bony structure which forms the majority of the lateral orbit and bridges the inferior and superior orbital fissures. Its robust nature makes it less prone for comminution and hence forms a predictable landmark to find even in severe trauma.

(d) *Orbital process of the palatine bone*: the Orbital process of the palatine bone forms the highest point of the posterior-medial bulge of the orbital floor. This is an integral part of the posterior orbit that needs to be reconstructed to get adequate positioning of the globe in the anteroposterior and vertical directions.

(e) *Orbital confluence*: the orbital confluence (Fig. 57.45a, b) is formed by the convergence of two bony shelves forming the genu of the internal orbital fissures. This signifies the safe limits of the dissection of the orbital floor. The confluence is formed by the perpendicular plate of the palatine bone on the medial aspect and the bony inferior margin of the greater wing of the sphenoid laterally.

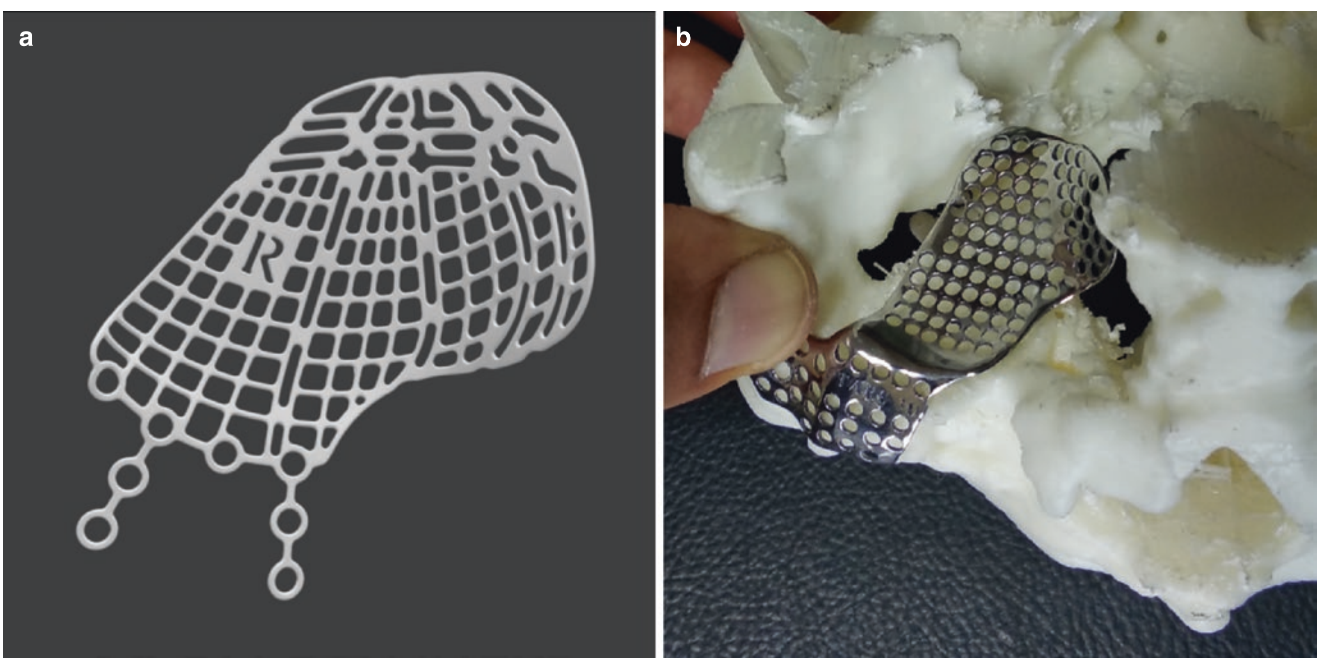

Fig. 57.44 Photographs of (**a**) Stryker[R] preformed anatomical orbital floor implant and (**b**) titanium "patient-specific implant" (PSI)

(f) *Safe distances within the orbit*: an important formula to remember safe distances within the orbit is 24-12-6, where 24 is the distance in mm of the anterior ethmoidal foramen from the medial orbital rim; an additional 12 mm deeper (36 mm) would indicate the posterior ethmoidal foramen followed by another 6 mm deep for the optic nerve (42 mm) [6].

(g) *Globe protection*: protection of the globe is of vital importance in orbital surgery. Adequate care should also be exercised for the protection of other vital structures like nerves and vessels also. Use of protection devices like specific retractors (Fig. 57.46a, b, c) and corneal shields is mandatory.

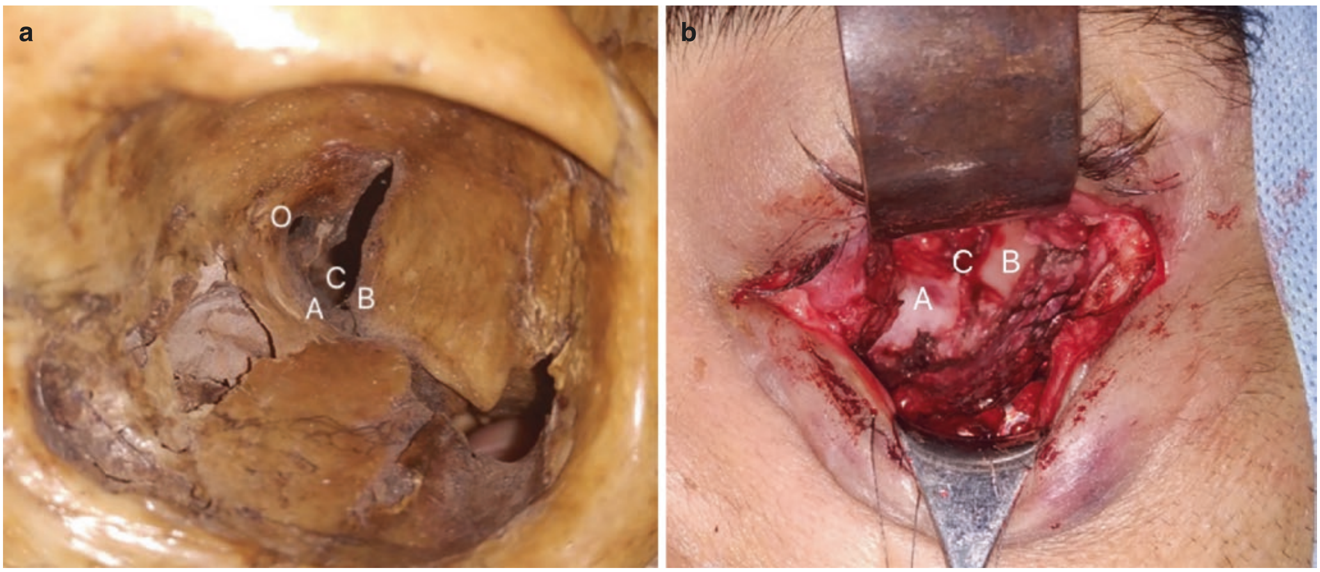

Fig. 57.45 (**a**) Demonstration of landmarks on dry skull. (A) Perpendicular plate of the palatine bone. (B) Medial lip of the greater wing of the sphenoid. (C) Orbital confluence and (O) Optic foramen. (**b**) Intraoperative photograph demonstrating the structures of the deep orbit in a patient undergoing secondary surgery for floor reconstruction with implant replacement

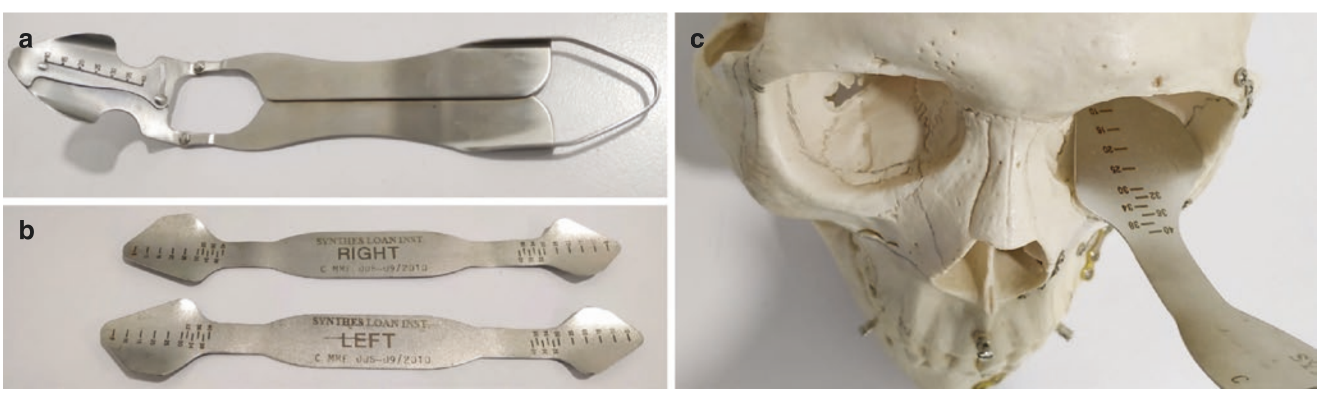

Fig. 57.46 Photographs showing globe protection devices. (**a**) Stryker[R] globe retractor, (**b**) Synthes[R] globe retractor and (**c**) Synthes[R] retractor in anatomical position demonstrating the use of calibration to aid intraoperatively

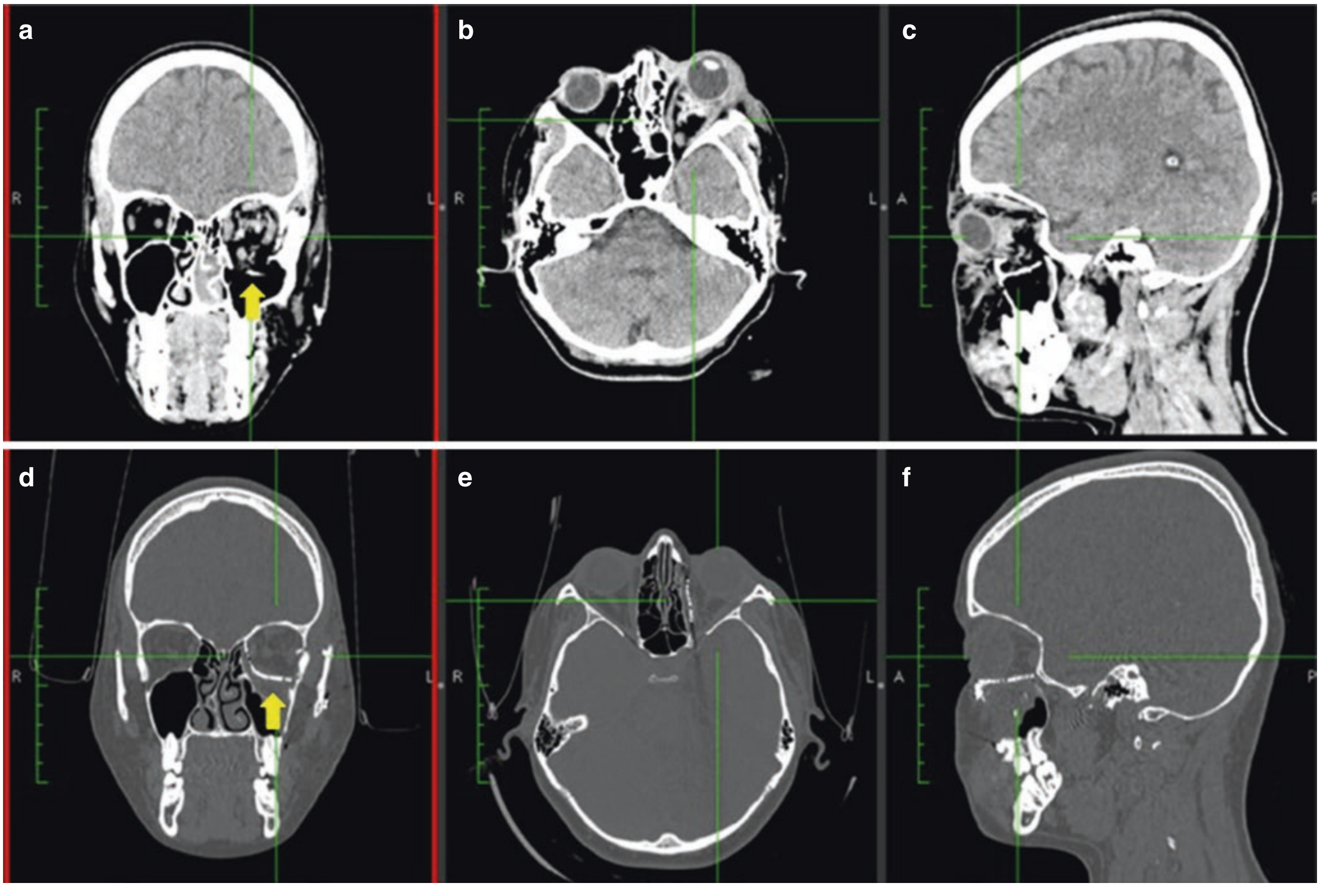

Fig. 57.47 CT scans images demonstrating optimal de-herniation of orbital contents and restoration of intra-orbital volume. (**a**–**c**) Pre-operative, (**d**–**f**) post-operative

De-herniation of the Orbital Contents and Locating the Posterior Ledge

Two important aspects of floor reconstruction are:

(i) De-herniation of the orbital (Fig. 57.47a–f) contents to *restore* the internal orbital volume

(ii) Locating the posterior ledge (Fig. 57.48a–d) for optimal implant positioning

However, locating the posterior ledge in large defects and secondary corrections may be a significant challenge. Absence of posterior ledge in severe orbital trauma is an indication for cantilevered implants which are secured to the infra-orbital rim alone.

57.8.3 Type III (Naso-Orbito-Ethmoid Type) (Refer Chap. 58)

The NOE-type fractures are the most challenging of all the orbital fractures to manage in terms of achieving predictable results. The management of the NOE complex reconstitutes the facial form of the central midface: a key element in facial esthetics. This type is also prone to have concomitant injuries to the lacrimal system which should be identified and treated.

Figure 57.49a–f demonstrates the CT images of a patient with a residual deformity following pan-facial trauma with a right-sided type I NOE and neglected orbital floor fractures.

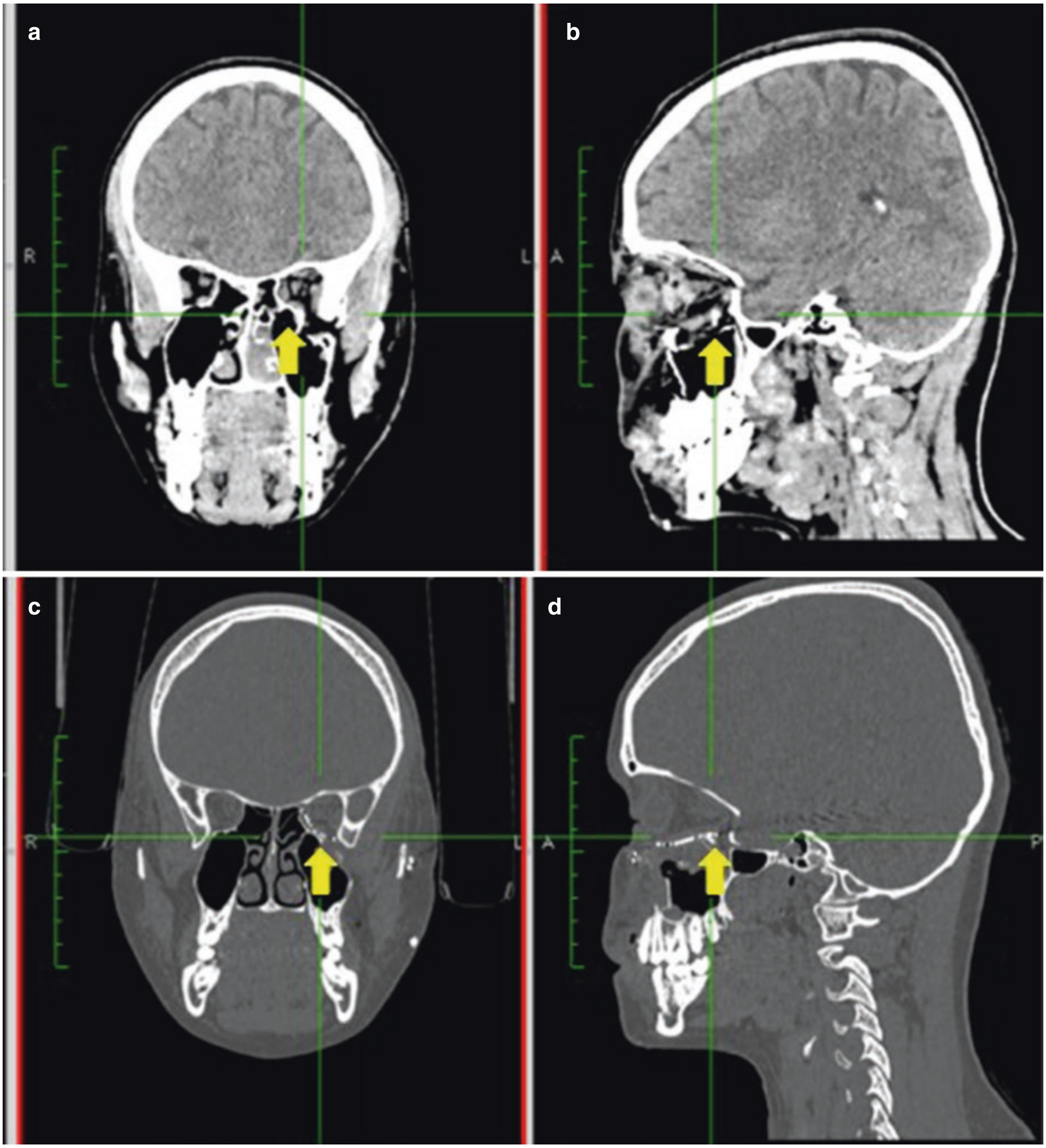

Fig. 57.48 (**a** and **b**) Pre-operative coronal and sagittal section CT images demonstrating the location of the posterior ledge of the floor defect. (**c** and **d**) Post-operative images showing the placement of the anatomical orbital floor implant in the appropriate position to bridge the defect

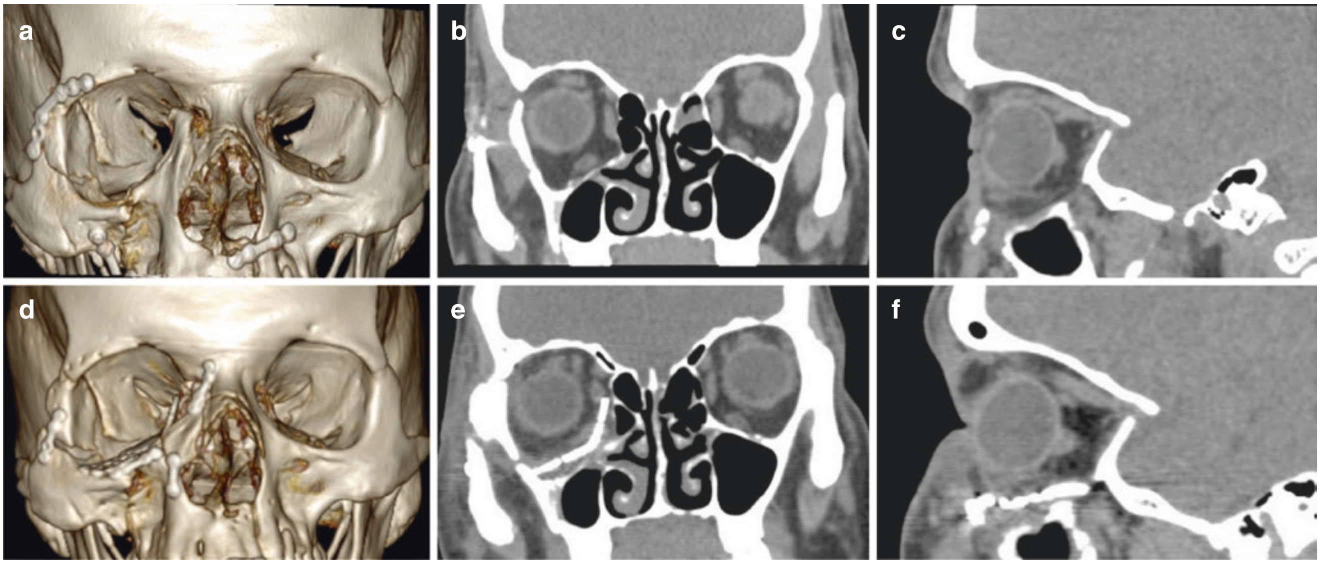

Fig. 57.49 CT scan images of patient with type I NOE fracture, plus orbito-zygomatic complex on the right side. (**a**–**c**) 3D, coronal and sagittal images demonstrating the fractures and the floor defect. (**d**–**f**) Post-operative images demonstrating ORIF of the right NOE fracture, redo of the orbito-zygomatic complex and floor reconstruction with anatomical orbital implant

Box 57.11 The *Key Elements* for Managing Type III Fractures

- Management of the medial canthal tendon (MCT) as indicated: this can be performed according to the description of Markowitz et al. [61] with the focus being the attachment or avulsion of the medial canthal tendon (MCT) to the fracture fragment
- Management of the soft tissue drape after reposition of the MCT
- Restoration of the nasal dorsum projection, which is of paramount importance
- Evaluation of injuries to the lacrimal system: canaliculi, sac and the nasolacrimal duct (NLD), and its management

57.8.4 Type IV (Complex Fractures of the Face with Orbital Fractures)

This type includes all the combinations of the fractures of the face which do not fall into the types described above. Sequencing of fractures (refer Chap. 60) such as these including pan-facial fractures requires a thorough understanding of the principles to obtain optimal outcomes. It is to be borne that sequencing and fixation of all facial fractures need to be completed prior to the reconstruction of the internal orbit.

Figures 57.50a–d and 57.51a–d demonstrate a patient with residual facial deformity following RTA. Patient had sub-optimally treated pan-facial and orbital fractures and a malunited mandible fracture. He was operated for a revision surgery addressing his midface and dental occlusion.

57.9 Management of Orbital Emergencies

(a) *Retrobulbar hemorrhage*: investigations with a CT scan or an MRI as the clinical situation mandates help us with a diagnosis of retrobulbar hemorrhage. 20% mannitol 2 g/kg body weight or 500 mg acetazolamide is administered to reduce the intraocular pressure in conjunction with 100 mg hydrocortisone for management of edema. Hourly examinations of pupils, visual acuity, and IOP are of great significance as stable ophthalmic status with diminishing signs of vision can be managed medically. Deterioration of vision or changes in visual fields may be considered an emergency [62]. Inferior cantholysis is the most commonly employed procedure for decompression of the retrobulbar space [63–65].

(b) *Traumatic optic neuropathy*: the management of traumatic optic neuropathy includes observation, use of steroids, and surgical decompression [66]. However, the use of corticosteroids in acute brain trauma is now debatable, and the general consensus is non-use of steroids in patients having concomitant brain trauma [67]. Many clinicians now restrict the use of steroids (bolus

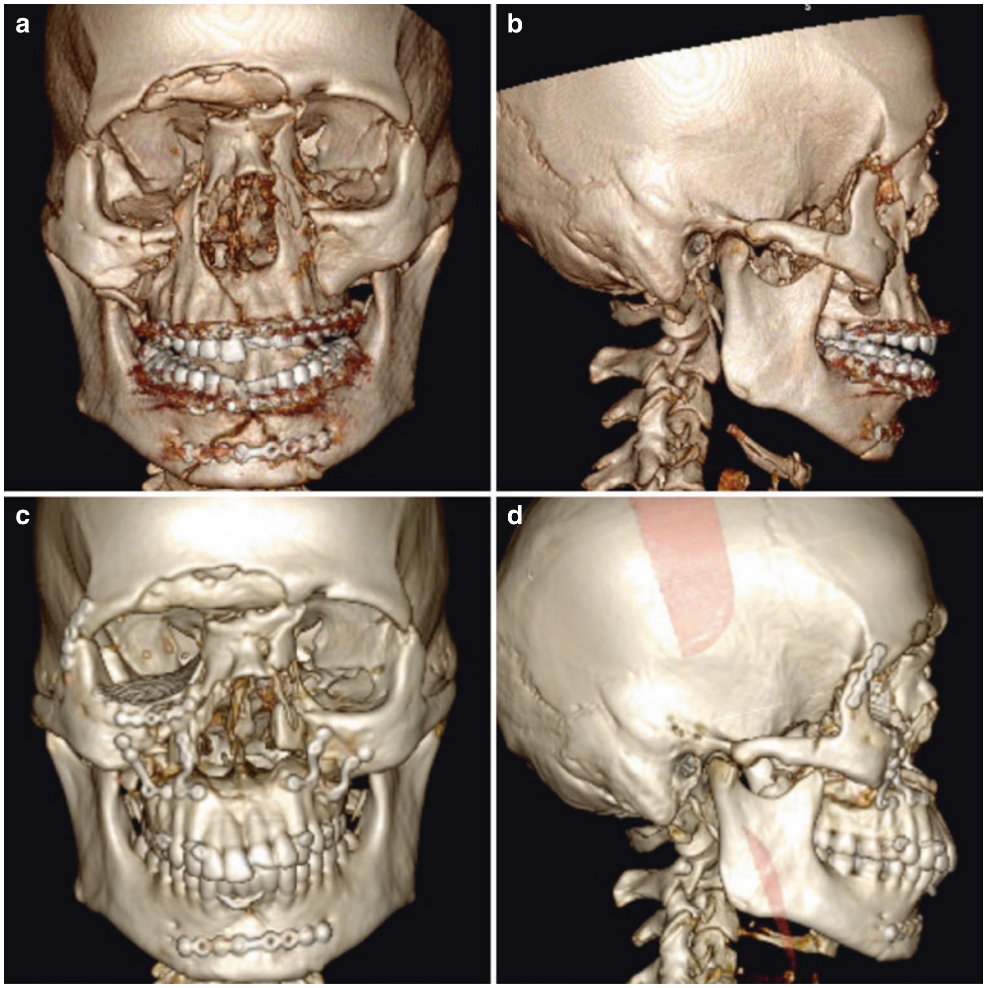

Fig. 57.50 3D CT images of patient with neglected pan facial injury and associated orbital fracture. (**a** and **b**) Images demonstrating frontal and lateral views showing malunited pan-facial fracture with facial deformity and significant dental malocclusion. (**c** and **d**) Post-operative images demonstrating ORIF of the right orbito-zygomatic complex and a Lefort I osteotomy with restoration of skeletal form, midface projection, and restoration of functional occlusion

dose of 30 mg/Kg body weight of methyl prednisolone followed by 3 mg/Kg/h for 24 h) within the first 8 h of injury, in cases of severe primary vision loss or progressive vision loss.

(c) *Compartment syndromes*: this includes both superior orbital fissure and orbital apex syndromes. The current protocols indicate early surgical decompression where indicated. The role of steroids is debatable as indicated above.

57.10 Pediatric Considerations (Figs. 57.52a–d and 57.53a, b)

Pediatric consideration in orbital trauma necessitates the discussion of four important aspects which clearly delineate the management principles from adults.

(a) *Ratio of cranium to facial fractures in children*
The face to cranium ratio of an infant is 1:8, while that of a child who is between 4 and 6 is about 1:4. This clearly establishes the fact that the cranium in an infant or a child is much larger than the face and is more exposed to potential trauma. The incidence of orbital roof fractures is much more common in children who are younger than 5 years, while beyond the age of 7, the floor fracture is more commonly seen.

(b) *Pediatric orbital roof fractures*
Roof fractures in children occur in the growing age [68] and cause an entity called the "growing skull fracture," where the fracture fragments continue to separate due to growth, causing "leptomeningeal" herniation which involves herniation of the meninges and part of the frontal lobe into the orbital cavity. Management of these need to be planned in conjunction with neurosurgical support.

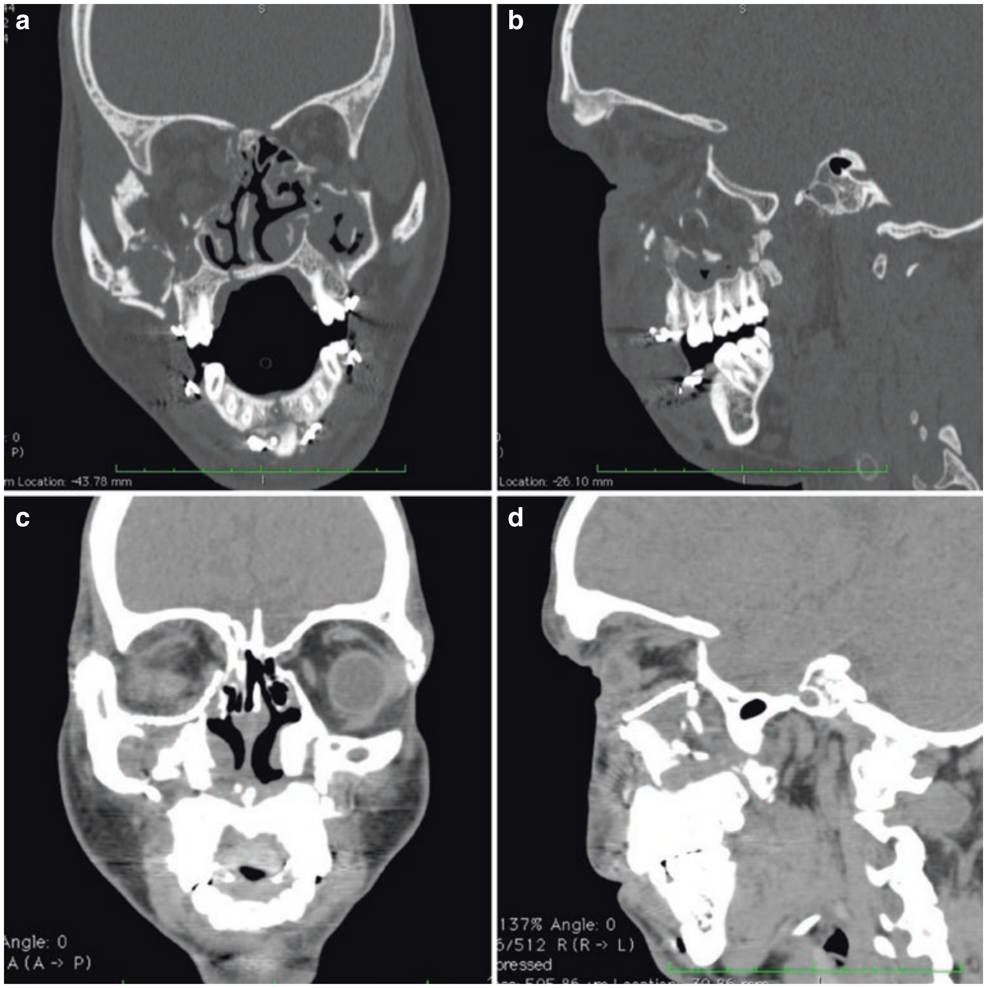

Fig. 57.51 Coronal and axial CT images of the patient in Fig 57.50. (**a** and **b**) Images demonstrating comminuted fractures of the midface and orbit. (**c** and **d**) Post-operative images showing optimal restoration of form of the face and orbit

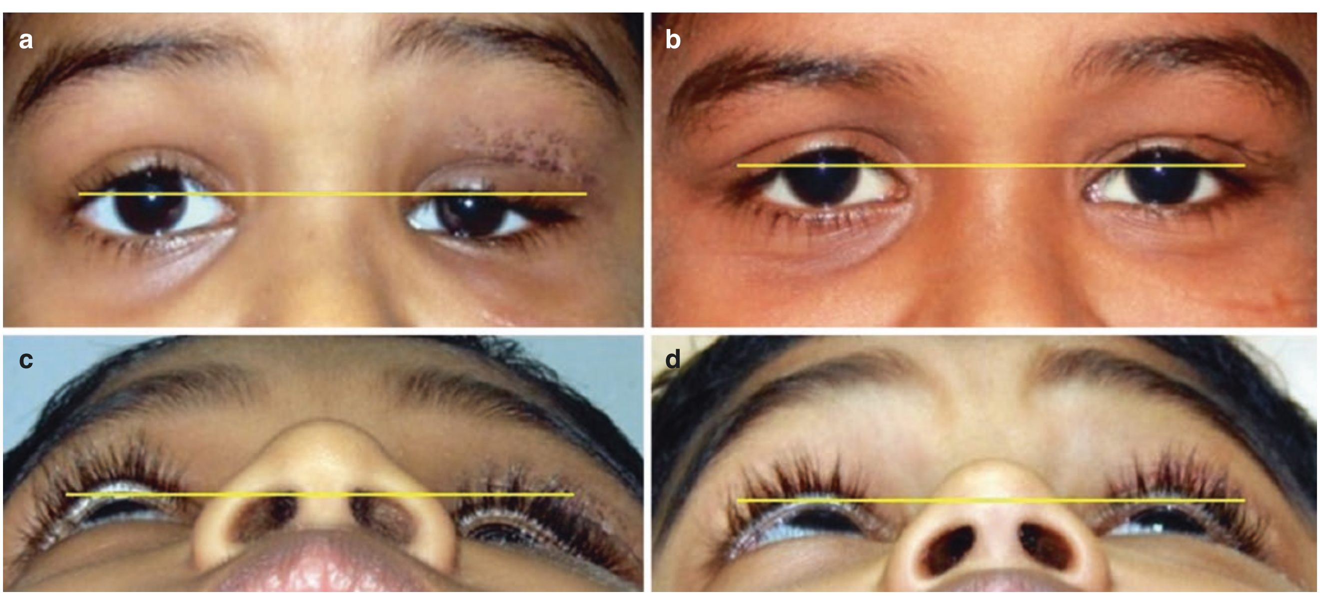

Fig. 57.52 Clinical photographs of a 6-year-old child with left sided orbital trauma (**a** and **c**) frontal and basal views demonstrating immediate-onset enophthalmos and hypophthalmos. (**b** and **d**) post-operative photographs showing optimal post-surgical outcome. (Courtesy: Dept of Orbit & Oculoplasty, Shankara Nethralaya, Chennai)

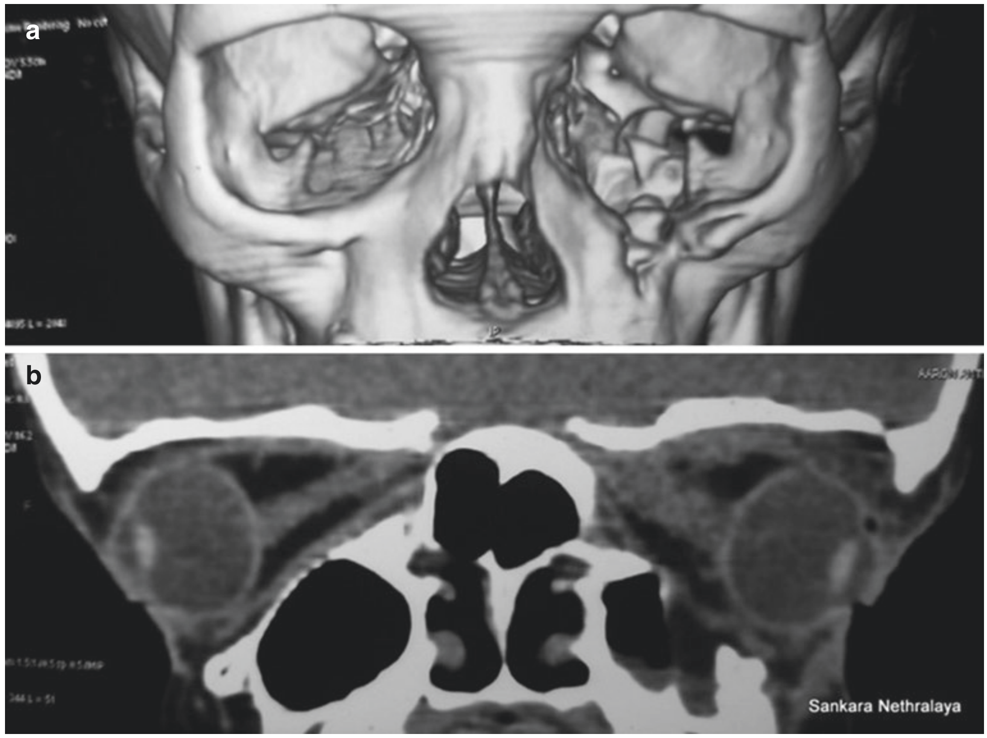

Fig. 57.53 CT scan images (**a**) 3D image demonstrating fracture involving the left infra-orbital rim and orbital floor in a 6 year-old child, (**b**) sagittal sections of both orbits showing left sided floor fracture. (Courtesy: Dept of Orbit & Oculoplasty, Shankara Nethralaya, Chennai)

(c) *White eye blowout*
The presence of floor fractures with restriction in superior gaze, with or without oculo-vagal responses and devoid of any physical signs of hemorrhage or ecchymosis in the eye or periorbital region [69–71]. This is a feature which may be seen in children and young adults as a result of a "self-reducing trapdoor" fracture which entraps the inferior rectus. The white eye blowout is considered a surgical emergency and necessitates immediate intervention.

(d) *Role of resorbable implants*
The cranium and upper face exhibit rapid growth in the early years. The orbit completes almost 80% of its growth within the first 2 years of life and another 10% within the next 2–3 years. Choice of implants in the growing orbit is to be taken into consideration by the surgeon who has to plan for the residual growth of the orbit and possible chances of migration of implants.

57.11 Secondary Correction of Orbital Deformities

Secondary corrections of the internal orbit demand great degrees of skill and are technically demanding even for the trained surgeon due to the nature of fibrosis and contracture that is already set in and the distortion of bony landmarks within the orbit. This may necessitate more extensive dissection and mobilization of the orbital contents and yet yield sub-optimal outcomes.

57.12 Complications

Complications associated with management of orbital fractures may be categorized into immediate and delayed complications.

Box 57.12 Indications for Secondary Deformity Correction of the Internal Orbit Generally Are

(a) Restricted ocular movement, which may be either due to muscle entrapments or adhesions of intra orbital and/or periorbita
(b) Diplopia due to physical impediments like bony interferences and/or soft tissue adhesion/entrapment
(c) Enophthalmos and/or hypophthalmos

57.12.1 Immediate Complications

The most common immediate complications that are secondary to orbital surgery include:

- edema,
- infection,
- would dehiscence,
- aberrant implant position,
- extrusion of implants.

Hemorrhage may be an infrequent complication which may happen during the surgery or in the immediate post-operative period.

Complications associated with specific ophthalmic implications like injuries to the cornea, extraocular muscles, lacrimal apparatus, or the optic nerve also may occur.

Blindness is a rare but grievous complication which has to be borne in mind.

The last group includes neurosensory disturbances like paresthesia or dysesthesia associated with the infra-orbital nerve and carrying grades of facial nerve palsy or weakness [72, 73].

57.12.2 Delayed Complications

Delayed complication may present in the form of:

- Persistent enophthalmos/hypophthalmos
- Persistent or worsened diplopia with altered vision
- Restricted ocular movement due to fibrosis and adhesion

Other adverse outcomes include:

- Entropion
- Ectropion
- Hypertrophic scars/keloids
- Change in the axis of the palpebral fissure

57.13 Recent Advances in Management of Orbital Fractures

Orbital reconstruction still remains one of the most challenging and enigmatic areas in the management of cranio-facial trauma and most certainly attracts the latest in terms of technology and developments to refine and improve outcomes. Significant advances in the field of orbital reconstruction include:

1. Computer-assisted surgery
2. Intraoperative imaging and navigation (refer Chap. 41)
3. Patient-specific implants for reconstruction

57.13.1 Navigation and CAS for Orbital Fractures and Reconstruction

Computer-assisted surgery allows virtual pre-operative planning of the desired reconstruction using pre-operative CT scans (Fig. 57.54a–d) [74]. This virtual plan gives real-time guidance during surgery. Navigation helps visualize the actual surgical outcome during surgery in relation to the pre-operative plan (Fig. 57.55). With this technique, sub-optimal reduction of fractures and positioning of implants can be identified and corrected during surgery, thereby reducing the need for secondary procedures [75–77].

57.13.2 Patient-Specific Implants (Fig. 57.56a–c)

Custom implants for the reconstruction of complex defects and deformities have become vogue now. They offer the advantages of accurate planning and infallible positioning intraoperatively which enormously improve post-surgical

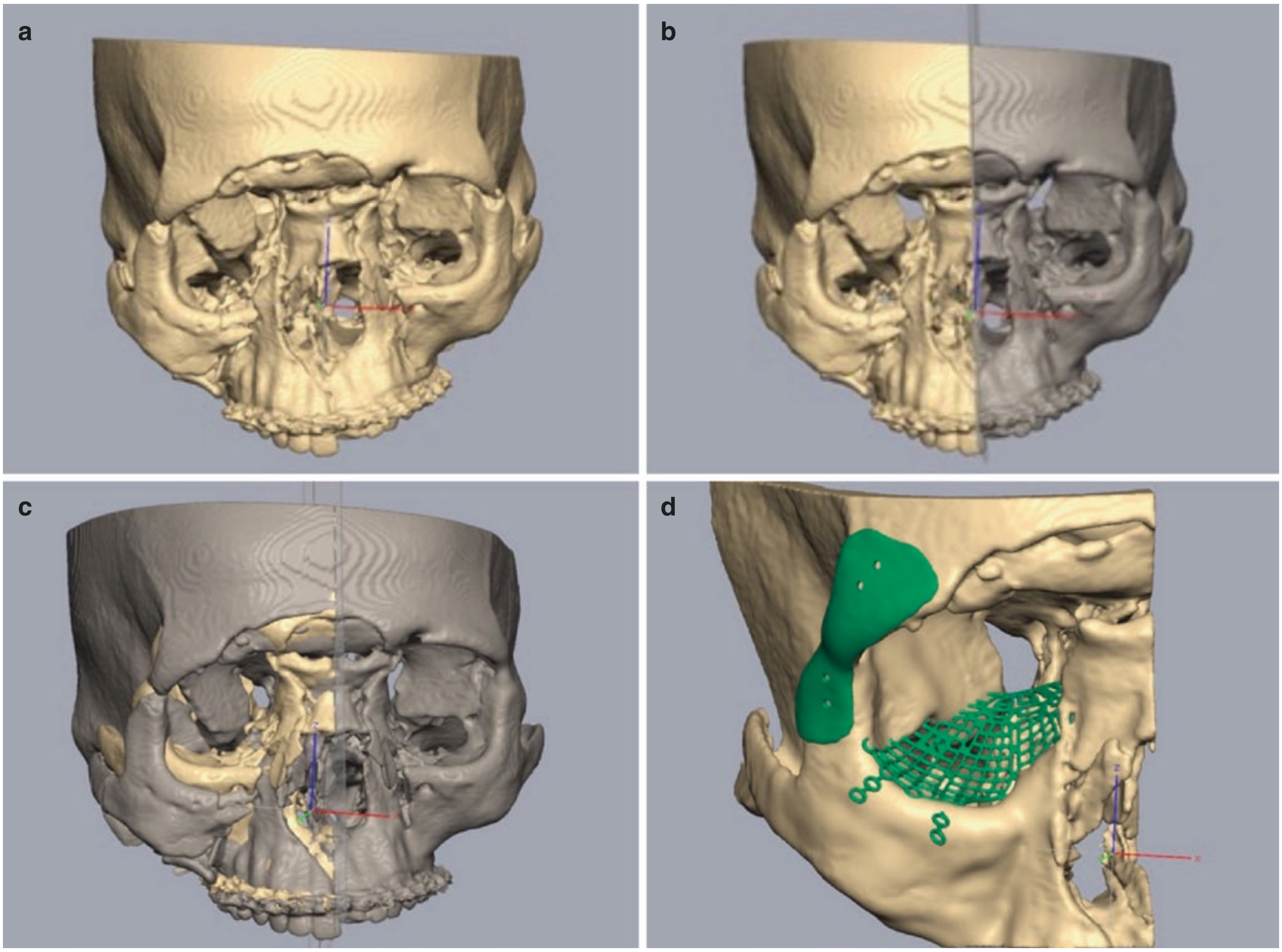

Fig. 57.54 Photographs depicting stages in computer-assisted surgery for orbito-facial reconstruction. (**a**) Generation of virtual 3D model; (**b**) segmentation and mirroring of normal side; (**c**) superimposition of the mirrored object on the affected side, enabling a better understanding of the deformity; and (**d**) creation of patient specific implant design for the fronto-zygomatic region and importing the virtual model of the anatomical orbital implant for floor reconstruction

outcomes. The defect can be mapped digitally and a construct can be made after virtual surgical planning to aid in intraoperative guidance. The implants may also function as guidance stents and double up as fixation devices too.

Box 57.13 Principles to Be Followed During Surgery for Orbital Floor Reconstruction

(i) Complete exposure of the fracture and defect
(ii) Meticulous de-herniation of the orbital soft tissues with restitution of intra-orbital volume
(iii) Identification of the posterior ledge in floor defects which is the posterior limit for reconstruction
(iv) Restoration of the posteromedial bulge of the orbit (Hammer's key area) [7]
(v) Choice for the reconstruction material should be based on the complexity of the defect (Dubois et al.) [55]

57.14 Conclusion

To conclude, all patients with orbital trauma need to be subjected to ophthalmological examinations both pre- and post-surgery. Globe protection, gentle retraction of tissues, and intraoperative testing for vision are mandatory during orbital surgery.

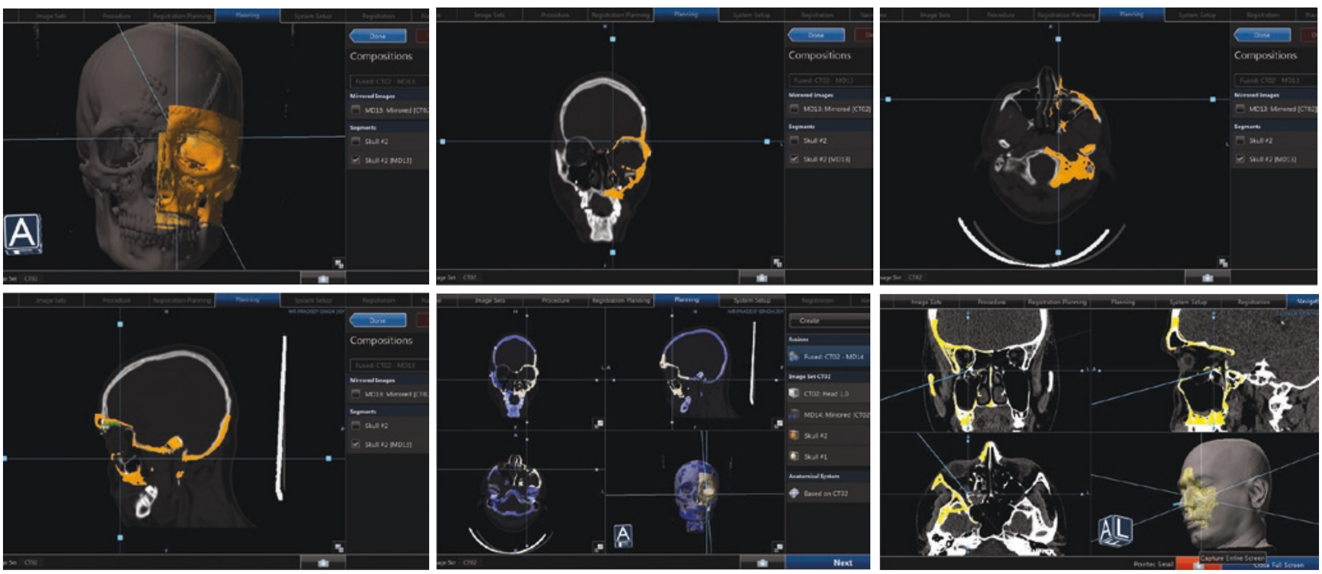

Fig. 57.55 Screenshot images of a left-sided orbital floor with an anatomical orbital floor implant that is virtually planned and executed with the help of intraoperative navigation

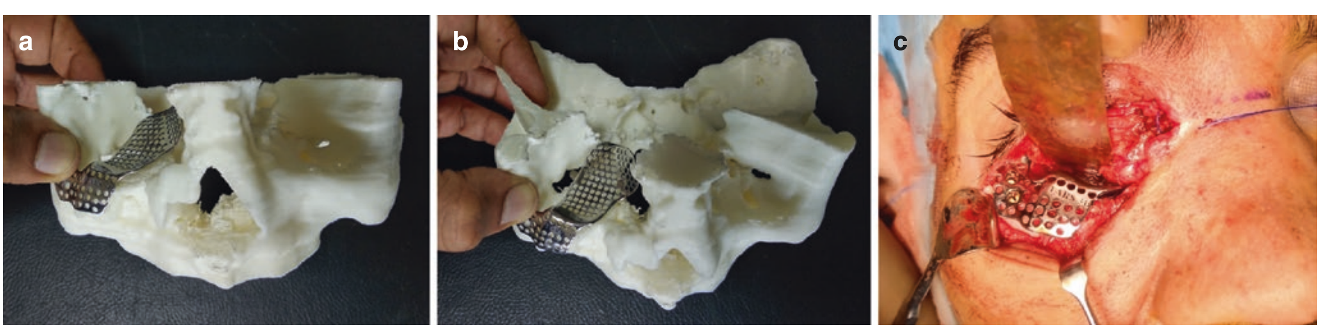

Fig. 57.56 PSI designed for reconstruction of a large floor and medial wall defect in the right orbit. (**a**) Frontal view of PSI on an STL model of the patient, (**b**) superior view, and (**c**) intraoperative photograph showing placement of the PSI "in situ"

57.15 Case Scenarios

Case 1

Patient with a history of facial trauma 8 months back presented with complaints of change in the position of his eyeballs. He had a history of surgical intervention for management of his pan-facial fractures immediately following the trauma. No intervention was performed for the orbital fractures primarily. Subsequent clinical evaluation performed 8 months later revealed enophthamos, hypophtalmos and restriction in superior gaze in the right eye. CT scans revealed a large orbital floor defect on the right side with fibrosis and adhesion of the inferior rectus to the posterior ledge of the floor defect. The patient was subjected to secondary surgery for correction of the above mentioned complaints. An orbital exploration was performed on the right side to release the inferior rectus, the infra-orbtial rim was augmented with a ramal graft and the floor defect was reconstructed with a "Stryker" anatomical orbital implant. Post-surgical evaluation revealed optimal corrections of the enophthalmos, hypophthalmos and good repositioning of the inferior rectus muscle (Figs. 57.57a–d, 57.58a, b and 57.59a–f).

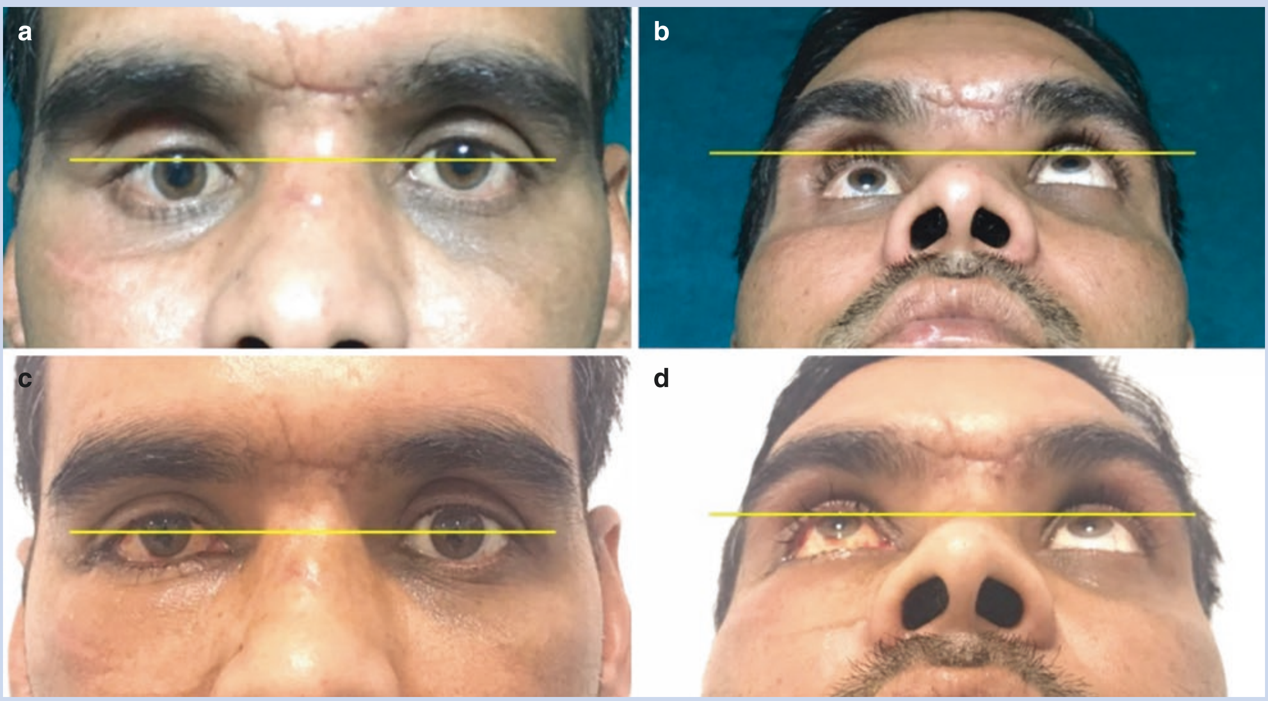

Fig. 57.57 (**a** and **b**) Pre-operative clinical photographs of patient demonstrating right sided enophthalmos and hypophthalmos. (**c** and **d**) Post-operative clinical photographs showing optimal surgical outcomes

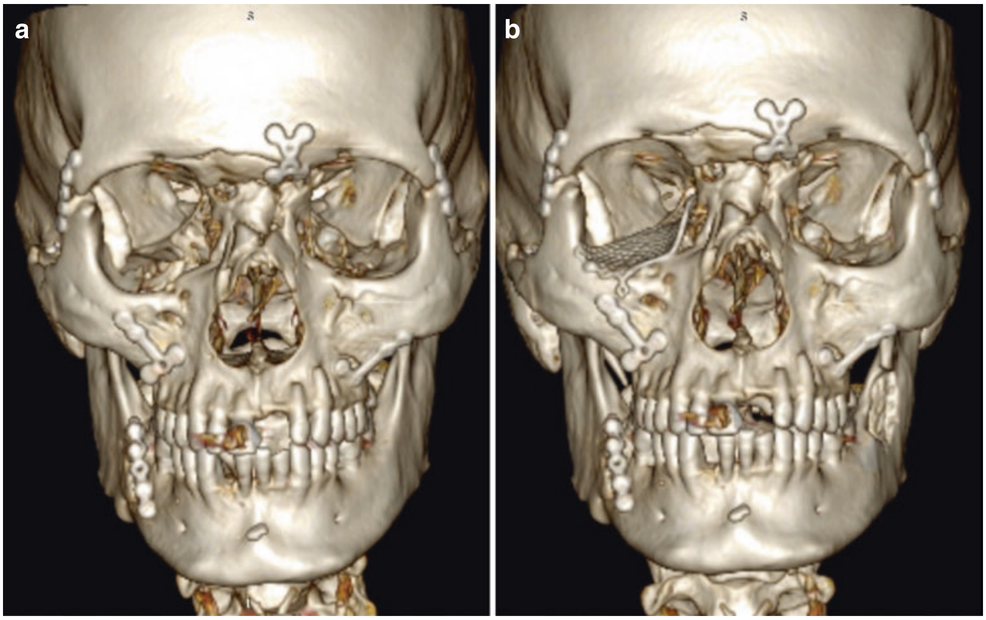

Fig. 57.58 3D CT reconstructions of patient in Fig 57.57 demonstrating (**a**) right-sided malunited zygomatic complex fracture with orbital floor defect and (**b**) post-surgical scan image showing reconstruction of the right orbital floor defect with an anatomical orbital implant after augmentation of the infra-orbital rim with a mandibular ramus bone graft

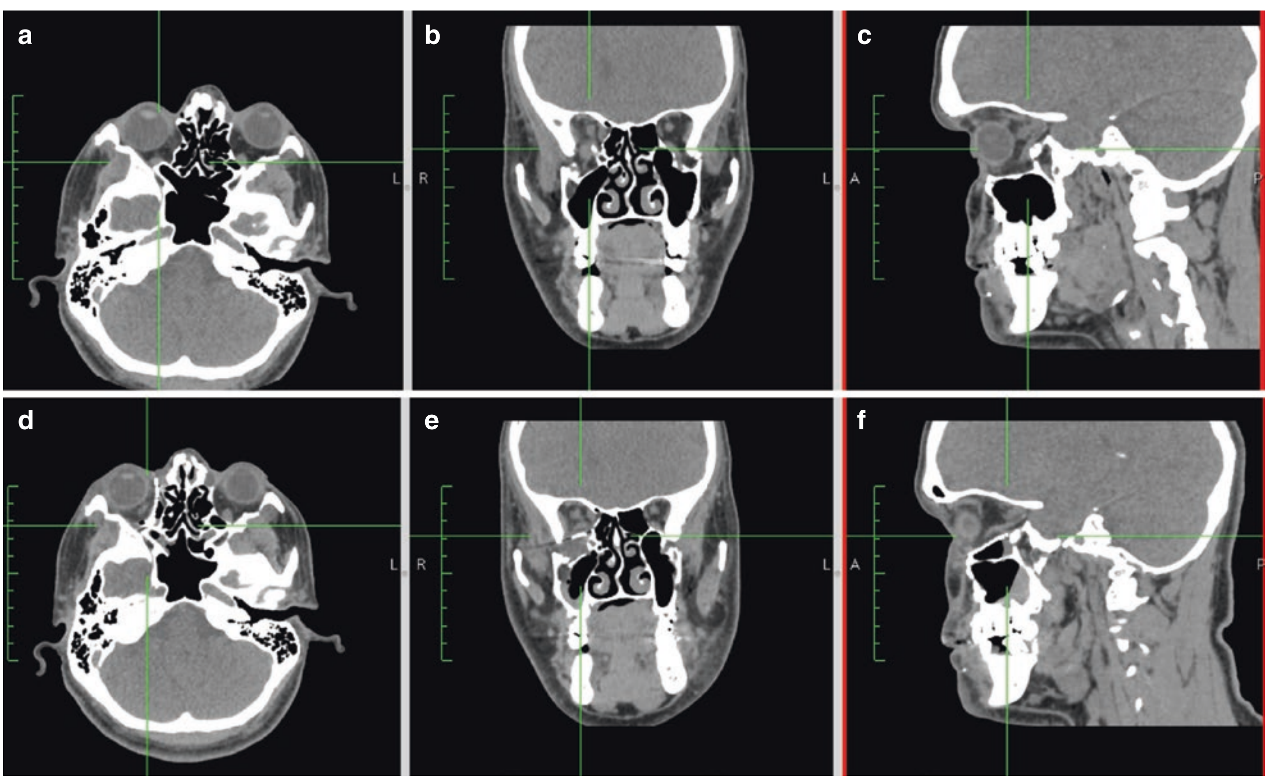

Fig. 57.59 (**a**–**c**) Pre-operative axial, coronal, and sagittal scans of patient in Fig 57.57 with large defect of the right orbital floor. (**d**–**f**) Post-operative sections demonstrating the correction of the floor defect with an anatomical orbital implant

Case 2

A 12 year old girl presented to the surgical OPD with history of blunt injury to the left eye. On examination she had no external signs of injury but revealed restriction in superior gaze in the left eye. CT scan revealed a springing trapdoor fracture of the left orbital floor with entrapment of the inferior rectus muscle. A diplopia charting was performed which revealed moderate to severe restriction of the left eye in the superior gaze. The patient was taken up for immediate surgery for orbital exploration and release of the entrapped muscle with/without floor reconstruction. The exploration was successful and the patient required no reconstruction of the floor. Post operatively the patient demonstrated complete resolution of the symptoms with the full range of ocular movements restored. (Figs. 57.60, 57.61, 57.62a, b) (Courtesy: Dept of Orbit & Oculoplasty, Shankara Nethralaya, Chennai)

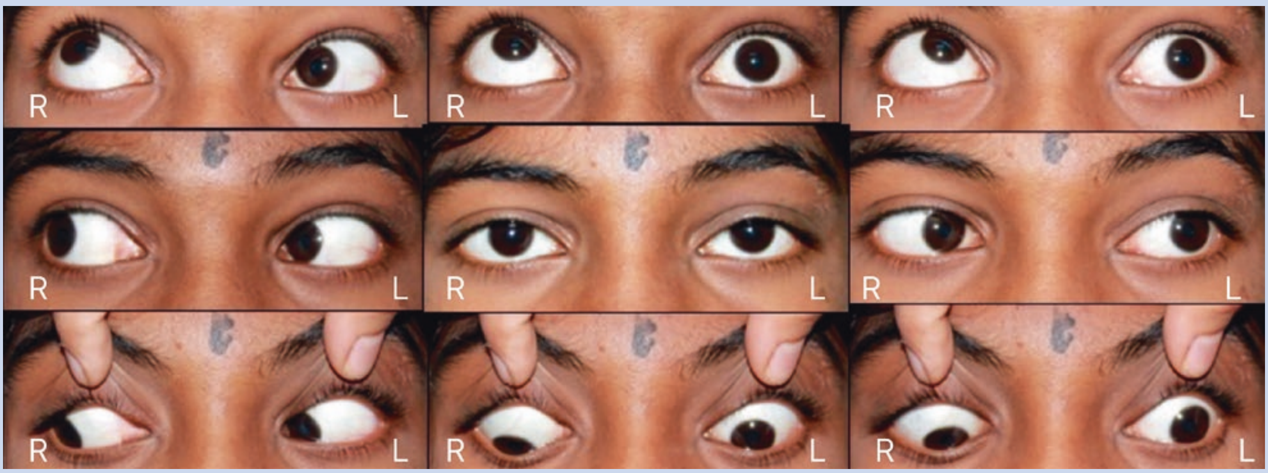

Fig. 57.60 Pre-operative photograph demonstrating the nine gazes of a young girl with a "White eye blowout" fracture of the left orbital floor with entrapment of the inferior rectus. (Courtesy: Dept of Orbit & Oculoplasty, Shankara Nethralaya, Chennai)

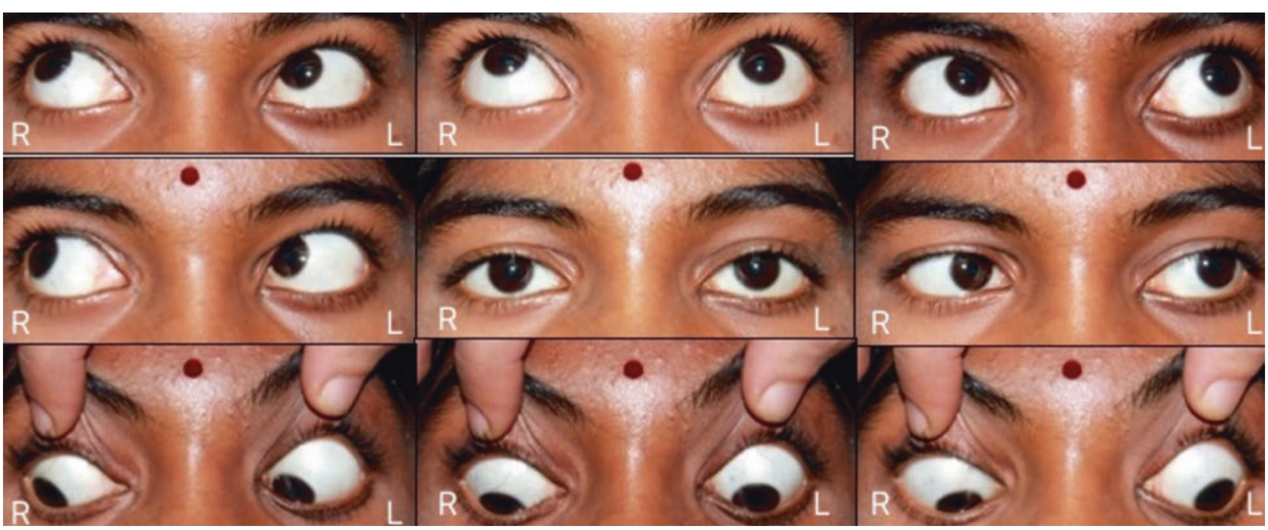

Fig. 57.61 Post-operative photograph demonstrating resolution of symptoms after 3 weeks of surgery (Courtesy: Dept of Orbit & Oculoplasty, Shankara Nethralaya, Chennai)

Fig. 57.62 Photograph of documentation of diplopia by charting with two colors (green for left and red for right eyes). The left and right sides are marked in the orientation that the patient sees an object in front of him/her. (**a**) Pre-operative and (**b**) post-operative (Courtesy: Dept of Orbit & Oculoplasty, Shankara Nethralaya, Chennai)

References

1. Turvey TA, Golden BA. Orbital anatomy for the surgeon. Oral Maxillofac Surg Clin North Am. 2012;24(4):525–36.
2. Ochs MW, Buckley MJ. Anatomy of the orbit. Oral Maxillofac Surg Clin North Am. 1993;5:419–29.
3. Rowe NL, Williams JL. Maxillofacial injuries. Edinburgh: Churchill Livingstone; 1985.
4. Furuta M. Measurement of orbital volume by computed tomography: especially on the growth of the orbit. Jpn J Ophthalmol. 2001;45(6):600–6.
5. Bron AJ, Tripathi RC. Wolff's anatomy of the eye and orbit. London: Chapman and Hall Medical; 1997.
6. Zide BM, editor. Surgical anatomy around the orbit: the system of zones. Philadelphia: Lippincott Williams & Wilkins; 2006.
7. Hammer B. Orbital fractures: diagnosis, operative treatment, secondary corrections. Toronto: Hogrefe & Huber; 1995.
8. Manson PN, Clifford CM, Su CT, Iliff NT, Morgan R. Mechanisms of global support and posttraumatic enophthalmos: I. The anatomy of the ligament sling and its relation to intramuscular cone orbital fat. Plast Reconstr Surg. 1986;77(2):193–202.
9. Martins C, Costa e Silva IE, Campero A, Yasuda A, Aguiar LR, Tatagiba M, Rhoton A. Microsurgical anatomy of the orbit: the rule of seven. Anat Res Int. 2011;2011:468727.
10. Manson PN, Markowitz B, Mirvis S, Dunham M, Yaremchuk M. Toward CT-based facial fracture treatment. Plast Reconstr Surg. 1990 Feb;85(2):202–12.
11. Converse JM, Smith B. Blowout fracture of the floor of the orbit. Trans Am Acad Ophthalmol Otolaryngol. 1960;64:676–88.
12. Dingman RO, Natvig P. Surgery of facial fractures. London: Saunders; 1964.
13. Fujino T. Experimental "blowout" fracture of the orbit. Plast Reconstr Surg. 1974;54(1):81–2.
14. Pfeiffer RL. Traumatic enophthalmos. Trans Am Ophthalmol Soc. 1943;41:293–306.
15. Brady SM, Mcmann MA, Mazzoli RA, Bushley DM, Ainbinder DJ, Carroll RB. The diagnosis and management of orbital blowout fractures: update 2001. Am J Emerg Med. 2001;19(2):147–54.
16. King EF, Samuel E. Fractures of the orbit. Trans Ophthalmol Soc U K. 1944;64:134–53.
17. Ahmad F, Kirkpatrick NA, Lyne J, Urdang M, Waterhouse N. Buckling and hydraulic mechanisms in orbital blowout fractures: fact or fiction? J Craniofac Surg. 2006;17(3):438–41.
18. Nagasao T, Miyamoto J, Shimizu Y, Jiang H, Nakajima T. What happens between pure hydraulic and buckling mechanisms of blowout fractures? J Cranio-Maxillofac Surg. 2010;38(4):306–13.
19. Al-Qurainy IA, Dutton GN, Titterington DM, Stassen LF, Moos KF, El-Attar A. Midfacial fractures and the eye: the development of a system for detecting patients at risk of eye injury. Br J Oral Maxillofac Surg. 1991;29(6):363–7.
20. Soparkar CN, Patrinely JR. The eye examination in facial trauma for the plastic surgeon. Plast Reconstr Surg. 2007;120(7):49S–56S.
21. AI-Qrainy IA, Dutton GN, Stassen LF, Moos KF, EI-Attar A. The characteristics of midfacial fractures and the association with ocular injury: a prospective study. Br J Oral Maxillofac Surg. 1991;29(5):291–301.
22. Ochs MW. Orbital and ocular trauma. In: Peterson's principles of oral and maxillofacial surgery. 2nd ed. Hamilton: London; 2004. p. 463–90.
23. American Academy of Ophthalmology. 8-point eye exam. Adopted May 24, 2016 (Cited May 21, 2019). Available from https://www.aao.org/young-ophthalmologists/yo-info/article/how-to-conduct-eight-point-ophthalmology-exam
24. AI-Qurainy IA, Dutton GN, Stassen LF, Moos KF, El-Attar A. Diplopia following midfacial fractures. Br J Oral Maxillofac Surg. 1991;29(5):302–7.
25. Tahernia A, Erdmann D, Follmar K, Mukundan S, Grimes J, Marcus JR. Clinical implications of orbital volume change in the management of isolated and zygomaticomaxillary complex–associated orbital floor injuries. Plast Reconstr Surg. 2009;123(3):968–75.
26. He D, Li Z, Shi W, Sun Y, Zhu H, Lin M, Shen G, Fan X. Orbitozygomatic fractures with enophthalmos: analysis of 64 cases treated late. J Oral Maxillofac Surg. 2012;70(3):562–76.
27. Goodall KL, Brahma A, Bates A, Leatherbarrow B. Lateral canthotomy and inferior cantholysis: an effective method of urgent orbital decompression for sight threatening acute retrobulbar haemorrhage. Injury. 1999;30(7):485–90.
28. Gruss JS, Hurwitz JJ, Nik NA, Kassel EE. The pattern and incidence of nasolacrimal injury in naso-orbital-ethmoid fractures: the role of delayed assessment and dacryocystorhinostomy. Br J Plast Surg. 1985;38(1):116–21.
29. Woernley TC, Wright TL, Lam DN, Jundt JS. Oculocardiac reflex in an orbital fracture without entrapment. J Oral Maxillofac Surg. 2017;75(8):1716–21.
30. Schaller B. Trigeminocardiac reflex. J Neurol. 2004;251(6):658–65.
31. Fonseca RJ, Marciani RD, Turvey TA. Oral and maxillofacial surgery. Missouri: Saunders Elsevier; 2009.

32. Chen CT, Chen YR. Traumatic superior orbital fissure syndrome: current management. Craniomaxillofac Trauma Reconstr. 2010 Mar;3(01):009–16.
33. Zachariades N. The superior orbital fissure syndrome: Review of the literature and report of a case. Oral Surg Oral Med Oral Pathol. 1982;53(3):237–40.
34. Warburton RE, Brookes CC, Golden BA, Turvey TA. Orbital apex disorders: a case series. Int J Oral Maxillofac Surg. 2016;45(4):497–506.
35. Antonyshyn O, Gruss JS, Kassel EE. Blow-in fractures of the orbit. Plast Reconstr Surg. 1989;84(1):10–20.
36. Lynch RC. The technique of a radical frontal sinus operation which has given me the best results.(original communications are received with the understanding) that they are contributed exclusively to the laryngoscope. Laryngoscope. 1921;31(1):1–5.
37. Ellis E, Zide MF, editors. Surgical approaches to the facial skeleton. Philadelphia: Lippincott Williams & Wilkins; 2006.
38. Perry M, Holmes S. Manual of operative maxillofacial trauma surgery. London: Springer; 2014.
39. Cline RA, Rootman J. Enophthalmos: a clinical review. Ophthalmology. 1984;91(3):229–37.
40. Athanasiov PA, Prabhakaran VC, Selva D. Non-traumatic enophthalmos: a review. Acta Ophthalmol. 2008;86(4):356–64.
41. Converse JM, Smith B, Obear MF, Wood-Smith D. Orbital blowout fractures: a ten-year survey. Plast Reconstr Surg. 1967;39(1):20–36.
42. Cossman JP, Morrison CS, Taylor HO, Salter AB, Klinge PM, Sullivan SR. Traumatic orbital roof fractures: interdisciplinary evaluation and management. Plast Reconstr Surg. 2014;133(3):335e–43e.
43. Alsuhaibani AH. Orbital fracture: significance of lateral wall. Saudi J Ophthalmol. 2010;24(2):49–55.
44. Stanley JR, Sires BS, Funk GF, Nerad JA. Management of displaced lateral orbital wall fractures associated with visual and ocular motility disturbances. Plast Reconstr Surg. 1998;102(4):972–9.
45. Manolidis S, Weeks BH, Kirby M, Scarlett M, Hollier L. Classification and surgical management of orbital fractures: experience with 111 orbital reconstructions. J Craniofac Surg. 2002;13(6):726–37.
46. McNichols CH, Hatef DA, Thornton JF, Cole PD, de Mitchell CA, Hollier LH Jr. A paradigm shift in correcting medial orbital fracture–related enophthalmos: volumetric augmentation through a lateral approach. J Craniofac Surg. 2012;23(3):762–6.
47. Nolasco FP, Mathog RH. Medial orbital wall fractures: classification and clinical profile. Otolaryngol Head Neck Surg. 1995 Apr;112(4):549–56.
48. Burm JS, Chung CH, Oh SJ. Pure orbital blowout fracture: new concepts and importance of medial orbital blowout fracture. Plast Reconstr Surg. 1999;103(7):1839–49.
49. Lee WT, Kim HK, Chung SM. Relationship between small-size medial orbital wall fracture and late enophthalmos. J Craniofac Surg. 2009;20(1):75–80.
50. Jin HR, Shin SO, Choo MJ, Choi YS. Relationship between the extent of fracture and the degree of enophthalmos in isolated blowout fractures of the medial orbital wall. J Oral Maxillofac Surg. 2000;58(6):617–20.
51. Saiepour D, Messo E, Hedlund AJ, Nowinski DJ. Radiologic and long-term clinical outcome from treatment of isolated medial orbital wall blowout fractures. J Craniofac Surg. 2012;23(5):1252–5.
52. Lee CS, Yoon JS, Lee SY. Combined transconjunctival and transcaruncular approach for repair of large medial orbital wall fractures. Arch Ophthalmol. 2009;127(3):291–6.
53. Dubois L, Steenen SA, Gooris PJ, Bos RR, Becking AG. Controversies in orbital reconstruction—III. Biomaterials for orbital reconstruction: a review with clinical recommendations. Int J Oral Maxillofac Surg. 2016;45(1):41–50.
54. Jaquiéry C, Aeppli C, Cornelius P, Palmowsky A, Kunz C, Hammer B. Reconstruction of orbital wall defects: critical review of 72 patients. Int J Oral Maxillofac Surg. 2007;36(3):193–9.
55. Dubois L, Steenen SA, Gooris PJ, Mourits MP, Becking AG. Controversies in orbital reconstruction—I. Defect-driven orbital reconstruction: a systematic review. Int J Oral Maxillofac Surg. 2015;44(3):308–15.
56. Palmieri CF, Ghali GE. Late correction of orbital deformities. Oral Maxillofac Surg Clin North Am. 2012;24(4):649–63.
57. Dubois L, Steenen SA, Gooris PJ, Mourits MP, Becking AG. Controversies in orbital reconstruction—II. Timing of post-traumatic orbital reconstruction: a systematic review. Int J Oral Maxillofac Surg. 2015;44(4):433–40.
58. Koo L, Hatton MP, Rubin PA. When is enophthalmos "significant"? Ophthalmic Plast Reconstr Surg. 2006;22(4):274–7.
59. Sung YS, Chung CM, Hong IP. The correlation between the degree of enophthalmos and the extent of fracture in medial orbital wall fracture left untreated for over six months: a retrospective analysis of 81 cases at a single institution. Arch Plast Surg. 2013;40(4):335.
60. Gooris PJ, Muller BS, Dubois L, Bergsma JE, Mensink G, van den Ham MF, Becking AG, Seubring K. Finding the ledge: sagittal analysis of bony landmarks of the orbit. J Oral Maxillofac Surg. 2017;75(12):2613–27.
61. Markowitz BL, Manson PN, Sargent L, Vander CAK, Yaremchuk M, Glassman D, et al. Management of the medial canthal tendon in nasoethmoid orbital fractures: the importance of the central fragment in classification and treatment. Plast Reconstr Surg. 1991;87(5):843–53.
62. Hayreh SS, Weingeist TA. Experimental occlusion of the central artery of the retina. IV: Retinal tolerance time to acute ischaemia. Br J Ophthalmol. 1980;64(11):818–25.
63. Vassallo S, Hartstein M, Howard D, Stetz J. Traumatic retrobulbar hemorrhage: emergent decompression by lateral canthotomy and cantholysis. J Emerg Med. 2002;22(3):251–6.
64. Gerbino G, Ramieri GA, Nasi A. Diagnosis and treatment of retrobulbar haematomas following blunt orbital trauma: a description of eight cases. Int J Oral Maxillofac Surg. 2005;34(2):127–31.
65. Amrith S, Saw SM, Lim TC, Lee TK. Ophthalmic involvement in cranio-facial trauma. J Cranio-Maxillofac Surg. 2000;28(3):140–7.
66. Levin LA, Beck RW, Joseph MP, Seiff S, Kraker R, International Optic Nerve Trauma Study Group. The treatment of traumatic optic neuropathy: the International Optic Nerve Trauma Study. Ophthalmology. 1999;106(7):1268–77.
67. Steinsapir KD, Goldberg RA. Traumatic optic neuropathy. Surv Ophthalmol. 1994;38(6):487–518.
68. Hoffmeister B. Pediatric maxillofacial trauma. In: Maxillofacial surgery. London: Churchill Livingstone; 2017. p. 193–9.
69. Sugamata A, Yoshizawa N. A case of blowout fracture of the orbital floor in early childhood. Int Med Case Rep J. 2015;8:155–8.
70. Tiwana PS, Vickers A. Pediatric cranio-maxillofacial trauma: mandibular fractures. In: Current therapy in oral and maxillofacial surgery. Philadelphia: WB Saunders; 2012. p. 841–50.
71. Yew CC, Shaari R, Rahman SA, Alam MK. White-eyed blowout fracture: diagnostic pitfalls and review of literature. Injury. 2015;46(9):1856–9.
72. Benoliel R, Birenboim R, Regev E, Eliav E. Neurosensory changes in the infraorbital nerve following zygomatic fractures. Oral Surg Oral Med Oral Pathol Oral Radiol Endod. 2005;99(6):657–65.

73. Kumar P, Godhi S, Lall AB, Ram CS. Evaluation of neurosensory changes in the infraorbital nerve following zygomatic fractures. J Maxillofac Oral Surg. 2012;11(4):394–9.
74. Bell RB, Markiewicz MR. Computer-assisted planning, stereolithographic modeling, and intraoperative navigation for complex orbital reconstruction: a descriptive study in a preliminary cohort. J Oral Maxillofac Surg. 2009;67(12):2559–70.
75. Lauer G, Pradel W, Schneider M, Eckelt U. Efficacy of computer-assisted surgery in secondary orbital reconstruction. J Cranio-Maxillofac Surg. 2006;34(5):299–305.
76. Wilde F, Lorenz K, Ebner AK, Krauss O, Mascha F, Schramm A. Intraoperative imaging with a 3D C-arm system after zygomatico-orbital complex fracture reduction. J Oral Maxillofac Surg. 2013;71(5):894–910.
77. Wilde F, Schramm A. Intraoperative imaging in orbital and midface reconstruction. Facial Plast Surg. 2014;30(05):545–53.

Additional Reading

Bater MC, Ramchandani PL, Brennan PA. Post-traumatic eye observations. Br J Oral Maxillofac Surg. 2005;43(5):410–6.